British Geological Survey
NATURAL ENVIRONMENT RESEARCH COUNCIL

JARÐFEINGI

A revised structural elements map for the Faroe-Shetland Basin and adjacent areas

Energy and Marine Geoscience Programme

Commissioned Report CR/14/059

Fully redacted version

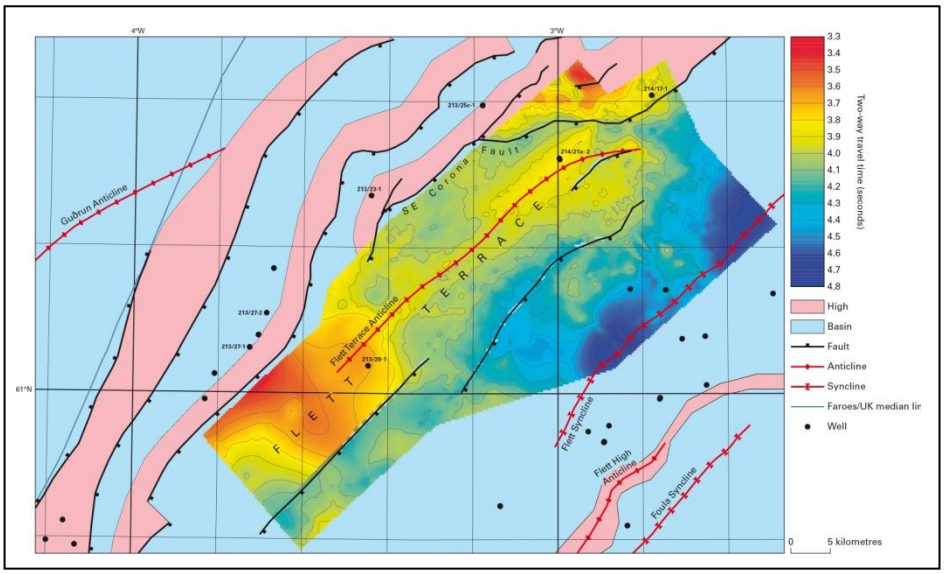

BRITISH GEOLOGICAL SURVEY

ENERGY AND MARINE GEOSCIENCE PROGRAMME

COMMISSIONED REPORT CR/14/059

A revised structural elements map for the Faroe-Shetland Basin and adjacent areas

M F Quinn[1], H Johnson[1], G S Kimbell[2], K Smith[1] and Ó Eidesgaard[3]

[1] *British Geological Survey, Edinburgh, UK*
[2] *British Geological Survey, Nottingham, UK*
[3] *Jarðfeingi, Faroe Islands*

Keywords

Structure, Faroe-Shetland Basin.

Front cover

Revised structural elements map for the Faroe-Shetland Basin and adjacent areas.

Bibliographical reference

QUINN, M F, JOHNSON, H, KIMBELL, G S, SMITH, K AND EIDESGAARD, Ó. 2011. A revised structural elements map for the Faroe-Shetland Basin and adjacent areas. *British Geological Survey Commissioned Report*, CR/14/059.

Edinburgh, British Geological Survey 2014

BRITISH GEOLOGICAL SURVEY

The full range of our publications is available from BGS shops at Nottingham, Edinburgh, London and Cardiff (Welsh publications only) see contact details below or shop online at www.geologyshop.com

The London Information Office also maintains a reference collection of BGS publications, including maps, for consultation.

We publish an annual catalogue of our maps and other publications; this catalogue is available online or from any of the BGS shops.

The British Geological Survey carries out the geological survey of Great Britain and Northern Ireland (the latter as an agency service for the government of Northern Ireland), and of the surrounding continental shelf, as well as basic research projects. It also undertakes programmes of technical aid in geology in developing countries.

The British Geological Survey is a component body of the Natural Environment Research Council.

British Geological Survey offices

BGS Central Enquiries Desk

Tel 0115 936 3143 Fax 0115 936 3276

email enquiries@bgs.ac.uk

Kingsley Dunham Centre, Keyworth, Nottingham NG12 5GG

Tel 0115 936 3241 Fax 0115 936 3488

email sales@bgs.ac.uk

Murchison House, West Mains Road, Edinburgh EH9 3LA

Tel 0131 667 1000 Fax 0131 668 2683

email scotsales@bgs.ac.uk

Natural History Museum, Cromwell Road, London SW7 5BD

Tel 020 7589 4090 Fax 020 7584 8270

Tel 020 7942 5344/45 email bgslondon@bgs.ac.uk

Columbus House, Greenmeadow Springs, Tongwynlais, Cardiff CF15 7NE

Tel 029 2052 1962 Fax 029 2052 1963

Maclean Building, Crowmarsh Gifford, Wallingford OX10 8BB

Tel 01491 838800 Fax 01491 692345

Geological Survey of Northern Ireland, Colby House, Stranmillis Court, Belfast BT9 5BF

Tel 028 9038 8462 Fax 028 9038 8461

www.bgs.ac.uk/gsni/

Parent Body

Natural Environment Research Council, Polaris House, North Star Avenue, Swindon SN2 1EU

Tel 01793 411500 Fax 01793 411501

www.nerc.ac.uk

Website www.bgs.ac.uk

Shop online at www.geologyshop.com

Foreword

This report describes the construction of a revised structural elements map for the Faroe-Shetland Basin (FSB) and adjacent areas by the British Geological Survey and Jarđfeingi, on behalf of the Faroe-Shetland Consortium (FSC). The revised map builds on the structural elements map of Ritchie et al. (2011) which was based primarily upon maps published in peer reviewed journals and books and further constrained by several commercial seismic profiles. The primary purpose of that map was to geographically delineate the main structural elements of the FSB for description in the published research report. However, recent work has highlighted some contrasting structural interpretations compared to the Ritchie et al. (2011) structural elements map and this study has addressed some of these issues. The revised map is based upon new seismic and potential field interpretations, using the extensive FSC seismic database with a particular focus upon the Corona High, Flett High and Erlend High areas. The revised map also incorporates some revisions on the basis of results from recent FSC projects and publications.

Acknowledgements

This report was commissioned by the BGS / Jarđfeingi / Faroe-Shetland Consortium, which includes the following oil companies: Centrica Energy Upstream, Chevron UK Limited, ConocoPhillips (UK) Ltd, Dana Petroleum Plc, DONG Energy, E.ON Ruhrgas UK North Sea Ltd, Faroe Petroleum, Nexen Petroleum UK Ltd, A/S Norske Shell, Statoil UK Ltd and TOTAL E&P UK Ltd. The participation and funding support of all these companies is gratefully acknowledged. Thanks also go to Michael Larsen of DONG for his insights into the geology adjacent to the Erlend High.

Responsibilities of individual authors during the production of the report have been as follows:

M F Quinn	Seismic interpretation and map compilation; report writing.
H Johnson	Project and Task management, significant contribution to the understanding and development of the FSB and map compilation; report editing.
G S Kimbell	Significant contribution to understanding and development of the FSB based primarily on interpretation of gravity and magnetic data. Input to ArcGis map development.
K Smith	Significant contribution to understanding and development of the FSB.
Ó Eidesgaard	General contribution to understanding and development of the FSB and map compilation.

We thank Faroe-Shetland Consortium oil company sponsors for allowing us to access their proprietary seismic data for the purpose of this report. In addition, BP is acknowledged for permission to use their seismic data. Jarđfeingi is thanked for release of geophysical data in the Faroese sector used in gravity and magnetic displays.

Common Data Access (CDA) Limited is acknowledged for allowing access to released well data for the purpose of this report. Well locations are based on information provided by DECC (the Department of Energy and Climate Change), which is available online at https://www.gov.uk/oil-and-gas-offshore-maps-and-gis-shapefiles.

The GSHHS /World Vector Shoreline used in this report is courtesy of National Geophysical Data Center (NGDC)/US Geological Survey (Wessel/Smith).

In compiling this report, the authors readily acknowledge the assistance of several BGS colleagues, including A F Henderson for technical support and drafting assistance, Craig Woodward for drafting assistance and Jennifer Bow and Diego Diaz Doce for guidance and assistance in building the GIS project. Derek Ritchie and Heri Ziska are acknowledged for review of this report.

Contents

FIGURES

Summary

This report details the rationale, methodology and results of a study in which we have carried out a revision of the structural elements of the Faroe Shetland Basin (FSB) (Figure 1), as defined in Ritchie et al. (2011) (Figure 2). The revision has involved a number of tasks including:

1. **Seismic interpretation** - carried out based upon the Faroe-Shetland Consortium (FSC) dataset (Figure 3) and was largely focused on three areas; the Corona High, the Flett High and the Erlend High (revised Erlend High interpretation subsequently redacted). These areas were specifically addressed because of known uncertainties and recent conflicting interpretations with respect to the structural summary map of Ritchie et al. (2011) (Figure 2). Results from the new interpretations have significantly changed the definition of these structures and provided new insights into their formation and the development of the FSB as a whole;
    a. **Corona High**
        a. More detailed mapping of faults has revealed a series of NE- to NNE-trending tilted fault blocks that dip to the NW; the majority of the significant faults on the Corona High throw to the SE;
        b. An area in the hanging wall of the SE-bounding faults of the Corona High has been informally named the Flett Terrace and is thought to comprise an inverted Cretaceous succession;
        c. Newly mapped Two-Way-Travel-Time (TWTT) to top crystalline basement reveals marked changes in its depth and orientation along the Corona High. The new mapping forms the basis for the informal naming of the North Corona High.

    b. **Flett High**
        a. FSC potential field and seismic data interpreted for this project show that the location and morphology of the Flett High, as defined in Ritchie et al. (2011), is only partly supported;
        b. The new interpretation of the Flett High suggests that it can be considered to be a NE-trending faulted and folded high comprising a succession of Mesozoic sediments intruded with Paleogene igneous sills;
        c. Crystalline basement may be present within the structure, but at a greater depth than previously supposed;
        d. The Flett High is interpreted to have been initiated as a fault block during Early Cretaceous rifting and subsequently subjected to Late Cretaceous/ early Paleocene compression tightening the structure to form the informally named Flett High Anticline and adjacent Foula Syncline;
        e. To the SW, in Blocks 205/09 & 10, the Flett High may have been influenced by Paleogene volcanic activity;
        f. The Flett High may mark the line of a NE-trending deep fault.

    c. **Erlend High**
        a. This section, largely based upon key 2D seismic data subsequently withdrawn from this project, has been redacted. Please refer to Larsen et al. (2010) for a regional overview.

The new interpretations have been integrated with the existing structural elements map of Ritchie et al. (2011).

2. **Review of rift-oblique lineaments** - The locations and extents of rift-oblique lineaments, already stored in the GIS, are also reviewed in this report. Ritchie et al. (2011) show nine

named NW-trending lineaments on their structural elements map plus the Wyville Thomson Lineament Complex (Figure 2), with mapped locations that are slightly modified from the transfer zones identified by Rumph et al. (1993). Ritchie et al. (2011) used the location of some of the lineaments to define the boundaries of the majority of their sub-basins in the FSB. Our new interpretations do not provide any definitive new evidence for the presence of these possible deep features and the lineaments are not included on the revised map.

3. **Review of Igneous Centres** - The current location and dimensions of igneous centres within the FSB is taken from the FSC Magnetic Signatures report (Kimbell, 2014). The limits of the Paleogene basalt and major volcanic escarpments are reproduced with slight modification from Ritchie et al. (2011).

4. **Review of additional features** - The location of the continent-ocean transition is taken from Kimbell (2014).

5. **Review of fold axes** - We have re-evaluated the locations of anticlinal axes from both externally published sources, from interpretations in recent FSC reports (e.g. Kimbell, 2014) and on the basis of FSC seismic mapping (e.g. Johnson et al., 2012). Additional axes, including two synclinal axes, have been mapped on the basis of seismic interpretation carried out in this study. A GIS database of the locations of the rationalised fold axes is stored in the project GIS **Fold_axes shapefile** resulting from this study. Where possible, the rationalised fold axes include a generalised age assignment from published literature and FSC reports.

6. The revised structural elements map of the Faroe-Shetland Basin resulting from this study is presented in GIS and hardcopy formats.

1 Introduction

1.1 RATIONALE AND BACKGROUND

This report describes a project to revise the structural elements map of the Faroe-Shetland Basin (FSB). The revised map is presented in a similar format to that shown in Ritchie et al. (2011) and shows the present day configuration of basins and highs, volcanic features and fold-axes (Figure 1; Figure 2). It was decided not to attribute the revised structural elements map with information on the ages of the sedimentary and volcanic successions similar to that shown in the Norwegian offshore area (Blystad et al., 1995) but to retain the relatively simple approach adopted by Ritchie et al. (2011). We hope that the revised map will ultimately inform a subsequent FSC study that will involve the preparation of a set of maps displaying stratigraphic distribution in a series of time slices from the Jurassic, Cretaceous, Paleocene and Eocene (scheduled to be compiled during 2014-2015).

The size and complexity of the FSB area, coupled with seismic imaging constraints due to thick lava and igneous intrusions and the geographical bias of well penetrations, result in considerable uncertainty of interpretation across the basin as a whole and precludes a systematic mapping exercise within the time and resources available to this project. Instead a focused approach was adopted, identifying specific areas where there are significant discrepancies between recent FSC gravity modelling and the structural elements shown in Ritchie et al. (2011).

The revision of the structural elements map of Ritchie et al. (2011) was guided by the FSC Steering Committee and involved:

- New focused seismic interpretations;
- Review and rationalisation of rift oblique lineaments and published anticlinal axes;
- Review of igneous centres and the Continent-Ocean Transition within the study area.

The new interpretations utilised the FSC seismic and released well datasets (Figure 3) and potential field information. Where the new seismic interpretations have been carried out, they have resulted in significant changes in the configuration of basins and highs; the new interpretations have been integrated with the existing structure map of Ritchie et al. (2011).

We have largely focused our seismic interpretation over three areas, the Corona, Flett and Erlend highs for the following reasons:

- The Corona High comprises a number of NE-trending crystalline basement cored faulted blocks onlapped and covered by late Jurassic, Cretaceous and Cenozoic sediments with a Paleogene basalt succession in some parts (and pervasive sill intrusions adjacent to the basement blocks). 3D gravity modelling (Kimbell et al., 2010) picks out the structure but extends beyond the seismically mapped boundary shown in Ritchie et al. (2011). In addition, the magnetic response shows a marked variation in intensity along its length. A new examination of the area, utilising the extensive seismic and well database, was carried out to try and resolve the mismatch between the 3D gravity modelling results compared to the limits of the High shown in Ritchie et al. (2011);
- The Flett High was also chosen as a focus for re-examination due to a mismatch between the 3D gravity modelling and the structure shown in Ritchie et al. (2011). The Flett High is described as a NE-trending segmented, deeply buried basement faulted block (Ritchie et al., 2011). However, along much of its length, 3D gravity modelling shows crystalline basement at a greater depth than the surrounding area;

- The Erlend High is described as a heavily intruded, fault-bounded basement terrace by Ritchie et al. (2011). However, Paleogene basalt and intrusive rocks associated with the Erlend and West Erlend Igneous Centres largely obscure Cretaceous and older rocks associated with the high. Recent mapping, using re-processed 2D data, has better defined these Cretaceous and older successions (Larsen et al., 2010), and this prompted a review of the Erlend High and adjacent area (revised Erlend High interpretation subsequently redacted).

In all three areas, an attempt was made to interpret a top crystalline basement seismic reflector, tied to a limited number of commercial wells that penetrated to crystalline basement level; this enabled the mapping of the main faulted basement blocks. Seismic reflectors representing Base Cretaceous, Top Lower Cretaceous and Top Upper Cretaceous were also interpreted where possible to help further define the basement blocks and associated basins. Interpretations of seismic reflectors for the Paleocene report (Smith et al., 2013) were utilised or extended to aid in the structural mapping of the three areas. The new interpretations are illustrated on geoseismic panels that are included in this report and whose locations are shown on Figure 4. Results from the new seismic interpretations were used to update the structure map of Ritchie et al. (2011) forming a revised framework of basement highs and basins in these areas.

The hardcopy structural elements map produced as part of this project has been constructed in ESRI ArcGis and supplied to FSC sponsors in Version 10.0. A set of attributed structural shapefiles, that together show the new structure, have been provided to partners as follows:

1. A set of polygons defining limits of basins and basement highs, igneous centres and the continent-ocean transition;
2. A set of attributed faults;
3. The limits of lava and main lava escarpments;
4. A set of mainly Late Cretaceous/ Cenozoic, fold axes.

1.2 DATA SOURCES

The revised structural elements map resulting from this study seeks to build on that of Ritchie et al. (2011) (Figure 2) in the light of more recent work that investigates known problem areas, new data and insights from recent FSC publications and external peer reviewed work from UK, Faroese and Norwegian parts of the Atlantic margin.

The Faroe-Shetland Consortium (FSC) seismic database utilised by this project, includes several 3D surveys and a regional grid of 2D lines (Figure 3). The location of seismic profiles to illustrate aspects of the structural interpretation is shown together with all well locations (including non-released wells that were not used in this project) in Figure 4; those wells referred to in this report are labelled. Unfortunately, we were unable to obtain permission to show some of the 2D seismic profiles interpreted in this study, particularly over the Erlend High, and any figures illustrating or utilising these profiles have been redacted.

Since the publication of Ritchie et al. (2011), several studies have been undertaken by the FSC, utilising extensive seismic, well and biostratigraphic databases. These studies provide new information and have extended our understanding of the Cretaceous, early Paleogene and Eocene (Stoker et al., 2010; Stoker et al., 2012; Smith et al., 2013; Smith et al., 2014). In addition, the production of structural TWTT maps of seismic reflectors within the Paleogene and Neogene (Johnson et al., 2012) and interpretation and modelling of potential field data (Kimbell et al., 2010) have underpinned this current project. Peer reviewed papers such as Larsen et al. (2010) and Ólavsdóttir et al. (2013) also add to our view of the FSB and adjacent areas and were not considered in the structural map compilation of Ritchie et al. (2011). Publications from the Norwegian sector (Blystad et al., 1995) have aided our structural interpretations, especially where they report potentially analogous structures (e.g. Osmundsen and Ebbing, 2008; Brekke, 2000).

2 Structural elements

2.1 STRUCTURAL HIGHS

In the study area, structural highs are generally elongated NE-trending, usually, but not exclusively basement cored, structures. For instance, the Corona, Rona and Erlend highs are crystalline basement cored highs, proven by well penetration, where the crystalline basement rocks are commonly overlain by Devono-Carboniferous, Permo-Triassic, Jurassic, Cretaceous and Cenozoic sedimentary strata. Jurassic and Lower Cretaceous rocks appear to onlap and then cover the highs and are succeeded by thick successions of Upper Cretaceous, Paleogene and Neogene sedimentary and volcanic rocks. However, where thick Paleogene basalt obscures the structure and succession beneath, and well information is sparse or absent, the nature of designated highs is equivocal. We follow Ritchie et al. (2011) in showing top Paleogene basalt defining the Munkagrunnur, Iceland Faroe and Wyville Thomson ridges, the Faroe Bank High and Faroe Platform. Some structural highs, such as Munkagrunnur and Wyville Thomson are commonly referred to as Ridges usually because they have bathymetric expression or for historical reasons. Platform areas that occur inboard of the buried highs are relatively stable blocks that form part of the continental land mass and tend to be covered with a thin, incomplete or condensed succession of younger rocks which are largely undeformed. These Platform areas, such as the East Shetland High, are also depicted on the map as structural highs.

The new structural interpretations over parts of the Corona, Flett and Erlend highs (revised Erlend High interpretation subsequently redacted) and adjacent areas have resulted in changes to these structures when compared to Ritchie et al. (2011) and resolved some of the mismatches between seismic mapping and 3D gravity modelling; top crystalline basement maps in TWTT have been produced for the Corona and Erlend high areas (revised Erlend High interpretation subsequently redacted). The re-mapped Corona and Flett highs have been integrated with the existing structural map of Ritchie et al. (2011) and their relationship within the regional structure is discussed. The interpretation process has improved our understanding in terms of the location, trend and style of faults in the three areas and helped redefine their boundaries. It should be noted that Kimbell (2014) interpreted a number of magnetic lineaments (e.g. his figure 14), postulated to be faults but was unable to verify this from seismic data because of poor resolution due to the presence of basalt.

2.2 NEW INTERPRETATIONS

2.2.1 The Corona High

Background **-** The Corona High was selected as an area for new interpretation because of a mismatch between depth to top crystalline basement, calculated from 3D gravity modelling (Kimbell et al., 2010) and the structural elements map compiled by Ritchie et al. (2011). Depth to crystalline basement derived from the 3D gravity model of Kimbell et al. (2010) shows shallow basement in front of the faults that define the SE limit of the Corona High as shown Ritchie et al. (2011) (Figure 5). Specifically, mismatches occur in the northern part of the High over Blocks 214/17, 18, 19, 21 and 22 and Block 214/10 and in the southern part over Blocks 205/02, 03 and 04 (Figure 5). It would be expected that basement would be at a deeper level in the hanging wall, SE of the Corona High, compared to that penetrated on the Corona High itself.

The Corona High is described by Ritchie et al. (2011) as an elongate, NE-trending intrabasinal fault block approximately 200 km long and up to 30 km wide (Figure 2; Figure 5). Ritchie et al. (2011) defined both NW- and SE-dipping north-east trending normal faults bounding the Corona High and this interpretation has been followed in recent publications (e.g. Larsen et al., 2010). However, Ritchie et al. (2011) also noted that several authors preferred to interpret the NW margin of the Corona High essentially as a ramp or fault-block dip slope (e.g. Dean et al., 1999).

Located on the Corona High, released wells 213/23- 1, 214/09- 1 and 204/10- 1 provide evidence that the High is cored by crystalline basement rocks. Although the basement in these wells was not considered by Ritchie et al. (2011), company reports describe the cores as comprising Lewisian gneiss. Well 213/23- 1 proved 1.5 m of crystalline basement unconformably overlain by 576 m of Devonian and Carboniferous sediments and 177 m of possible Triassic rocks. A faulted boundary separates the Triassic succession from a thin (19.5m) Lower Cretaceous claystone, 466 m of Upper Cretaceous and 1855 m of younger sediments (Figure 6). Well 214/09- 1 to the northeast, proved 12.2 m of crystalline basement unconformably overlain by an undated succession comprising 73.1 m of gneissic conglomerate, claystone and sandstone, which is in turn overlain by 64 m of Upper Jurassic Kimmeridge Clay Formation and 122 m of Lower Cretaceous strata. These are succeeded by 503 m of Upper Cretaceous and 2393 m of younger Cenozoic sediments (Figure 7).

Released well 204/10- 1, located at the SW end of the Corona High, reached total depth in crystalline basement comprising an acid igneous granodiorite (Ritchie et al., 2011).

Dataset **-** The new seismic interpretation over the Corona High utilised two 3D seismic datasets covering the central part of the High around well 213/23- 1 and a grid of 2D seismic profiles with variable spacing (Figure 3). Observations from 3D gravity modelling (Kimbell et al., 2010; Figure 5; Figure 10) and the reduced to pole magnetic response (Figure 12) were also utilised. Around the NE part of the Corona High, 2D seismic profiles have a separation of approximately 3 km between NW-trending profiles and a minimum of 8 km between NE-trending profiles. Elsewhere, over the Corona High, spacing varies from a maximum of 20 km to a minimum of 3 km. Key released commercial wells 213/23- 1, Rosebank wells 213/27- 1 and 2, and 214/09- 1, located in the northeastern part Corona High, were utilised to identify seismic horizons (Figure 4).

Interpretation **-** Seismic interpretation primarily focused on mapping the top crystalline basement with associated fault displacements, however where possible, other seismic horizons were interpreted, specifically Base and Top Cretaceous (Figure 6). Although seismic reflector relationships around and over the Corona High are difficult to resolve with any certainty, seismic interpretation, tied with limited the well penetrations described above, suggests that a Jurassic and Cretaceous succession is present on the dip slopes of the fault blocks that comprise the Corona High and that higher parts of the Upper Cretaceous succession pass over the top of the high (Figure 6). The Jurassic succession may be absent up-dip, for instance in well 213/23- 1 (Figure 6), but appears to thicken down-dip and is also present in Rosebank discovery wells 213/27- 1 and 2 and well 214/09- 1 to the north. Sills are common adjacent to the Corona High, especially within the Upper Cretaceous and lower part of the Paleocene successions (Trude, 2004). Seismic reflections beneath and close to these Paleogene igneous intrusions are obscured and disrupted, thus mapping sills and understanding their relationships with surrounding rock successions and how they affect the seismic response helped in the overall interpretation; some sills were interpreted where this would aid in the mapping of the Corona High structure. Sills are recognised in the seismic data by a very strong amplitude response, due to their high impedance value compared to the surrounding country rock (Smallwood and Maresh, 2002) and their structural relationships with the rock successions into which they have been intruded; to be seen on seismic profiles, sills must have a thickness greater than between 10 to 15 m (Smallwood and Maresh, 2002). Sills may be intruded along bedding planes and thus be concordant with the general dip of the country rock; the near top of the Upper Cretaceous is often marked by sill intrusion **(**Figure 7; Figure 8). Sills can often be distinguished from other high amplitude events by following them to their culminations where they often form a dyke that cuts through the rock succession sometimes ending in some form of hydrothermal vent (Planke et al., 2005). Sills may also be discordant and cut across bedding planes forming saucer shape profiles. The limbs of saucers sometimes connect to a higher saucer forming a climbing set of sills (Trude, 2004; Møller Hansen and Cartwright, 2006). In 3D volumes, time slices that cut across sills often show curving, oval semi-circular events, and sills mapped in 3D often show lobate architecture.

The new interpretation presented in this study has generated a more detailed view of the structural configuration of the Corona High compared to Ritchie et al. (2011) and images a series of generally south-easterly dipping faults (Figure 9). The mapped location of the newly interpreted faults, constrained by wells drilled on the Corona High (e.g. Figure 6), enlarges the extent of the mismatch between top basement from gravity modelling and that based on seismic interpretation carried out for this project (Figure 10; Kimbell et al., 2010). The new interpretation depicts three major NE-trending *en echelon* faults that define the southeastern flanks of the significant Cambo and Rosebank discoveries and the Eriboll and (unreleased) North Uist exploration wells located on tilted fault block culminations along the Corona High (Figure 9). Depth to top of crystalline basement, based on interpreted TWTT and two well penetrations, is quite variable along the length of the Corona High (Figure 11). For instance, at the SW end of the Corona High, around the Cambo discovery, top crystalline basement is interpreted at around 4 seconds TWTT rising to around 2.0 seconds at its shallowest point in the Rosebank area. At well 213/23- 1, top basement is recorded at a TWTT of 4.162 seconds (4308.6 m). Continuing in a north-easterly direction, at the location drilled by the currently unreleased well, 213/25c- 1, 1Z, (North Uist prospect) top basement is interpreted at around 5 seconds TWTT. Only 3 km NE beyond this well there is a marked northeastward change in the residual magnetic field (reduced-to-pole), from high to low response (Figure 12). This change in the magnetic response was utilised by Rumph et al. (1993) to map the NW-trending Clair Lineament at this location (Figure 11; Figure 12) and may mark increasing depth of crystalline basement (thus lowering observed magnetic response). Makris et al. (2009) interpreted long offset seismic data and generated a 3D model over the part of the Corona High close to where the reduction in magnetic response occurs and showed an E-W oriented ridge at top of the crystalline basement at around 5 km increasing to around 9 km to the east (Figure 11). Makris et al. (2009) noted that the ridge marked the separation between the Corona Sub-basin to the north and the Faroe-Shetland Basin to the south. Immediately north of the E-W trending ridge defined by Makris et al. (2009), interpretation of seismic profiles shows depth to basement increasing to more than 6 seconds (Figure 11). We interpret this mapped basement low, also with an E-W trend, as separating the main Corona High from a northerly extension comprising a buried NNE-trending basement block drilled by well 214/09- 1 where top basement was encountered at 4.768 seconds TWTT (Figure 10; Figure 11). This northerly extension of the Corona High has been informally named by Loizou et al. (2006) as the North Corona Ridge and we follow their naming here. However, we follow Ritchie et al. (2011) by designating it a High as opposed to a Ridge and referring to the area north of the mapped shallow basement as the North Corona High (Figure 9). It is worth noting the change in orientation from the NE trend of the main Corona High, veering to a more northerly NNE trend over the North Corona High (Loizou et al., 2006 their figure 1; Figure 9); this mirrors the more northerly trends of the faults on the opposite side of the Faroe-Shetland Basin, to the SW of the Erlend High (***see section 2.2.4***), thought to be controlled by the Walls Boundary Fault and possibly the older NW-SE 'Tornquist' trend (Larson et al., 2010; Figure 1).

The most easterly of the three *en echelon* faults is informally named here as the SE Corona Fault and has the Eriboll and North Uist discoveries located on its footwall. It is 60 km in length, and is interpreted as marking the south-easternmost boundary of the Corona High (Figure 9; e.g. Figure 13). The SE Corona Fault may be a composite of two *en echelon* faults linked by a step-over similar to the progressive linkage of faults described by Larsen et al. (2010) in the Erlend area. It is interpreted to extend from the northern part of Block 213/28 for 22 km before veering to a more EW trend through Blocks 213/25 and 214/21 for approximately 17 km (the 'step-over') before returning to a NE orientation and tipping out in the northern part of Block 214/19 to the south of the NE Corona High (Figure 9). The location of the E-W trend in the SE Corona Fault appears to correspond to the E-W cross-trend in shallow basement mapped by Makris et al. (2009) and E-W trend of the basement low that separates the Corona and North Corona highs (Figure 11).

2.2.2 The Flett Terrace

Loizou et al. (2006) informally named an area of downfaulted crystalline basement between the Corona High and the Flett Sub-basin as the Flett Terrace. We adopt this informal nomenclature and broadly concur with Loizou et al. (2006) in terms of the limits of the Terrace (Figure 9). Furthermore, we interpret much of this area as an inverted part of the Flett Sub-basin. Seismic interpretation of the depth to top basement across the Flett Terrace remains difficult but it is interpreted to be much deeper than that predicted by 3D gravity modelling (Figure 8; Figure 10). Modelling (Kimbell et al., 2010) suggests basement occurs at depths of less than 5 km (around 4 to 4.5 seconds TWTT on Figure 8) whereas the new interpretation has top crystalline basement at around 6 to 6.5 seconds TWTT (Figure 8).

Within the Foula Sub-basin, between the Rona High and Flett High, a thick Cretaceous succession is penetrated by wells and can be interpreted on seismic profiles. For example, well 206/03- 1 in the Foula Sub-basin proved 1492 m of Cretaceous sediments before reaching TD in the Lower Cretaceous Aptian (Figure 14; Stoker et al., 2010, Fig. 2.7; Dean et al., 1999). The Top Cretaceous is fairly well constrained and this and the Top Lower Cretaceous seismic reflector are seen to continue down into the Flett Sub-basin to approximately 4.7 seconds and 5.7 seconds TWTT, respectively (Figure 14; Stoker et al., 2010 their Figure 2.7). The base Cretaceous seismic reflector cannot be traced with any certainty to the NW beyond the Flett High but with reference to the TWTT interpretation of Top and Base Upper Cretaceous, it may now lie at more than 6.0 seconds TWTT within some parts of the Flett Sub-basin (Figure 14); ConocoPhillips show Base Cretaceous at more than 7.0 seconds TWTT (ConocoPhillips UKCS Licence P799; their geo-seismic section). Adjacent to the Corona High, in the hanging wall of the informally named SE Corona Fault, there is a marked angular unconformity at early Paleocene/ Top Cretaceous level and this succession lies at a shallower level than the equivalent succession in the adjacent Flett Sub-basin; truncation of seismic reflectors indicates at least 0.5 secs of missing section (Figure 13; Figure 14). This relationship could be due to relative subsidence of the Flett Sub-basin during the early Paleocene or relative uplift and inversion of the succession adjacent to the Corona High. Our favoured interpretation is that in the area where 3D modelling of depth to basement (Kimbell et al., 2010) indicated shallow depth to basement in the hanging wall of the SE Corona Fault (Figure 10), an uplifted and inverted thick Cretaceous and older sedimentary succession is present (Figure 13). A TWTT map of the Top Cretaceous in the hanging wall of the SE Corona Fault clearly shows a NE-trending anticlinal surface that veers to a more ENE trend in front of the step-over or dog-leg of the Fault (Figure 15). The topography is most pronounced at this location and here the mapped surface comprises a composite of the Upper Cretaceous, intra-Vaila and intra-Flett unconformities (Figure 13). A seismic profile across the structure, flattened on the intra-Vaila Unconformity reinforces the marked unconformity between the Cretaceous and Paleogene at this location (Figure 16).

As stated above, we interpret much of the Flett Terrace as an inverted part of the Flett Sub-basin. An inverted and uplifted Cretaceous succession, located in the hanging wall of the SE Corona Fault, would be expected to have a higher density than normally compacted sediments and this might provide an explanation for the anomalous 3D gravity modelling results recorded in this area. Two-dimensional potential field modelling was carried out across the Flett Terrace to validate the 3D gravity modelling results and examine their implications for the magnetic responses across this structure. A 2D model, constructed from a section through the 3D model and attributed with similar densities, does replicate the observed gravity signature reasonably well (Figure 17; Figure 4 and Figure 5 for location). However, there is a marked difference between the observed and calculated magnetic field if the apparent broad basement high is assumed to have a uniformly high magnetic susceptibility (Figure 17). This difference between the observed and calculated magnetic response corresponds to the interpreted position of one of the NE-trending faults mapped in the area and suggests that the rocks in the hanging wall of the fault are non-magnetic. However, assigning them the normal density (compaction) trend assumed for the sedimentary sequence generates a substantial (>10 mGal) gravity mismatch, so

the conclusion is that these rocks have a relatively high density and low magnetisation (Figure 17). An inverted (overcompacted) Cretaceous succession would be expected to have this combination of properties, but a large thickness of material would have had to be eroded from it for the density to approach that of the basement, as indicated in the model. The alternative form for the top of the magnetic basement includes features that could be deep expressions, around 8 and 9 km below mean sea level of the Flett Terrace and Flett High respectively (Figure 18; Figure 4 and Figure 5 for location); in Figures 13 and 14 top basement on the Flett Terrace and Flett High are shown 6 and around 7 seconds TWTT respectively. Since the modelling was carried out, South Uist exploration well 214/21a- 2 has been released and associated density and sonic transit times are now available (Figure 19); the well lies 34.5 km to the NE of the model line. A plot of density against depth that also marks the depths of the Sullom, intra-Vaila and intra-Flett unconformities, shows that the densities sit significantly above the shale compaction curve of Sclater and Christie (1980). Although there is some variation of the densities over the interval marked by the early Paleocene unconformities it is difficult to discern a marked difference in density here and in the overlying Eocene succession (Figure 19). In addition, other wells in the area (e.g. 214/17- 1 and 214/19- 1) have sedimentary densities that sit above the shale compaction curve (Kimbell et al., 2010) so densities from the South Uist well are not unique in this regard. The plot of velocity against depth shows generally higher velocity values through the Upper Cretaceous and early Paleocene and a large drop at the start of the Eocene before they increase to sit on the shale compaction curve. In the Upper Cretaceous, velocity values are significantly higher than the Eocene (Figure 19). Although seismic interpretation shows significant unconformities at Top Cretaceous/ early Paleocene level we cannot show that the higher densities recorded in well 214/21a- 2 are attributable to deeper burial followed by uplift and erosion. In conclusion, although the density and velocity profiles recorded in well 214/21a- 2 do not counter our suggestion that the Flett Terrace comprises a thick uplifted Cretaceous succession, they are not unequivocal evidence for substantial uplift. It is possible that the succession is at maximum depth of burial at the present day and any anomalous densities/ velocities have been overprinted by subsequent burial. The reason(s) for the anomalous gravity field SE of the Corona High is still uncertain, with possible explanations being the presence of a high density of sills, secondary processes which have modified the rock densities in this area or a metasedimentary succession which may include pre-Cretaceous units (e.g. Neoproterozoic strata coeval with the Torridonian).

Smith et al. (2013) suggest that the intra-Vaila unconformity marks an important change in the structural configuration of the FSB and postulated an associated phase of local inversion. One such area of inversion is interpreted to lie on the Flett Terrace immediately south-east of the dog-leg in the SE Corona Fault (Figure 13; Figure 15). Considering this location, a likely mechanism by which this structure formed would be uplift associated with this restraining bend on the SE Corona Fault.

The NNE-trending basement horst, drilled by well 214/09- 1, forming part of the North Corona High has modelled depth to basement at a shallow level in the hanging wall of the SE bounding fault, the same as that in the hanging wall of the SE-Corona Fault (Figure 10). Seismic data images a high concentration of sills at this location and it is speculated that this might explain the high gravity response (Figure 7)**.**

2.2.3 The Flett High

Background - The Flett 'Ridge' was first described in the late eighties where two papers in the 3rd 'Barbican' Conference show the structure as a NE-trending tilted basement block with a SE-dipping bounding fault (Mudge and Rashid, 1987; Duindam and van Hoorn, 1987). In the same volume, Hitchen and Ritchie (1987), describe the structure as a 'constituent part of an intrusive sill complex' also with a generally NE trend. Roberts et al. (1999), Dean et al. (1999), Lamers and Carmichael (1999) and Grant et al. (1999) all show the Flett High as a NE-trending basement cored high; Dean et al. (1999) show the structure offset for the first time. However,

Ashcroft et al. (1999) noted that the interpretation of the Flett High as a basement cored structure could not be reconciled with the gravity data (see below).

The depiction of the Flett High in Ritchie et al. (2011) (Figure 2) is based on that shown in Dean et al. (1999) and its description summarises published studies from different locations along its length (e.g. Robinson et al., 2004; Lamers and Carmichael, 1999). Ritchie et al. (2011) describe the Flett High as a narrow NE-trending, segmented, deeply buried horst block that is interpreted to be sinistrally offset by the Grimur Kamban Lineament (Keser Neish, 2004; Figure 2; Figure 5). South-west of the offset, the Flett High is described by Robinson et al. (2004) who record its influence on structuration and sedimentation of Paleocene and younger rocks (Figure 20**)**. Robinson et al. (2004) suggest a volcanic origin for the Flett 'Ridge' at this location (see also Smallwood et al., 2004 and Smallwood and Maresh, 2002). North-eastwards, the effect of the high on the Paleocene succession diminishes and the Upper Cretaceous and overlying successions appear relatively unaffected by the deeper buried high (Figure 21; Figure 22). Here, Ritchie et al. (2011) are guided by Lamers and Carmichael (1999), in depicting the Flett High as a basement horst block, capped by a Devonian to Cretaceous succession that formed during Early to Late Cretaceous extensional movements on northern and southern flanking faults. However, Ashcroft et al. (1999) carried out two-dimensional gravity modelling along a regional seismic profile across the NE Flett High (Ritchie et al., 2011). On the basis of the gravity modelling, Ashcroft et al. (1999) suggested that the Flett High has a cap of pre-Cretaceous sediment about 2 km thick resting on basement. This interpretation is supported by Kimbell et al. (2010) whose modelled depth to top crystalline basement show the axis of the Flett High, as depicted by Ritchie et al. (2011), to be where basement is at its deepest in the Flett and Foula sub-basins (Figure 5). This mismatch between the existing interpretation of the Flett High as a basement cored high and potential field modelling showing only minimal elevation of basement coupled with apparently different interpretations of the Flett High along its length, prompted a review of available seismic data over the area.

The Foula Sub-basin was defined by Ritchie et al. (2011) as a NW-dipping half-graben bounded to the NW by the Flett High whose SE faulted boundary formed the master fault for the half-graben. The NE and SW boundaries of the Sub-basin were defined by the locations of the Victory and Corona lineaments respectively. The new interpretation of the Flett High, described below, has resulted in the NE boundary of the Foula Sub-basin being re-defined (Figure 1; Figure 2).

Dataset – North-east of the sinistral offset associated with the postulated location of the Grimur Kamban Lineament, the Flett High, as described by Ritchie et al. (2011), has complete coverage from a combined set of 3D seismic surveys as well as a variably spaced grid of 2D seismic profiles. However, over much of the Flett High south-west of the offset, interpretation relied on a small number of NW-trending 2D profiles (Figure 3). Seismic profiles published in Robinson et al. (2004) and Smallwood et al. (2004) aided in our interpretation of the Flett High in this area. A large number of commercial wells are situated over the Flett High of Ritchie et al. (2011) however the majority reach TD in early Paleocene or the Upper Cretaceous. Key wells used in this interpretation are 206/04- 1 (recorded Lower Cretaceous on crystalline basement at TD), 206/05- 1 (recorded Lower Cretaceous on Upper Jurassic reaching TD in undifferentiated ?Middle Jurassic), 206/05- 2 (recorded Lower Cretaceous on Lower Jurassic reaching TD in the Triassic), 206/03- 1 and 214/29- 1 (recorded Lower Cretaceous at TD) (for location see Figure 4).

Interpretation **–** Seismic reflectors over the Flett High are often discontinuous and poorly resolved and as a consequence seismic interpretation was equivocal. However, the overall trend and limits of the high could be interpreted and the approximate location of the crest of the high mapped; this feature is shown as a linear polygon on the revised map (Figure 1**;** Figure 9). Interpretation of the Flett High began where it is best seismically imaged (Figure 21; Figure 22), in the area adjacent to a marked Cretaceous synclinal depocentre in blocks 206/01, 206/02,

206/03 and 206/06 that we informally name here the Foula Syncline (Figure 21; ***section 2.2.3.1***). We then proceeded to examine any evidence for the high extending northeastwards (***section 2.2.3.2***; see Figure 4 for location) and then considered a continuation of the high to the southwest (***section 2.2.3.3***; see Figure 4 for location).

2.2.3.1 FLETT HIGH, ADJACENT TO THE FOULA SYNCLINE

At this location, the Flett High is recognised on seismic profiles by a series of high amplitude reflections within the Lower Cretaceous and older succession that rise up from the deep Flett Sub-basin, culminate and then either terminate or descend again into the Foula Sub-basin in front of the Rona High (Figure 21; Figure 22). Nearby well 206/04- 1, located on the flanks of the Rona High, penetrated a 639 m Lower Cretaceous sedimentary succession, including 82 m of Lower Cretaceous Royal Sovereign Fm. conglomerate resting on crystalline basement (see Figures 9 and 10 for location), while to the NE, wells 206/05- 1 and 206/05- 2 record successions of Early to Late Jurassic sediments 1054 m and 339 m thick, respectively (Figure 23). These wells and others (206/03- 1 and 214/29- 1) on and adjacent to the NW flank of the Rona High provide good ties to seismic reflectors that can be traced into the Foula Sub-basin and enable the depocentre to be interpreted as a thick succession of Cretaceous and Jurassic sediments (Figure 21; Figure 22). We interpret many of the high amplitude seismic reflections rising from the Flett Sub-basin as sills whereas others, especially within the Lower Cretaceous succession in the Foula Syncline within the Foula Sub-basin, are considered to represent sandstone or limestone units within the mudstone dominated Lower Cretaceous and lower part of Upper Cretaceous successions (e.g. the Commodore Sandstone Formation penetrated in well 206/04- 1).

Seismic interpretation, constrained by the wells 206/05- 1 and 206/05- 2 located on the NW flank of the Rona High, indicates a succession of Jurassic and possibly some Triassic sandstone and shale resting on Palaeozoic and older rocks (Figure 23). To the NE along the Rona High, the Jurassic seismic package appears to be absent and Cretaceous sediments rest directly on pre-Jurassic rocks. Where present, the Jurassic and older succession thins updip onto the flank of the Rona High, and is overlapped by a Lower Cretaceous succession, the latter eventually resting directly on crystalline basement (e.g. well 206/04- 1); downdip, the Jurassic seismic package is interpreted to thicken into the Foula Sub-basin (Figure 22). Locally, particularly high on the flanks of the Rona High, an angular unconformity is observed between the Jurassic and the Lower Cretaceous (Figure 23). From examination of a seismic profile tied to well 206/05- 1, Haszeldine et al. (1987) interpreted the Upper, Middle Jurassic and older sediments within tilted fault blocks separated from pre-Cambrian basement. Haszeldine et al. (1987) interpreted subtle thickness changes in the Jurassic succession and based upon this, coupled with examination of facies in well 206/5- 1, proposed a submarine fan depositional model requiring active faulting along the Rona High during the mid-Jurassic. However, in a contrasting study based upon Jurassic core from wells in the SW part of the Faroe-Shetland Basin, Verstralen et al. (1995) identified a sub-aerial and fan delta facies of Late Jurassic age interpreted to have been deposited over an irregular weathered Lewisianoid basement topography in a subsiding basin setting. Rising sea level eventually covered Lewisianoid source areas, cutting off this source for clastic material and resulted in the deposition of Kimmeridge Clay Formation mudstone. In this study, we observe no convincing evidence of significant thickening or wedge shape geometry within the Jurassic seismic package adjacent to faults close to well 206/05- 1. Locally, we recognise the high-angle seismic events in the Jurassic succession that contrast with the overlying, almost horizontal seismic reflectors within the Lower Cretaceous, and interpret the former as having been faulted and rotated by low angle, NW-dipping, displacements that sole out on the deeper, pre-Triassic, possibly crystalline basement-sedimentary rock interface (Figure 23). The faulting is interpreted to have taken place during Early Cretaceous rifting, prior to onlap of the Cretaceous sediments; the faulted Jurassic sediments are interpreted as a pre-rift succession. The low angle NW-dipping faults are cut by later SE-dipping faults (Figure 23). Stoker et al. (2010) also record the initiation of widespread rifting in the FSB in Aptian-Albian times and on the

Norwegian Atlantic Margin, specifically in the northern Vøring Basin, Early Cretaceous rifting and hyperextension, is interpreted to have taken place (Lundin et al., 2013).

The Cretaceous and Jurassic succession increases in thickness away from the Rona High and is interpreted to be cut by both NW- and SE-dipping relatively high angle faults some of which bound the Flett High (Figure 22). Although seismic evidence is equivocal, we interpret the NW-dipping steeper faults to sole out upon or cut the low angle NW-dipping faults on the Rona High (Figure 22). The SE-dipping faults are considered to be antithetic to the low angle NW-dipping faults; they generally terminate upwards within the Upper Cretaceous (Figure 21; Figure 22) and some are interpreted to displace the NW-dipping faults that they intersect (Figure 23). Further downdip, seismic reflections are poorly resolved, however the Jurassic and older successions do appear conformable with the overlying Lower Cretaceous.

Low angle NW-dipping faults on the flanks of the Rona High progressively down-throw crystalline basement, overlying Palaeozoic and younger rocks into the Foula Sub-basin. The deepest fault, interpreted to separate Palaeozoic and younger rocks from the crystalline basement, is projected to pass beneath the Flett High, an interpretation that places crystalline basement at a depth greater than previously shown (Ritchie et al., 2011 their figures 30 & 31; Figure 21; Figure 22).

A low total magnetic field response marks the location of the Foula Syncline and the associated crest of the Flett High (Figure 12). To the east of the Foula Syncline, the magnetic response increases markedly as it approaches the Rona High. Anomalously higher magnetic values, north of the Foula Syncline, associated with the termination of the crest of the Flett High in Blocks 214/29 and 30 are also observed (Figure 12). The high magnetic response could be an indication of shallow (magnetised) basement at this location (see also Osmundsen and Ebbing, 2008). The change in depth to basement could be explained by a variation in dip along strike of the low angle NW-dipping detachments. A change in dip of the low angle NW-dipping faults along the strike of the Rona High may coincide with the location of the postulated NW-trending rift-oblique Clair lineament (Figure 2; Figure 12; Rumph et al., 1993).

Truncation of seismic reflectors within the Upper Cretaceous seismic package at top Cretaceous level (Figure 22), doming of seismic reflectors within the Upper Cretaceous above the Flett High with complementary synclinal geometry in the adjacent Foula Sub-basin (Figure 21) and onlap of Paleocene seismic reflectors (Figure 22) are interpreted here as evidence for Late Cretaceous/ early Paleocene compression. Stoker et al. (2010), record folding in the Foula Sub-basin during the Cenomanian-Turonian as well as regional exposure, due either to regional uplift and/ or a lowering of eustatic sea level, at the Cretaceous/ Paleogene boundary. Similarly, Lundin et al. (2013) interpret phases of compression in the north Vøring Basin during the Turonian, Campanian and Maastrichtian/ early Paleocene.

The stratigraphic relationships of the Cretaceous and Jurassic sedimentary successions within the Foula Syncline and with respect to the adjacent Rona and Flett highs together with the difficulty in differentiation of sediments from sills (Figure 21; Figure 22) results in considerable uncertainties regarding the nature and timing of Flett High development. However, from our observations of this portion of the high, we postulate the following sequence of events in the formation of the Flett High:

1. The main episode in the formation of the Flett High is interpreted to have taken place during the Early Cretaceous when a succession of Jurassic and older sediments that thickens basinward, was faulted down into the extending Foula Sub-basin on low angle NW-dipping faults (Figure 22); some rotation of the faulted succession could have occurred, analogous to that seen in the Jurassic succession on the flanks of the Rona High (Figure 23);
    - It is possible that some Jurassic rifting occurred within the FSB (Larsen et al., 2010; Dean et al., 1999; Haszeldine et al., 1987), but evidence to date from sedimentary facies and thickness distribution does not suggest deposition

controlled by major active fault scarps (Verstralen et al., 1995); the observed angular unconformity between the Jurassic and Lower Cretaceous sediments described above is interpreted to be the result of Early Cretaceous rifting (see above).

2. The Flett High is interpreted to be bounded by NW- and SE-dipping faults that are steeper than the low angle NW-dipping faults on the western flank of the Rona High (Figure 22). On some seismic profiles, the SE-dipping faults do not appear to propagate significantly above the Top Lower Cretaceous seismic reflector, however, some of the NW-dipping steep faults propagate upwards into the Paleogene section but have larger displacements within the Lower Cretaceous succession (Figure 22). These NW-dipping steeper faults, active in the Lower Cretaceous, are interpreted to have been reactivated in Late Cretaceous to early Paleocene times as the Flett Sub-basin was subjected to extension and subsidence;

3. Doming and truncation of the Top Upper Cretaceous seismic horizons together with accompanying onlap of early Paleocene seismic reflectors (Figure 21; Figure 22) is interpreted to indicate Late Cretaceous or early Paleogene compression and uplift of the Cretaceous depocentre. Such compression may have also tightened the limbs of the Foula Syncline and steepened the bounding faults of the adjacent Flett High forming an anticlinal structure, named informally here as the Flett High Anticline (Figure 21; ***see section 2.7 below***);
    - Supporting evidence for uplift within the Foula Sub-basin is provided in a study by Tassone et al. (2014), on the basis of sonic transit times within Upper Cretaceous shales from the Faroe-Shetland Basin. Tassone et al. (2014) identify Cretaceous successions not at maximum depth of burial and quantified the amounts of net exhumation. Three wells were examined in the Foula Sub-basin, from SW to NE, 206/11- 1, 206/05- 1 and 208/26- 1. All of these wells showed the Cretaceous succession has been uplifted with an increasing net exhumation to the NE of 183 m, 353 m and 411 m, respectively.

The highly localised nature and synclinal deformation of the thick Cretaceous sedimentary succession and the low ratio of the areal dimensions of the Foula Syncline is perhaps suggestive of 'pull-apart' basin architecture and, if this is the case, a transtensional regime during formation of the Flett High and associated depocentre could be postulated. In this interpretation, the Flett High adjacent to the Cretaceous depocentre is considered to comprise a faulted block of Jurassic and older sediments resting on low angle NW-dipping fault(s) that separate these younger sediments from crystalline basement.

2.2.3.2 Flett High, NE of the Foula Syncline

The Flett High could not be recognised on seismic data to the NE of the Foula Syncline (Figure 24) and it is thought that the presence of the Flett High depicted in Ritchie et al. (2011) in Blocks 214/27, 214/28, 214/24 and 214/25 is unlikely. Several NE-trending shale diapirs have been mapped in the Foula Sub-basin (Lamers and Carmichael, 1999) and it is possible that associated structure may have been mis-interpreted as an extension of the Flett High. For instance, at the approximate location of a seismic profile shown in Ritchie et al. (2011) (their figure 30) defining the Flett High over Block 214/24, FSC seismic interpretation postulated Cretaceous shale diapirism (Smith et al., 2013, their figure 15; see Figure 4 for location). It is possible however, that the Flett High may be obscured by Paleogene igneous sills intruded in the Upper Cretaceous succession.

2.2.3.3 FLETT HIGH, SW OF THE FOULA SYNCLINE

FSC seismic coverage is poor over the Flett High to the SW of the Foula Syncline. In this area, the seismic expression of the Flett High becomes well defined to the SW of Block 205/10 where Robinson et al. (2004) report 'detailed mapping of the Mesozoic structure' and describe the Flett 'Ridge' as a NE-SW trending high. They note onlap and later thinning of an Early and Late Paleocene seismic package of reflectors onto the Flett 'Ridge' from both a northwesterly and southeasterly direction (Figure 20). Robinson et al. (2004) note that this part of the Flett High has structural expression at Top Cretaceous level and appears to have actively grown during the early Paleogene times, influencing Paleocene and early Eocene sedimentation. The Flett High at this location is associated with numerous sill intrusions some of which, Smallwood and Maresh (2002) suggest, may have influenced Lower Paleocene sedimentation. Robinson et al. (2004) identify a 'near perfect circular feature' at this location on a deep time slice (4.25 seconds) and suggest that it could indicate an igneous pluton at depth. However there is no anomalous gravity response over this area suggesting that the feature is not likely to be a pluton as there is no excess mass (basic) or mass deficit (acidic pluton); it is possible that the feature could be volcanic in nature.

Discussion - There are similarities in the structural and sedimentary relationships observed along parts of the Flett High and those reported for the Fles Fault Complex in the Vøring Basin in the Norwegian sector (Brekke 2000). For example, both the Flett and Fles structures form a faulted NE-trending boundary between a Cretaceous depocentre to the SE and Paleocene depocentre to the NW (Figure 21; Brekke, 2000 their figures 5 & 6). Interestingly, along parts of the Fles Complex, faulting displays flower structure geometry. Speculatively and by analogy with the Fles Fault Complex, it is possible that the formation of the Flett High itself had a strike-slip component and its mapped location marks the line of a deep crustal fault; interaction with faults associated with the postulated NW-trending Clair lineament and NE-trending Rona Fault may have controlled the formation of an associated Cretaceous pull-apart basin (the Foula Syncline). Further south-westwards in Block 205/10, this fault line could have been a focus for igneous activity and associated uplift during the early Paleogene (Robinson et al., 2004).

Interpretation by England et al. (2005) of the WNW-ESE trending FAST deep seismic reflection profile (see Figure 12 for location) reveals steep west-dipping normal faults just west of the Rona High. Further west at the location of the Corona High, a series of east-dipping reflectors, one interpreted at a depth of 8-12 km, can be delineated (England et al., 2005). It is possible that the SE-dipping bounding faults that define the Corona High sole out on these easterly-dipping reflectors (England et al., 2005). Considering the interpretation of the Flett High in the context of the Faroe Shetland Basin as a whole, it is suggested in this study that the NW-dipping faults bounding the Rona High, may project beneath the Flett High and intersect with continuations of the low angle east-dipping reflectors beneath the Corona High. These shallow detachments controlling the Mesozoic and Cenozoic structures sit above and are younger than the proposed vertical fault line beneath the Flett High.

In summary, examination of the FSC seismic and well database has resulted in significant revision regarding the location and extent of the Flett High and this is reflected on the revised structural elements map **(**Figure 1). The location and morphology of the Flett High, as defined in Ritchie et al. (2011), is only partly supported by the new examination of potential field and seismic data within this study. Late Cretaceous or early Paleogene compression has enhanced the Flett High by increasing the dip of sedimentary layers on its flanks and also producing an anticlinal form to the Upper Cretaceous and early Paleogene (Figure 21; ***see section 2.7 below***).

2.2.4 The Erlend High

Background **-** Ritchie et al. (2011) describe the Erlend High as a heavily intruded, fault-bounded basement terrace with dimensions of about 65 to 70 km in both NE and NW directions (their figure 7; Figure 2). Paleogene basalt and intrusive rocks associated with the Erlend and West

Erlend igneous centres largely obscure Cretaceous and older rocks associated with the high. The Erlend igneous centres are well imaged as circular positive gravity anomalies (Figure 1; Kimbell, 2014). Ritchie et al. (2011) show the Erlend High to be bounded to the SW and NE, respectively, by the Erlend and Magnus lineaments. To the SE, the Erlend High passes into the East Shetland High that comprises crystalline basement (Figure 2). Ritchie et al. (2011) noted a mismatch between their mapped limit of the Erlend High and the extent of an associated positive gravity anomaly, which extends westwards, with an E-W trend, beyond the mapped limit of the high (Figure 25).

Larsen et al. (2010) reinterpreted the structural geology of the Erlend High using high quality seismic data that was acquired in 2005 and 2006 with a regular line grid of approximately 5 km spacing. They recognised two NE-trending Cretaceous half-graben, informally termed the Yell Sub-basin and Muckle Basin, of opposite polarity located adjacent to the West and North Shetland platforms respectively (terminology from Larsen et al., 2010). They suggested the polarity shift may be due to deep-seated basement structures (rift-oblique lineaments). Larsen et al. (2010) also noted the NS trend in some of their mapped faults as probably being associated with trends similar to the Walls Boundary fault (WBF), the north veering extension of the Great Glen Fault. The Yell Sub-basin is located southwest of the Erlend High, here the Cretaceous succession dips and thickens to the SE against the NW-dipping, NE-trending, master faults that step down into the deeper Flett Sub-basin (Larsen et al., 2010, their figure 3). The Muckle Basin is located between the Erlend High and North Shetland Platform (East Shetland High of Ritchie et al., 2011). The Cretaceous succession dips and thickens to the NW against SE-dipping master faults (Larsen et al., 2010, their figure 3). The reinterpretation of the area by Larsen et al. (2010) significantly contrasted with the structural elements mapping of Ritchie et al. (2011) and prompted a detailed review of the area within this study.

Dataset - There are no FSC 3D datasets available over the area and a key 2D seismic dataset was withdrawn from this FSC project upon which our interpretation was originally based. Six commercial released wells have been drilled on the Erlend High as described by Ritchie et al. (2011). To the NE, three further wells aided in the interpretation of the Erlend Sub-basin and one of these wells, 219/28- 2Z, reached total depth in psammitic gneiss. To the SW, most of the wells reach TD in the Upper Cretaceous section however well 208/27- 1 terminated in possible weathered basement. Potential field data and modelled depth to top basement (Kimbell et al., 2010) provided insights into the disposition and depth of basement while published information, in particular Larsen et al. (2010), provided additional information as to structural style and aided in the interpretation.

Interpretation – This section has been redacted following withdrawal of the key 2D seismic dataset upon which our revised interpretation was based.

2.3 BASINAL AREAS

Ritchie et al. (2011) defined the basins within the designated Faroe-Shetland Basin as 'sub-basins' and this naming distinction has been retained on the revised map. Two new basins, the Yell Sub-basin and Muckle Basin (Larsen et al., 2010) have also been mapped and described in this study (***see section 2.2.4,*** subsequently redacted) and this has resulted in alteration to the south-eastern boundaries of the Flett and Erlend sub-basins respectively. In addition, the north-eastern boundary of the Foula Sub-basin has been changed slightly from Ritchie et al. (2011). We explored the possibility of attributing the age of basinal fill in various ways, however, this was considered inappropriate as the map would be too complicated with the boundaries, contours and limits of the different sedimentary and volcanic successions. Furthermore, the location and extents of sedimentary and volcanic depocentres are likely to be refined as we begin to build our maps displaying sediment distribution from Jurassic to the Eocene and it was considered premature and possibly misleading to show them on the map at this stage.

2.4 LINEAMENTS

Rift-oblique lineaments are often inferred to segment rift basins and passive margins. They have been observed and mapped onshore and often mark along-strike changes in polarity of half-grabens and compartmentalisation of dissected basins influencing their sedimentary evolution (see Moy and Imber, 2009, for summary and references). Following Rumph et al. (1993), Ellis et al. (2009) have postulated the controlling influence of such features on thickness changes in lava successions and sediments on the Faroe Islands.

Rumph et al. (1993) utilised gravity and magnetic data to define 17 NW-trending transfer zones, some of which had been previously postulated (Duindam and van Hoorn, 1987). They envisaged these as significant transcurrent crustal features of varying magnitude within the FSB area. Kimbell et al. (2005) used the term 'lineament' for features that may have acted as transfer zones during the evolution of the NE Atlantic margin. Moy and Imber (2009) preferred the use of the term 'lineament' or 'rift-oblique lineament' rather than 'transfer zone' to distinguish features identified primarily by potential field data from those that could be more specifically identified using well calibrated seismic reflection data. Stoker et al. (2010) followed Moy and Imber (2009) in their use of this term and we also adopt the term rift-oblique lineament for such features.

Rumph et al. (1993) introduced informal names for six of their 17 proposed transfer zones: Judd, Westray, Clair, Victory, Erlend and Magnus (they cite Duindam and van Hoorn, 1987, regarding the Judd, Erlend and Magnus lineaments). Ritchie et al. (2011) show nine named and two unnamed NW-trending lineaments (plus the Wyville Thomson Lineament Complex to the SW) on their structural elements map (their figure 7; Figure 2) with mapped locations that are slightly modified from the transfer zones identified by Rumph et al. (1993). The informal nomenclature within this study follows that of Ritchie et al. (2011) (Figure 2) who follow Rumph et al. (1993) in the naming of these lineaments. Ritchie et al. (2011) reduced the four unnamed lineaments between the Victory and Erlend lineaments (Rumph et al., 1993) to one shortened version that marks their NE limit of the Rona High (Figure 2), and did not include one relatively short unnamed lineament between the Victory and Clair transfer zones. Three unnamed transfer zones between the Clair and Westray lineaments were reduced to two and these were termed the Corona Lineament (Ritchie et al., 2011) and the Grimur Kamban Lineament by Keser Neish (2004). The most northerly (unnamed) transfer zone identified by Rumph et al. (1993) was termed the Brendan Lineament by Ritchie et al. (2011). Finally Ellis et al. (2009) identified the Brynhild Lineament from onshore evidence on the island of Streymoy in the Faroes and continued this into the south-western part of the FSB.

Several workers have proposed that the rift-oblique lineaments influenced the distribution of sediments in the FSB (e.g. Ellis et al., 2009; Larsen and Whitham, 2005; Naylor et al., 1999; Rumph et al., 1993) and this topic has attracted much debate. A study by Moy and Imber (2009) based on the interpretation of 3D seismic data volumes, questions the influence that three of the lineaments, specifically the Judd, Corona and Clair features (naming from Rumph et al., 1993 and Ritchie et al., 2011), and by analogy other rift oblique lineaments, may have had on Cenozoic sediment distribution. However, Moy and Imber (2009) do not discount the possibility that rift-oblique lineaments marked changes in deep crustal structure during Mesozoic extension (e.g. England et al., 2005).

We have not included any rift-oblique lineaments on the revised map as we have not observed any unequivocal evidence for the influence or effects that these structures may have had on the present day structural configuration. However, the rift-oblique lineaments, as shown in Ritchie et al. (2011) and with the addition of the Brynhild Lineament southeast of the Faroe Islands that was defined by Ellis et al. (2009) are included as layer in the FSC GIS.

2.5 PALEOGENE IGNEOUS CENTRES AND LIMIT OF PALEOGENE BASALT

The revised structural elements map incorporates the location of Paleogene igneous centres as recently modified on behalf of the FSC by Kimbell (2014). The outlines are based on isostatic gravity anomaly gradients, magnetic signatures and comparison with the quantitative models generated for each centre; the methodology for defining and delineating the igneous centres is detailed in Kimbell (2014). In order to be consistent with the Magnetic Signatures report (Kimbell, 2014), we adopt the term igneous centre rather than volcanic centre as favoured by Ritchie et al. (2011). This change of terminology is to avoid distinction between the extrusive and intrusive components of the complexes. We also note here that the Brendan Igneous Centre (Ritchie et al., 2011) has now been remapped as two centres, named as Brendan and West Brendan (Figure 1). The limits of Paleogene basalt and key basalt escarpments depicted on the revised structural elements map have been slightly modified from Ritchie et al. (2011) (Figure 1).

2.6 CONTINENT OCEAN BOUNDARY AND TRANSITION ZONE

The revised map shows the Continent-Ocean Transition whose southerly limit has been redefined by Kimbell (2014) from the location of the Continent-Ocean Boundary shown in Ritchie et al. (2011) and modified on the basis of new magnetic data (Kimbell, 2014).

2.7 ANTICLINES

We have re-evaluated the locations of anticlinal axes from both externally published sources and from FSC reports (i.e. Johnson et al., 2012; Kimbell, 2014); the revised set of anticlinal axes is shown in Figure 34. The majority of these structures are considered to have evolved during compressional episodes in the Cenozoic. The GIS for this project holds the digitised location and attribution of published anticlinal axes as reported by Boldreel and Anderson (1998), Lamers and Carmichael (1999), Ritchie et al. (2003), Davies et al. (2004), Johnson et al. (2005), Ritchie et al. (2008), Tuitt et al. (2010), Stoker et al. (2012) and Ólavsdóttir et al. (2013) which were all consulted in the compilation of the revised set of anticlines.

The methodology we have adopted in compiling this revised set of fold axes is as follows. Where a published axial trace has a structural expression on one or more of the TWTT structure surfaces shown in Johnson et al. (2012) then they are shown on the map that accompanies this report. The Westray Anticline, is also included although it occurs close to the mapped limits of Johnson et al. (2012) and cannot therefore be fully verified on these maps. However, the anticline has been defined by several authors including Smallwood (2004), who published maps at Top Balder level showing the Judd and Westray complexes although the axis shown in this report is based on Ritchie et al. (2008). The Wyville Thomson Ridge Anticline, located in the SW of the study area, is also described from published sources. In addition the Ben Nevis Anticline, described by Hodges et al. (1999), has been mapped from a 3D seismic timeslice by Kimbell (2014). The location of anticlinal axes have been rationalised over the Munkagrunnur Ridge and Faroe Platform following consideration of interpretations of the magnetic signature made by Kimbell (2014) and consultation with the Jarðfeingi. The locations of the Flett High Anticline and a NE-trending anticlinal axis on the Flett Terrace, the Flett Terrace Anticline are based upon seismic mapping carried out in this study (Figure 9; Figure 15). The rationalised set of structures, a comprehensive summary of the significant anticlines, is grouped in a separate shapefile (named **Fold_axes** shapefile) and incorporated on our revised structural elements map; the interpreted timing of development is recorded as part of their attribution characteristics.

The majority of anticlines described below are located within basins such as the Annika, Guđrun and Corona sub-basins (Figure 34) and all of the anticlines described below record phases of growth, of varying intensity, during the Paleogene and Neogene.

As far as we are aware there are no published maps of pre-Cenozoic anticlinal structures in the study area. However, Lundin et al. (2013) illustrate and describe early Late Cretaceous (Cenomanian/ Turonian) structures in the northern Vøring Basin and in particular refer to the Vigrid Syncline and the Rås and Træn basins located west and east respectively of the NE-trending Utgard High-Fles Fault Complex. As stated above (***see section 2.2.3***), the Flett High has similarities to the Fles Fault Complex and it is possible that the Flett High Anticline (***see below***) and adjacent Foula Syncline (***see below***), have a Late Cretaceous initiation. High-angle reverse faulting with associated folding in the south-western part of the FSB, specifically the East and South Solan basins, provide evidence for an episode of Cenomanian to Turonian compression (Booth et al., 1993; Stoker et al., 2010). The entire southeast Faroe-Shetland region along and adjacent to the Rona High may have been subjected to Late Cretaceous tectonism. In the Solan basins, Late Cretaceous (Roberts et al., 1999) to earliest Paleocene (Booth et al., 1993) formation of several localised inversion structures formed by transpressional reactivation has been recorded (Johnson et al., 2012). In addition, Roberts et al. (1999) noted evidence of Late Cretaceous tectonism shown by anticlinal subcrop down to the Turonian along the Clair Ridge and Stoker et al. (2010) record a regional unconformity at the Cretaceous/ Paleogene boundary along the south-eastern edge of the FSB.

The anticlinal axes (Figure 34) are described below beginning with the highs bounding the Faroe-Shetland Basin, moving counter-clockwise and then moving inboard to consider sub-basins and their adjacent highs moving from the north to the south.

- The ***Ben Nevis Anticline*** has been described by Hodges et al. (1999) who identified a dome-like structure beneath a succession of basalt immediately SE of a potential field anomaly marking the location of the Brendan Igneous Centre. Hodges et al. (1999) interpreted the dome as an inverted Cretaceous succession of mudstone and sandstone onlapped by early Eocene sediments and covered by a basalt plateau; a thick succession of mid-late Eocene sediment was interpreted to cover the basalt. Well 219/21- 1, drilled on the structure in 2003, showed it to comprise a mudstone dominated Cretaceous succession, intruded by sills, and covered by a thin succession of Paleogene basalts. Results from this well enabled Smith et al. (2013) to interpret the succession of onlapping early Eocene sediments, postulated by Hodges et al. (1999), as a westerly thickening interval of Paleogene volcanic rocks.

  The anticline was drawn with reference to a seismic timeslice at 3.2 s TWTT, that includes part of the Upper Cretaceous succession, covering the structure and the south-eastern part of the Brendan Igneous Centre (The timeslice is illustrated by Kimbell, 2014, his figure 44). The timeslice images an ENE trend and enabled an axis to be drawn. The ENE-trending axis is approximately 42 km in length and is located immediately south of the Brendan Igneous Centre (Figure 1; Figure 34).

- The ***Fugloy – North Faroe Anticline***, east of the Faroe Platform, is well imaged on the TWTT structure map of Johnson et al. (2012) at Top Paleogene Basalt level and the digitised anticlinal axis in the **Fold_axes** shapefile has been guided by this map. Ritchie et al. (2003) equate the Fugloy Ridge Anticline with their Anticline C and show the axis with a dextral displacement on the postulated Erlend Lineament. Boldreel and Anderson (1998) locate an unnamed ENE-trending anticlinal axis along the Fugloy Ridge. On the Faroes Platform, the location of the axis was guided by Rasmussen and Noe-Nygaard (1970) and passes through the northern parts of the islands of Viðoy, Borðoy, Kunoy, Kalsoy, Eysturoy and Streymoy. West of the Faroe islands, the location of the fold axis was guided by the subcrop of normally magnetised basalt layers mapped by Kimbell (2014) and an inversion structure mapped by Ólavsdóttir et al. (2013).

East of the Faroe Platform, the anticline is interpreted to have formed during a phase of compression from mid Eocene to mid Miocene with mild compression in late Pliocene to the present day (Johnson et al., 2012).

Ritchie et al. (2011) note that the Fugloy Ridge is interpreted as a deeply buried structure at Mesozoic and older stratigraphical levels. The large asymmetrical anticline, defined at top Paleogene basalt and younger sediments, is slightly offset from the older structure (Johnson et al. 2012, their figure 5).

- The ***Munkagrunnur Ridge Anticline*** is a flat-topped (caused by truncation of Paleogene basalt) anticline, approximately 158 km long (e.g. Ritchie et al., 2011; Keser Neish, 2003; Roberts et al., 1999). Johnson et al. (2005), Davies et al. (2004), Boldreel and Anderson (1998) and Lamers and Carmichael (1999) all show a NNW-trending axis along different parts of the Munkagrunnur Ridge south of the Faroe Islands. Ólavsdóttir et al. (2013) map an anticlinal axis (No. 6) just west and south-west of the island of Suðuroy. In addition, Kimbell (2014) shows an NNW-trending anticline at this location (Kimbell, 2014, his figure 14). The digitised anticlinal axis in the **Fold_axes** shapefile is a composite of these different axial traces and runs from the southern tip of the Munkagrunnur Ridge to just west of the northern tip of the island of Suðuroy. Doré et al. (2008) interpret the timing of inversion as predominantly Eocene with another pulse in the mid-Miocene.

  Ritchie et al. (2011) and Keser Neish (2003) interpret the boundary of the ridge as marked by steep extensional and reverse faults and the presence of a deep structure is implied, but is obscured by Paleogene basalt.

- The ***Wyville Thomson Ridge Anticline*** is described in Ritchie et al. (2011) as a WNW-trending symmetrical basalt anticline. The anticlinal axis is also mapped in Tuitt et al. (2010), Johnson et al. (2005) and Boldreel and Anderson (1998); a composite of these has been digitised for the **Fold_axes** shapefile. Ziska and Varming (2008) show, through interpretation of seismic data, that the Wyville Thomson Ridge was a positive feature prior to extrusion of the basalt succession and discuss the possibility that the structure was formed during early Paleocene rifting. Johnson et al. (2005) also suggest an early initiation (in the Late Paleocene, Thanetian) but during a phase of mild compression. The main period of growth of the ***Wyville Thomson Ridge Anticline***, by a series of compressional pulses, is thought to have been through the Eocene, Oligocene and Early Miocene finally ceasing with a period of mild compression in the mid-Miocene (Johnson et al., 2012) although more recent growth is postulated by Tuitt et al. (2010) and Tate et al. (1999).

- **Erlend Sub-basin**
  - The ***Pilot Whale Anticline*** is mapped as a NNE-trending anticline at Top Paleogene Basalt (Johnson et al., 2012) and the axial trace in the 'summary shapefile' has been digitised from this structure (closed on 3.2 sec TWTT). The anticline is also well defined at Intra-Neogene Unconformity (INU) level (closed on 2.6 secs TWTT); it is described as having been formed during two phases of mild compression in mid to late Eocene and mid to late Miocene and continuing to the present day (Johnson et al., 2012). The structure is also shown on figures 2 and 9 of Ritchie et al. (2003) where it comprises their NNE-trending Anticline F.
  - ***Anticline E*** was named by Ritchie et al. (2003) and is equivalent to Anticline A2 of Davies et al. (2004). Anticline E is a NNE-trending anticline at the Top Eocene T2a horizon and the axial trace in the **Fold_axes** shapefile has been digitised from

this structure (closed on 3.1 sec TWTT). It is also depicted on the INU, Intra-Miocene Unconformity (IMU), Top Paleogene Unconformity (TPU), Intra-Oligocene Unconformity (IOU), and T2b (late Priabonian) maps of Johnson et al. (2012); it is described as having been formed during one phase of mild compression mainly in mid to late Miocene times, but possibly extending to the present day.

- ***Anticline A1*** was located and named by Davies et al. (2004) and the axial trace in the **Fold_axes** shapefile is a copy of their structure. Several of the TWTT structure maps of Johnson et al. (2012) show a generally NE-trending culmination at this location (e.g. INU, TPU, T2a (Late Eocene/ Early Oligocene Unconformity), T2b). Anticline A1 also coincides with an unnamed anticlinal axis in figure 2 of Ritchie et al. (2003). Davies et al. (2004), date the formation of the anticlinal domes they identified, including Anticline A1, as having been formed by compression during the mid to late Miocene.

- **Corona Sub-basin**
  - ***Anticline D* / *Tobermory Anticline*** has been digitised for the summary shapefile, following a ridge and minor culminations on the IMU surface of Johnson et al. (2012); this corresponds quite closely to the trace shown in Ritchie et al. (2003) (their Anticline D). It is depicted as a NE-trending gently sinuous anticlinal axis approximately 55 km long. Davies et al. (2004) show two axes at this location (A4 and A5), roughly corresponding to the single trace shown in Ritchie et al. (2003). The anticline has some structural expression at several horizons in Johnson et al. (2012) where it has small closures on the T2b, T2a, IOU, TPU and IMU surfaces. Davies op. cit show (their figure 10) another anticlinal axis, A3, along trend from their A5 and A4 which would extend Anticline D further to the NE. However, there is only a minor suggestion of this on the Johnson op. cit. maps and so has not been included in the **Fold_axes** shapefile. Anticline D is described as having been formed during one phase of mild compression in mid to late Miocene, which possibly extended into the early Pliocene.
  - ***Anticline A6*** is located and named by Davies et al. (2004) and the axial trace in the **Fold_axes** shapefile is a copy of their structure. Several of the TWTT structure maps of Johnson et al. (2012) show a generally NE-trending culmination (e.g. IMU, intra-Oligocene unconformity and Top Balder). Anticline A6 also coincides with an unnamed anticlinal axis in Figure 2 of Ritchie et al. (2003).
  - ***Anticline A14*** (named in Davies et al., 2004) is shown in Ritchie et al. (2003) as an unnamed NE-trending gently sinuous anticlinal axis. The anticline has some structural expression at several horizons in Johnson et al. (2012). The axial trace in the **Fold_axes** shapefile and depicted on the structural map has been digitised following culminations, specifically on the Intra Oligocene Unconformity surface of Johnson et al. (2012); this corresponds quite closely to the trace shown in Davies et al. (2004) and Ritchie et al. (2003).
  - ***Anticline A15*** is located and named by Davies et al. (2004). Two of the TWTT structure maps of Johnson et al. (2012) show a generally NNE-trending culmination (T2c (intra-Bartonian), T2b) that corresponds to A15 of Davies et al. (2004). Ritchie et al. (2003) also show an unnamed anticlinal axis at this location. For our **Fold_axes** shapefile, part of A15 has been digitised to follow the mapped culmination of Johnson et al. (2012).
  - ***Anticline A16*** is located and named by Davies et al. (2004). The Top Paleogene Basalt TWTT structure map of Johnson et al. (2012) shows a NE-trending area of erosion, while T2c, T2b, T2a, Intra Oligocene Unconformity and IMU all depict the structure to varying degrees. Ritchie et al. (2003) also show an unnamed

anticlinal axis at this location. For our **Fold_axes** shapefile, the northeastern part of A16 (Davies et al., 2004) has been digitised to follow the mapped culmination.

- **Annika Sub-basin**
  - The ***Annika Anticline*** is a term introduced in this study for a NE-trending anticline mapped by Ólavsdóttir et al. (2013) in the Annika Sub-basin (their structure number 3); the axial trace in the **Fold_axes** shapefile is a copy of their structure. Boldreel and Anderson (1998) show an unnamed anticlinal axis, with a longer length at roughly the same location and date its formation as mid-Oligocene. From interpretation of seismic profiles, Ólavsdóttir et al. (2013) give a later time of formation from mid-Miocene to Recent times. The structure is well defined on several TWTT structure maps from Johnson et al. (2012) (e.g. Top Paleogene Basalt and Top Balder Formation).

- The ***East Faroe High Anticline*** has been mapped by Ritchie et al. (2003) as Anticline A and in Davies et al. (2004) as Anticline A17. Boldreel and Anderson (1998) also show a NE-trending anticlinal axis adjacent to the East Faroe High and date its formation as mid-Oligocene. The form of the anticline can be recognised on several of the surfaces mapped by Johnson et al. (2012) (e.g. Top Paleogene Basalt, Top Balder, IMU – absent over structure) but it has been digitised for the **Fold_axes** shapefile from the T2b structure map (1.9 secs TWTT closure). The digitised trace is not as extensive as that depicted on the published traces.

  The East Faroe High Anticline is located above the northern extremity of the north-eastern segment (Ritchie et al., 2011) of the East Faroe High (Figure 34) and is described as having been formed during possible pulses of mild compression from mid Eocene culminating in a final pulse of compression in the mid Miocene (Johnson et al., 2012). The presence of a basement cored high, the northeast segment of the East Faroe High, at this location is equivocal on the basis of 3D gravity modelling. The depth to modelled crystalline basement is between 8 and 10 km at this location compared to 5 km over the rest of the East Faroe High (Kimbell et al., 2010).

- **Guđrun Sub-basin**
  - The ***Guđrun Anticline*** can be recognised on some of the surfaces mapped by Johnson et al. (2012). At sea bed, INU and T2a it is shown as a NE-trending anticline traversing the Guđrun Sub-basin and the digitised trace in the summary shapefile is based on these three maps. On the T2d (intra-Lutetian) surface, and to a lesser extent on Top Paleogene Basalt, the structure has been mapped as an ESE-trending anticline (Johnson et al., 2012). Ólavsdóttir et al. (2013, their structure number 5) shows a NNE-trending anticline traversing the Guđrun sub-Basin. The Gudrun Anticline is described as having mainly formed during one phase of compression in the mid Miocene, but possibly extending to the present day (Ólavsdóttir et al., 2013; Johnson et al., 2012).

- **Brynhild Sub-basin**
  - The ***Brynhild Anticline*** is a term introduced in this study for a NNE-trending anticline mapped by Ólavsdóttir et al. 2013 (their structure number 2) and located within the Brynhild Sub-basin. Ólavsdóttir et al. (2013) interpret the structure as having formed between the mid Miocene and the present day (Ólavsdóttir et al., 2013). The Brynhild Anticline intersects the line of the postulated NW-trending Judd Lineament. Several maps from Johnson et al. (2012) indicate a NW-trending structure at this location (e.g. T2c and T2a) and an anticlinal axis has been

digitised for the **Fold_axes** shapefile guided by the T2c surface from Johnson et al. (2012).

- **Flett Sub-basin**
  - The informally named ***Flett Terrace Anticline,*** a term introduced here, is located within the Flett Terrace (Figure 9; Figure 15), which is interpreted to have developed in early Paleogene times through inversion of a thick Cretaceous succession in the hanging wall of the SE-Corona Fault (***see section 2.2.2***). The crest of the anticline is drawn from a TWTT map at Top Upper Cretaceous level that shows a NE-trending linear anticline whose axial trace veers to a more ENE trend in front of the stepover in the SE-Corona Fault (Figure 15).

- The ***Westray Anticline*** is recognised by Ritchie et al. (2008) as a NW-trending anticline; the axial trace in the **Fold_axes** shapefile replicates its structure. Lamers and Carmichael (1999) also show a NW-trending anticlinal axis close to this location. The structure lies beyond the mapped extents in Johnson et al. (2012). Its location does not correspond to that shown on the map of Top Balder from Smallwood (2004). The general form and trend of the anticline can be partially recognised (its NW end) on some of the surfaces mapped by Johnson et al. (2012, e.g. Top Balder, T2d, T2c and T2b). The Westray Anticline is described as having been initiated at the beginning of the mid-Eocene and enhanced by pulses of compression through the mid and late Eocene and Oligocene. It has continued to be affected by pulses of mild compression to the present day (Johnson et al., 2012; Ritchie et al., 2008).

- **Judd Sub-basin**
  - The ***Judd Anticline*** is mapped in Ritchie et al. (2008) where it is shown as an EW-trending anticlinal axis; the axial trace in the **Fold_axes** shapefile is a copy of their structure. Its location corresponds to that shown on maps of Top Balder from Smallwood (2004) and an EW-trending area of erosion is shown on several maps in Johnson et al. (2012, T2d, T2c, T2b and INU). Ólavsdóttir et al. 2013 (their structure number 1), Tuitt et al. (2010) and Boldreel and Anderson (1998) all show EW-trending anticlines at this location. The Judd Anticline is described as having been formed over a period from mid Eocene to the end of the Oligocene (Johnson et al., 2012).
  - The ***South Judd Anticline*** is mapped by Ritchie et al. (2008) where it is shown as a NW-trending anticlinal axis; the axial trace in the **Fold_axes** shapefile is a copy of their structure. Ritchie et al. (2008) show its formation to have been confined to a pulse of compression at the Oligocene/ Miocene boundary. Lamers and Carmichael (1999) also show a NW-trending anticlinal axis close to this location. The structure is well imaged on the TWTT structure contour map of the Top Balder Formation in Johnson et al. (2012) where its orientation is defined on the 1.9 second TWTT contour.

- The term ***Flett High Anticline*** is introduced in this study for a faulted NE-trending anticline (Figure 9; Figure 21) located between the Flett Sub-basin (and Flett Syncline) to the NW and the Foula Sub-basin (and Foula Syncline) to the SE. It comprises a fault-bounded, folded Lower Cretaceous, Jurassic and older succession overlain by a folded Upper Cretaceous sediments (***see section 2.2.3 above***). The structure is interpreted to have developed during Late Cretaceous to early Paleocene compression (Figure 21).

A number of anticlinal axes, mapped by others particularly Ritchie et al. (2003) and (2008) could not be recognised on the maps of Johnson et al. (2012) and were therefore not included on the

revised map. The majority are of quite small length and therefore may not have been resolved on these maps.

2.8 SYNCLINES

Two synclinal axes were mapped from selected FSC seismic profiles. They show evidence for compression in the areas where they are shown.

- **Flett Sub-basin**
  - The ***Flett Syncline*** is a NE-trending synclinal axis that marks the main Paleocene depocentre within the FSB; the depocentre is likely to have been enhanced by later compression forming the syncline (Figure 9; Figure 14). The axial trace was digitised with reference to selected NW-orientated seismic profiles across the FSB and the 1500 m isopach (Top Balder to Base Tertiary) shown in Knox et al. (1997).

- **Foula Sub-basin**
  - The ***Foula Syncline*** is a synclinal axis (informally named here as the Foula Syncline) located in the Foula Sub-basin and associated with a marked Cretaceous depocentre and adjacent to the Flett High faulted anticline (Figure 9; Figure 14). The flanks of the syncline are thought to have been steepened during late Cretaceous/ early Paleocene compression. Stoker et al. (2010) suggest possible initiation of the Foula Syncline (and the North Rona Basin) in a Cenomanian to Turonian compressional phase.

3 Conclusions

This study has produced a revision of the structural elements of the Faroe-Shetland Basin delivered in the form of a hardcopy summary map, an explanatory report and a GIS database. The revised map displays a simple 'basin and high' framework that is generally derived from the structural elements map of Ritchie et al. (2011); we follow Ritchie et al. (2011) with regard to their symbology that distinguishes 'structural highs', 'highs defined at top Paleogene basalt level', 'basins' and 'Paleogene igneous centres'. The revised map differs from the structural elements map of Ritchie et al. (2011) in several ways:

1. Focused interpretations have significantly changed the configuration of basins and highs in the Corona, Flett and Erlend high areas (revised Erlend High interpretation subsequently redacted). These areas where chosen due to observed mismatches between potential field information and mapped extents of basement highs and basins. For the Erlend High area, recent published mapping results prompted a new look at the FSC seismic dataset. Geoseismic profiles illustrating the revised structural interpretation are included in the report.

   Corona High:

   a. The new interpretation of the Corona High shows it to comprise a series of NE-trending fault blocks bounded by predominantly SE-dipping, relatively steep, *en echelon* faults. The informally named SE Corona Fault forms the south-easternmost boundary of the Corona High and incorporates a dog-leg with a change in orientation from NE-trending to approximately E-W before returning to a NE trend along its length;

   b. An area in the hanging wall of the faults bounding the SE side of the Corona High is interpreted to contain a thick Cretaceous succession and following Loizou et al. (2006) has been termed the Flett Terrace. The Cretaceous succession within the Flett Terrace area is interpreted to have been inverted and eroded at the Intra-Vaila Unconformity (Smith et al., 2013) and a NE-trending anticlinal axis has been mapped across it;

   c. The area where inversion appears greatest is located immediately south-east of the dog-leg in the SE Corona Fault. Considering this location, the structure could be the result of local inversion associated with this restraining bend on the SE Corona Fault;

   d. The Corona High is separated from the informally named North Corona High by an EW-trending area of deeper crystalline basement interpreted from seismic data; this area of deeper basement sits adjacent to and immediately north of an EW-trending area of shallow basement interpreted by Makris et al. (2009);

   e. An abrupt reduction in the magnetic field is a response to the deeper basement and is coincident with the published location of the Clair Lineament.

   Flett High:

   a. The new seismic interpretation has significantly changed our view of the location, extents and formation of the NE-trending Flett High**.** Where best imaged on seismic data adjacent to blocks 206/02, 03 and 06, the Flett High forms the NW boundary of a marked Cretaceous depocentre, the Foula Sub-basin and is informally named the Foula Syncline;

b. The Flett High also bounds the SE edge of the Flett Sub-basin, a marked Paleocene depocentre;

c. The Flett High is interpreted to comprise a succession of Jurassic and older rocks separated from deep crystalline basement by low-angle, NW-dipping faults and onlapped and overlain by a Cretaceous succession. The Cretaceous sediments surrounding the Flett High are interpreted to be intruded by several Paleocene sills. The SW part of the Flett High, in Block 205/10, exhibits sedimentary onlap relationships that indicate the Flett High at this location developed during early Paleogene times. However, further to the NE the main period of formation of the Flett High appears to have been during the early Cretaceous with little effect on Paleogene sedimentation. On the basis of the seismic interpretation carried out in this study, the sinistral offset of the Flett High described in Ritchie et al. (2011) associated with the published location of the Grimur Kamban Lineament could not be recognised. The Flett High could not be interpreted beyond Block 214/29 and its NE extent corresponds only approximately to the published location of the inferred Clair Lineament;

d. The Flett High appears to show some similarities in its structural and sedimentary relationships compared with the Fles Complex in the Vøring Basin in that they both show similar positioning of Paleogene basin and Cretaceous synclines. In addition, the Fles Complex displays flower structure geometry in parts and by analogy it is possible that the Flett High has a strike-slip component with its mapped location marking the line of a deep crustal fault.

Erlend High – The revised interpretation of the Erlend High has been redacted following withdrawal of the key 2D seismic dataset from the FSC database upon which our revised interpretation was based.

2. The interpretation of seismic data utilised in this study did not provide unequivocal evidence to support the presence of rift-oblique lineaments and consequently none are shown on the final map.

3. A new GIS layer comprising the location and extents of igneous centres, including a new addition following the recognition of a possible West Brendan Igneous Centre, has been added to the revised map following review and new interpretation by Kimbell (2014).

4. A new interpretation of the edge of the continent-ocean transition has been added to the revised map following new interpretation of magnetic data by Kimbell (2014).

5. The location and extents of 23 fold axes are shown on the revised map and included as a new layer in the GIS accompanying this report. Published anticlinal axes have been compared with mapped Cenozoic surfaces depicted in Johnson et al. (2012) and fold structures interpreted by Kimbell (2014). These comparisons have resulted in a rationalisation of fold axes in the FSB and adjacent areas. In addition, new axes mapped in this study are the Flett Terrace and Flett High anticlines and the Foula and Flett synclines and these folds are also depicted on the map.

6. Minor alteration to the limit of the basalts and primary basalt escarpments are included on the revised map.

References

British Geological Survey holds most of the references listed below, and copies may be obtained via the library service subject to copyright legislation (contact libuser@bgs.ac.uk for details). The library catalogue is available at: http://geolib.bgs.ac.uk.

ASHCROFT, W A., HURST, A. and MORGAN, C J. 1999. Reconciling gravity and seismic data in the Faroe-Shetland Basin, West of Shetland. 595-600 in *Petroleum Geology of Northwest Europe: Proceedings of the 5th Conference*. FLEET, A J and BOLDY, S A R (editors). (London: The Geological Society).

BLYSTAD, P, BREKKE, H, FÆRSETH, R B, LARSEN, B T, SKOGSEID, J, and TØRUDBAKKEN, B. 1995. *Structural elements of the Norwegian continental shelf. Part II: the Norwegian Sea region.* NPD, Norwegian Petroleum Directorate Bulletin, Vol. 8, 45p.

BOLDREEL, L O. and ANDERSEN, M S. 1998. Tertiary compressional structures on the Faroe-Rockall Plateau in relation to northeast Atlantic ridge-push and Alpine foreland stresses. *Tectonophysics*, Vol. **300**, pp. 13–28.

BOOTH, J., SWIECICKI, T. and WILCOCKSON, P. 1993. The tectono-stratigraphy of the Solan Basin, west of Shetland. 987–998 in *Petroleum Geology of Northwest Europe: Proceedings of the 4th Conference*. PARKER, J R (editor). (London: The Geological Society).

BREKKE, H. 2000. The tectonic evolution of the Norwegian Sea Continental Margin with emphasis on the Vøring and Møre Basins. 327–378 in *Dynamics of the Norwegian Margin*. NØTTVEDT, A and seven others (editors). Geological Society, London, Special Publications, No. 167.

CONOCOPHILLIPS. 2009. UKCS Licence P799, Blocks 213/25a & 214/21a; South Uist Prospect, Atlantic Margin.

DAVIES, R, CLOKE, I, CARTWRIGHT, J, ROBINSON, A, and FERRERO, C. 2004. Post-breakup compression of a passive margin and its impact on hydrocarbon prospectivity: An example from the Tertiary of the Faroe-Shetland Basin, United Kingdom. *American Association of Petroleum Geologists Bulletin*, Vol. **88**, pp. 1–20.

DEAN, K, MCLAUCHLAN, K and CHAMBERS, A. 1999. Rifting and the development of the Faeroe-Shetland Basin. 533–544 in *Petroleum Geology of Northwest Europe, Proceedings of the 5th Conference*. FLEET, A J, AND BOLDY, S A R (editors). (London: The Geological Society).

DORÉ, A G., LUNDIN, E.R., FICHLER, C. & OLESEN, O. 1997. Patterns of basement structure and reactivation along the NE Atlantic margin. Journal of the Geological Society, London, **154**, 85–92.

DORÉ, A G, LUNDIN, E R, JENSEN, L N, BIRKELAND, Ø, ELIASSEN, P E. and FICHLER, C. 1999. Principal tectonic events in the evolution of the northwest European Atlantic margin. 41–61 in *Petroleum Geology of Northwest Europe: Proceedings of the 5th Conference*. FLEET, A J and BOLDY, S A R (editors). (London: The Geological Society).

DORÉ, A G, LUNDIN, E R, KUSZNIR, N J. and PASCAL, C. 2008. Potential mechanisms for the genesis of Cenozoic domal structures on the NE Atlantic margin: pros, cons and some new ideas. 1–26 in *The Nature and Origin of Compression in Passive Margins.* JOHNSON, H, DORÉ, A.G, HOLDSWORTH, R.E, GATLIFF, R.W, LUNDIN, E.R. and RITCHIE, J.D (editors). *The Geological Society, London, Special Publication*, No. 306.

DUINDAM, P, and VAN HOORN, B. 1987. Structural evolution of the West Shetland continental margin. 765-773 in *Petroleum Geology of NW Europe, Proceedings of the 3rd Conference*. BROOKS, J, AND GLENNIE, K W (editors). (London: Graham and Trotman).

ELLIS, D, PASSEY, S R, JOLLEY, D W, and BELL, B R. 2009. Transfer zones: The application of new geological information from the Faroe Islands applied to the offshore exploration of intra-basalt and sub-basalt strata. 205–226 in *Faroe Islands Exploration Conference: Proceedings of the 2nd Conference*. VARMING, T, and ZISKA, H (editors). Annales Societatis Scientiarum Færoensis, Supplementum **50**.

ENGLAND, R W., MCBRIDE, J H. and HOBBS, R W. 2005. The role of Mesozoic rifting in the opening of the NE Atlantic: evidence from deep seismic profiling across the Faroe-Shetland Trough. *Journal of the Geological Society, London*, Vol. **162**, pp. 661-673.

GALLAGHER, J W. and DROMGOOLE, P W. 2007. Exploring below the basalt, offshore Faroes: a case history of sub-basalt imaging. *Petroleum Geoscience*, Vol. **13**, pp. 213-225.

GRANT, N, BOUMA, A, and MCINTYRE, A. 1999. The Turonian play in the Faeroe-Shetland Basin. 661–673 in *Petroleum Geology of Northwest Europe, Proceedings of the 5th Conference*. FLEET, A J, and BOLDY, S A R (editors). (London: The Geological Society).

HASZELDINE, R S., RITCHIE, J D. and HITCHEN, K. 1987. Seismic and well evidence for the early development of the Faroe-Shetland Basin. *Scottish Journal of Geology*, Vol. **23**, (3), pp. 283-300.

HITCHEN, K. and RITCHIE, J D. 1987. Geological review of the West Shetland area. 737-749 in *Petroleum Geology of NW Europe, Proceedings of the 3rd Conference*. BROOKS, J. and GLENNIE, K.W (editors). (London: Graham and Trotman).

HODGES, S., LINE, C. and Evans, R. 1999. The Other Millenium Dome. *1999 Offshore Europe Conference*, Society of Petroleum Engineers, SPE 56895.R

JOHNSON, H, RITCHIE, J D, HITCHEN, K, MCINROY, D B. and KIMBELL, G S. 2005. Aspects of the Cenozoic deformational history of the northeast Faroe-Shetland Basin, Wyville-Thomson Ridge and Hatton Bank areas. 993–1007 in *Petroleum Geology: NW Europe and Global Perspectives: Proceedings of the 6th Conference*. DORÉ, A.G. and VINING, B (editors). (London: The Geological Society).

JOHNSON, H., QUINN, M F., KIMBELL, G S., STOKER, M S., SMITH, K., ÓLAVSDÓTTIR, J. and VARMING, T. 2012. Cenozoic pre- and post-breakup compression in the Faroe-Shetland area, within the context of the NE Atlantic. British Geological Survey Commissioned Report, CR/12/017.

KESER NEISH, J C. 2003. The Faroese Region: A Standard Structural Nomenclature System. Faroese Geological Survey, Tórshavn, Faroe Islands.

KIMBELL, G S, RITCHIE, J D, JOHNSON, H. and GATLIFF, R W. 2005. Controls on the structure and evolution of the NE Atlantic margin revealed by regional potential field imaging and 3D modelling. 933–945 in *Petroleum Geology: North-West Europe and Global Perspectives, Proceedings of the 6th Petroleum Geology Conference*. DORÉ, A G, and VINING, B A (editors). (London: The Geological Society).

KIMBELL, G S, MCINROY, D B, QUINN, M F. and ZISKA, H. 2010. The three-dimensional crustal structure of the Faroe-Shetland region. British Geological Survey Commissioned Report, CR/10/110.

KIMBELL, G S. 2014. Magnetic signatures of Paleogene igneous rocks in the Faroe-Shetland area. British Geological Survey Commissioned Report, CR/14/054.

KNOX, R W O'B., HOLLOWAY, S., KIRBY, G A. and BAILY, H E. 1997. Stratigraphic nomenclature of the UK North West Margin. 2. Early Paleogene lithostratigraphy and sequence stratigraphy. *In*: Knox, R.W.O'B. & Cordey, W.G. (eds) British Geological Survey, Nottingham.

LAMERS, E. and CARMICHAEL, S M M. 1999. The Paleocene deepwater sandstone play West of Shetland. 645–659 in *Petroleum Geology of Northwest Europe, Proceedings of the 5th Conference*. FLEET, A J, and BOLDY, S A R (editors). (London: The Geological Society).

LARSEN, M. and WHITHAM, A G. 2005. Evidence for a major sediment input point into the Faroe-Shetland Basin from the Kangerlussuaq region of southern East Greenland. 913–922 in *Petroleum Geology: North-West Europe and Global Perspectives, Proceedings of the 6th Petroleum Geology Conference*. DORÉ, A G, and VINING, B A (editors). (London: The Geological Society).

LARSEN, M., RASMUSSEN, T. and HJELM, L. 2010. Cretaceous revisited: exploring the syn-rift play of the Faroe-Shetland Basin. pp. 953-962 in *Petroleum Geology: From Mature Basins to New Frontiers – Proceedings of the 7th Petroleum Geology Conference.* VINING, B. A. & PICKERING, S.C. (editors). (London: The Geological Society).

LOIZOU, N., ANDREWS, I J. STOKER, S J. and CAMERON, D. 2006. West of Shetland revisited: the search for stratigraphic traps. pp. 225-245, *In* ALLEN, M R., GOFFEY, G P., MORGAN, R K. and WALKER, I M. (eds) 2006. *The Deliberate Search for the Stratigraphic Trap*. Geological Society, London, Special Publications, **254**, pp. 225–245.

LUNDIN, E R., DORÉ, A G., RØNNING, K. and KYRKJEBØ, R. 2013. Repeated inversion and collapse in the Late Cretaceous-Cenozoic northern Vøring Basin, offshore Norway. *Petroleum Geoscience*, Vol. **19**, pp. 329-341.

MAKRIS, J., PAPOULIA, I. and ZISKA, H. 2009. Crustal structure of the Shetland-Faroe Basin from long offset data. 30-42 in *Faroe Islands Exploration Conference. Proceedings of the 2nd Conference.* VARMING, T. and ZISKA, H. (editors). Annales Societatis Scientiarum Færoensis, Supplementum **50**.

MØLLER HANSEN, D and CARTWRIGHT, J. 2006. Saucer-shaped sill with lobate morphology revealed by 3D seismic data: implications for resolving a shallow-level sill emplacement mechanism. *Journal of the Geological Society, London*, Vol. **163**, pp. 509–523.

MOY, D J, and IMBER, J. 2009. A critical analysis of the structure and tectonic significance of rift-oblique lineaments ('transfer zones') in the Mesozoic–Cenozoic succession of the Faroe-Shetland Basin, NE Atlantic margin. *Journal of the Geological Society, London*, Vol. **166**, pp. 831–844.

MUDGE, D C. and RASHID, B. 1987. The geology of the Faeroe Basin area. 751-763 in *Petroleum Geology of NW Europe, Proceedings of the 3rd Conference*. BROOKS, J, AND GLENNIE, K W (editors). (London: Graham and Trotman).

NAYLOR, P H., BELL, B R., JOLLEY, D W., DURNALL, P. and FREDSTED, R. 1999. Paleogene magmatism in the Faroe-Shetland Basin: influences on uplift history and sedimentation. 545–558 in *Petroleum Geology of Northwest Europe, Proceedings of the 5th Conference*. FLEET, A J, and BOLDY, S A R (editors). (London: The Geological Society).

ÓLAVSDÓTTIR, J., ANDERSEN, M S. and BOLDREEL, L O. 2013. Seismic stratigraphic analysis of the Cenozoic sediments in the NW Faroe Shetland Basin – implications for inherited structural control of sediment distribution. *Marine and Petroleum Geology*, Vol. **46**, pp. 19-35.

OSMUNDSEN, P T. and EBBING, J. 2008. Styles of extension offshore mid-Norway and implications for mechanisms of crustal thinning at passive margins. *Tectonics*, Vol. 27. doi:10.1029/2007tc002242.

PLANKE, S., RASMUSSEN, T, REY, S S. and MYKLEBUST, R. 2005. Seismic characteristics and distribution of volcanic intrusions and hydrothermal vent complexes in the Vøring and Møre basins. Pp. 833-844 in *Petroleum Geology: North-West Europe and Global Perspectives, Proceedings of the 6th Petroleum Geology Conference*. DORÉ, A G, and VINING, B A (editors). (London: The Geological Society).

RASMUSSEN, J. and NOE-NYGAARD, A. 1970 (1969). Geology of the Faeroe Islands (Pre- Quaternary). Trans:Henderson,G. Geological Survey of Denmark, Copenhagen1/25.

RITCHIE, J D, JOHNSON, H. and KIMBELL, G S. 2003. The nature and age of Cenozoic contractional deformation within the NE Faroe-Shetland Basin. *Marine and Petroleum Geology*, Vol. **20**, pp. 399–409.

RITCHIE, J D, JOHNSON, H, QUINN, M F. and GATLIFF, R W. 2008. Cenozoic compressional deformation within the Faroe-Shetland Basin and adjacent areas. 121–136 in *The Nature and Origin of Compression in Passive Margins*. JOHNSON, H, DORÉ, A G, HOLDSWORTH, R E, GATLIFF, R W, LUNDIN, E R, and RITCHIE, J.D (editors). *The Geological Society, London, Special Publication*, No. 306.

RITCHIE, J D, ZISKA, H, JOHNSON, H. and EVANS, D (compilers). 2011. The Geology of the Faroe-Shetland Basin, and adjacent areas. *British Geological Survey Research Report*, RR/11/01, *Jarðfeingi Research Report*, RR/11/01.

RITCHIE, J D, ZISKA, H, KIMBELL, G, QUINN, M, and CHADWICK, A. 2011. Structure. 9–70 in *The Geology of the Faroe-Shetland Basin, and adjacent areas*. RITCHIE, J D, ZISKA, H, JOHNSON, H, and EVANS, D. (compilers). British Geological Survey, Edinburgh and Jarðfeingi, Torshavn.

ROBERTS, D G, THOMSON, M, MITCHENER, B, HOSSACK, J, CARMICHAEL, S. and BJORNSETH, H -M. 1999. Palaeozoic to Tertiary rift and basin dynamics: mid-Norway to the Bay of Biscay- a new context for hydrocarbon prospectivity in the deep water frontier. pp. 7–40 in *Petroleum Geology of Northwest Europe, Proceedings of the 5th Conference*. FLEET, A J, and BOLDY, S A R (editors). (London: The Geological Society).

ROBINSON, A M., CARTWRIGHT, J A., BURGESS, P.M. and DAVIES, R J. 2004. Interactions between topography and channel development from 3D seismic analysis: an example from the Tertiary of the Flett Ridge, Faroe-Shetland Basin, UK. pp.73-82 in *3D Seismic Technology: Application to the Exploration of Sedimentary Basins,* Geological Society, London. Memoirs, **29** DAVIES, R.J., CARTWRIGHT, J.A., STEWART, S.A., LAPPIN, M and UNDERHILL, J.R. (eds).

RUMPH, B, REAVES, C M, ORANGE, V G. and ROBINSON, D L. 1993. Structuring and transfer zones in the Faeroe Basin in a regional tectonic context. pp. 999–1009 in *Petroleum Geology of Northwest Europe, Proceedings of the 4th Conference*. PARKER, J.R. (editor). (London: The Geological Society).

SCLATER, J G. and CHRISTIE, P A F. 1980. Continental stretching: an explanation of the post-mid-Cretaceous subsidence of the central North Sea basin. *Journal of Geophysical Research*, Vol. 85, 3711–3739.

SMALLWOOD, J R. and MARESH, J. 2002. The properties, morphology and distribution of igneous sills: modelling, borehole data and 3D seismic from the Faroe-Shetland area. 271-306 in *The North Atlantic Igneous Province: Stratigraphy, Tectonic, Volcanic and Magmatic Processes.* JOLLEY, D.W. and BELL, B.R. (editors). *The Geological Society, London, Special Publication*, No. 197.

SMALLWOOD, J R., PRESCOTT, D. and KIRK, W. 2004. Alternatives in Paleocene exploration West of Shetland: a case study. *Scottish Journal of Geology*, Vol. **40** (2), pp. 131–143.

SMALLWOOD, J R. 2004. Tertiary inversion in the Faroe-Shetland Channel and the development of major erosional scarps. pp.187-198 in *3D Seismic Technology: Application to the Exploration of Sedimentary Basins,* Geological Society, London. Memoirs, **29** DAVIES, R J., CARTWRIGHT, J A., STEWART, S A., LAPPIN, M and UNDERHILL, J R. (eds).

SMITH, K., STOKER, M.S., JOHNSON, H. and EIDESGAARD, Ó. 2013. Early Paleogene stratigraphy, volcanism and tectonics of the Faroe-Shetland region. British Geological Survey Commissioned Report, CR/13/006.

SMITH, K., STOKER, M S., JOHNSON, H. and ÓLAVSDÓTTIR, J. 2014. Seismic stratigraphy and tectonics of the Stronsay Group (Eocene) in the Faroe-Shetland region. British Geological Survey Commissioned Report, CR/14/024.

STOKER, M S., McINROY, D B., JOHNSON, H. and RITCHIE, J D. 2010. Cretaceous tectonostratigraphy of the Faroe-Shetland Region. British Geological Survey Commissioned Report, CR/10/144.

STOKER, M S., SMITH, K., VARMING, T., JOHNSON, H. and ÓLAVSDÓTTIR, J. 2012. Eocene (Stronsay Group) post-rift stratigraphy of the Faroe-Shetland region. British Geological Survey Commissioned Report, CR/12/009.

TASSONE, D R., HOLFORD, S P., STOKER, M S., GREEN, P., JOHNSON, H., UNDERHILL, J R. and HILLIS, R R. 2014. Constraining Cenozoic exhumation in the Faroe-Shetland region using sonic transit time data. *Basin Research*, Vol. **26**, pp. 38-72.

TATE, M.P., DODD, C.D. and GRANT, N.T. 1999. The Northeast Rockall Basin and its significance in the evolution of the Rockall-Faroes/East Greenland rift system. pp. 391–406 in *Petroleum Geology of Northwest Europe, Proceedings of the 5th Conference*. FLEET, A J, and BOLDY, S A R (editors). (London: The Geological Society).

TRUDE, K.J. 2004. Kinematic indicators for shallow level igneous intrusions from 3D seismic data: evidence of flow direction and feeder location. pp.209-217 in *3D Seismic Technology: Application to the Exploration of Sedimentary Basins,* Geological Society, London. Memoirs, **29** DAVIES, R J., CARTWRIGHT, J A., STEWART, S A., LAPPIN, M and UNDERHILL, J R. (eds).

TUITT, A., UNDERHILL, J R., RITCHIE, J D., JOHNSON, H. & HITCHEN, K. 2010. Timing, controls and consequences of compression in the Rockall–Faroe area of the NE Atlantic Margin. *In*: Vining, B A. & Pickering, S C. (eds) *Petroleum Geology: From Mature Basins to New Frontiers –Proceedings of the 7th Petroleum Geology Conference*. Geological Society, London, 963–977, http://dx.doi.org/: 10.1144/0070963.

VERSTRALEN, I., HARTLEY, A. and HURST, A. 1995. The sedimentological record of a late Jurassic transgression: Rona Member (Kimmeridge Clay Formation equivalent), West Shetland Basin, UKCS. 155–176 in *Characterisation of Deep Marine Clastic Systems*. HARTLEY, A.J. and PROSSER, D.J. (editors). *The Geological Society, London, Special Publication*, No. 94.

ZISKA, H. and VARMING, T. 2008. Paleogene evolution of the Ymir and Wyville Thomson ridges, European North Atlantic margin. 153-168 in *The Nature and Origin of Compression in Passive Margins.* JOHNSON, H, DORÉ, A G, HOLDSWORTH, R E, GATLIFF, R W, LUNDIN, E R, and RITCHIE, J D (editors). *The Geological Society, London, Special Publication*, No. 306.

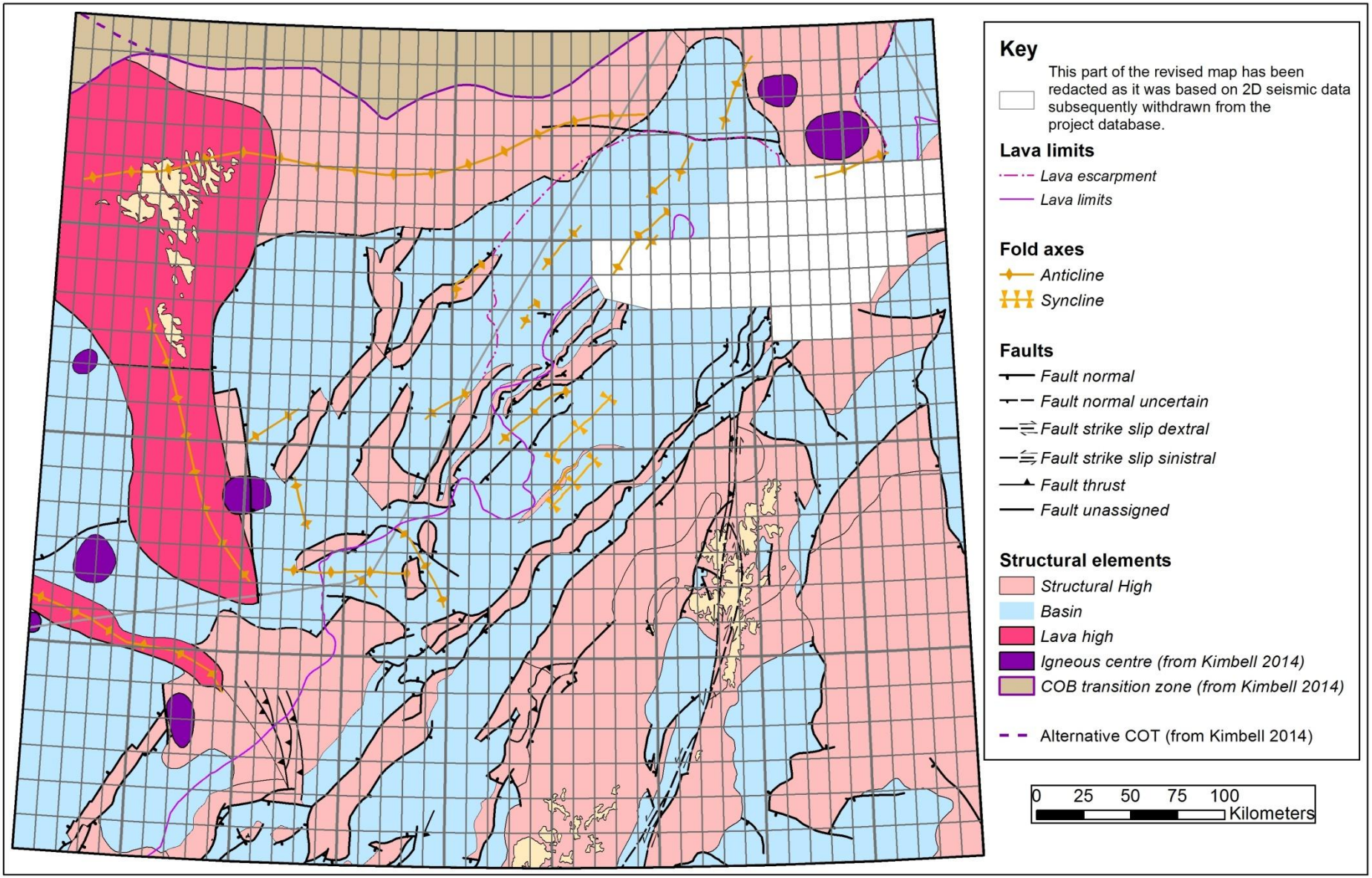

Figure 1. A revised structural elements map for the Faroe-Shetland Basin and adjacent areas, see text for details.

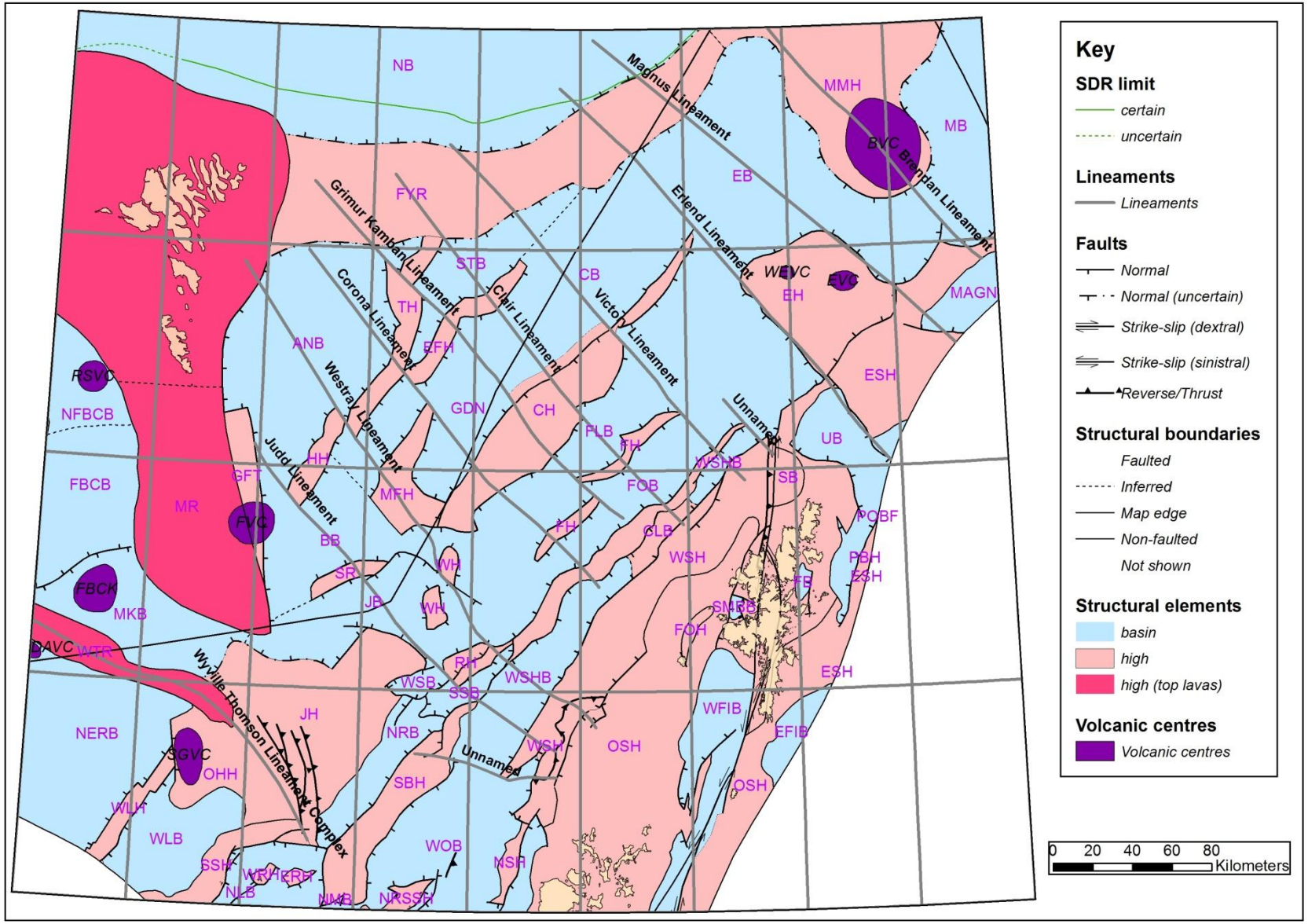

Figure 2. Detail from the structural elements map of the Faroe-Shetland area of Ritchie et al. (2011) (their Figure 7), covering the study area.

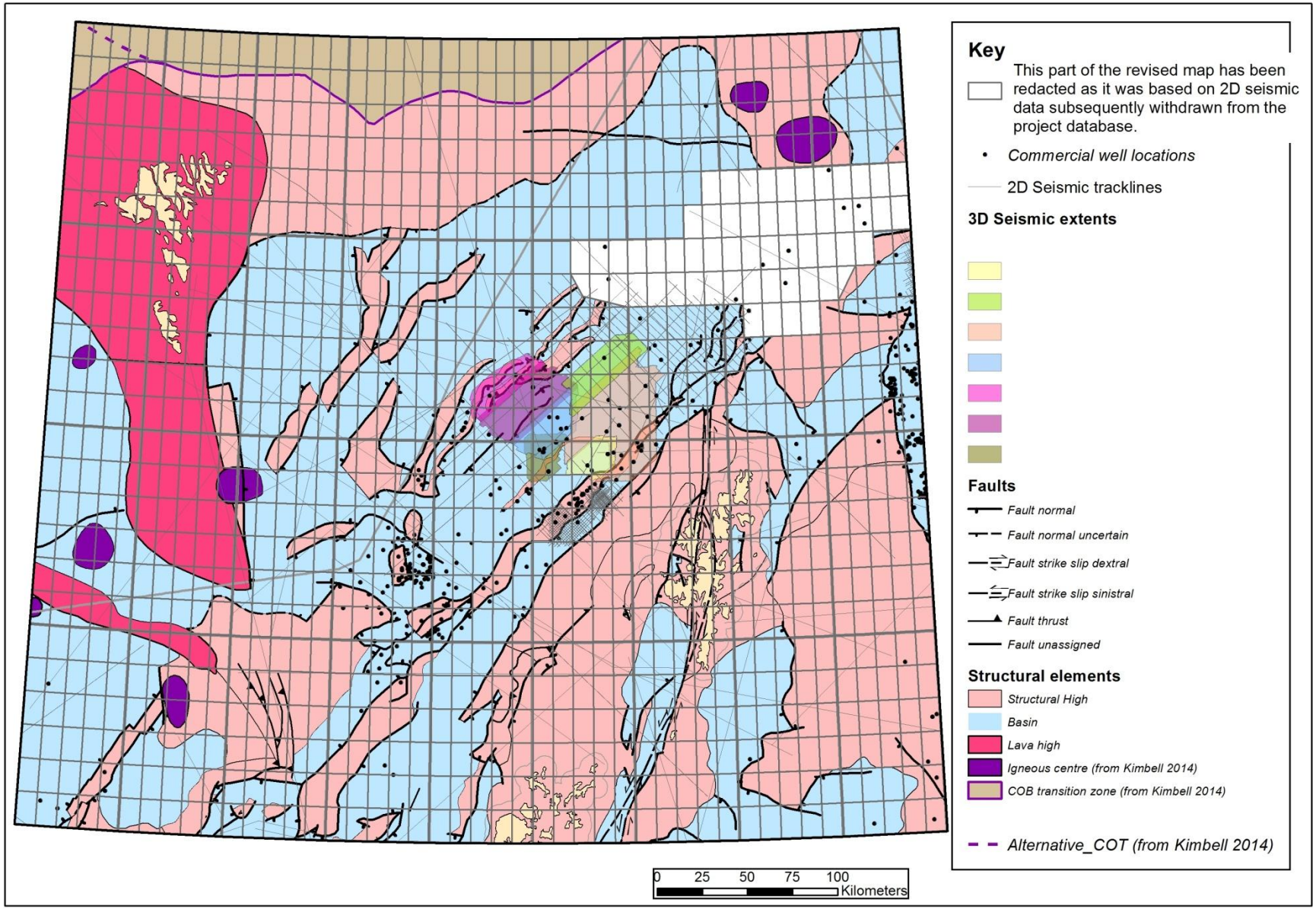

Figure 3. FSC seismic and (released) well database used in this study, superimposed on the revised structural element map.

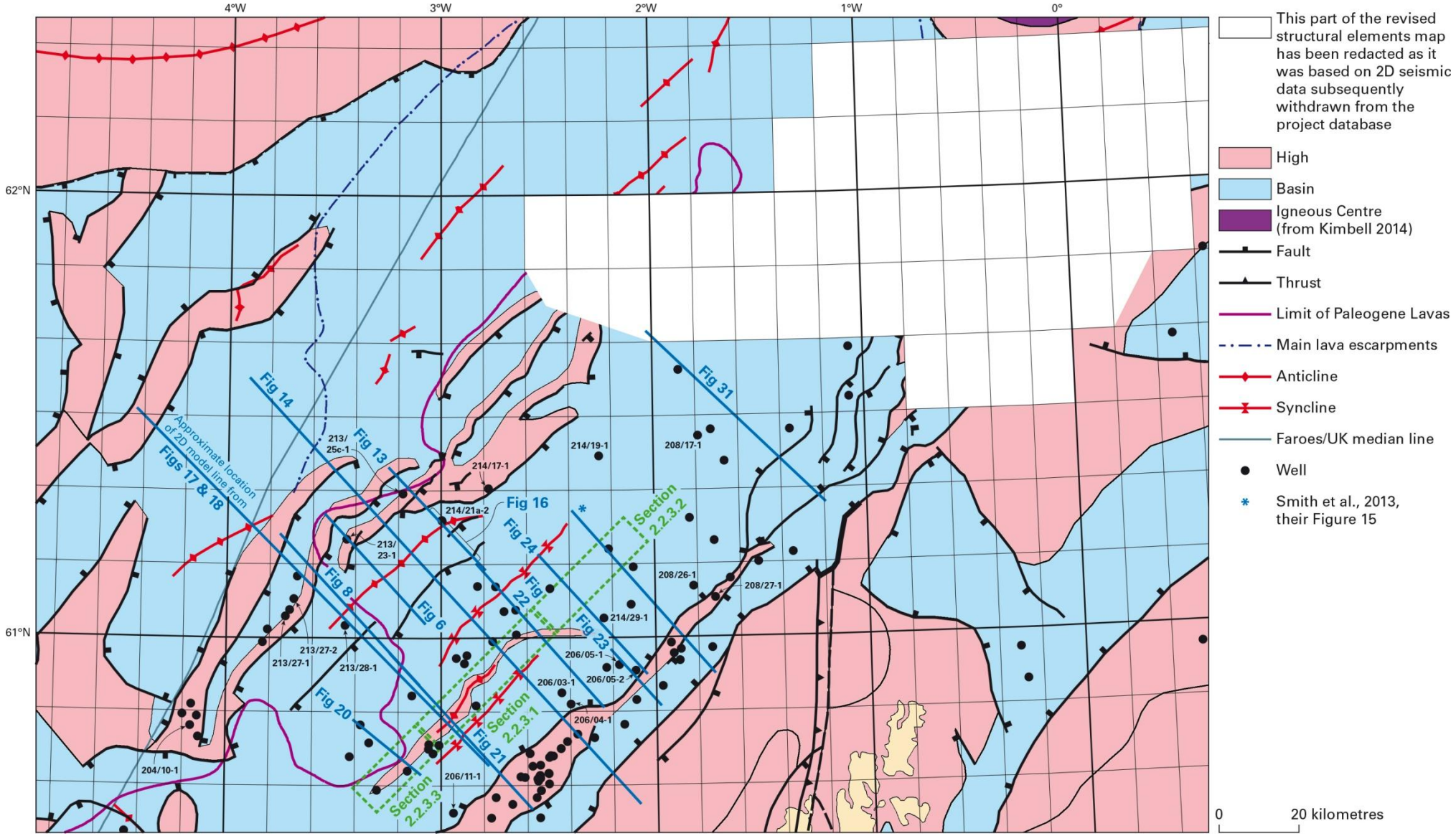

Figure 4. Detail of the revised structural elements map showing location of illustrated seismic profiles and figures adapted from published sources referred to in this report.

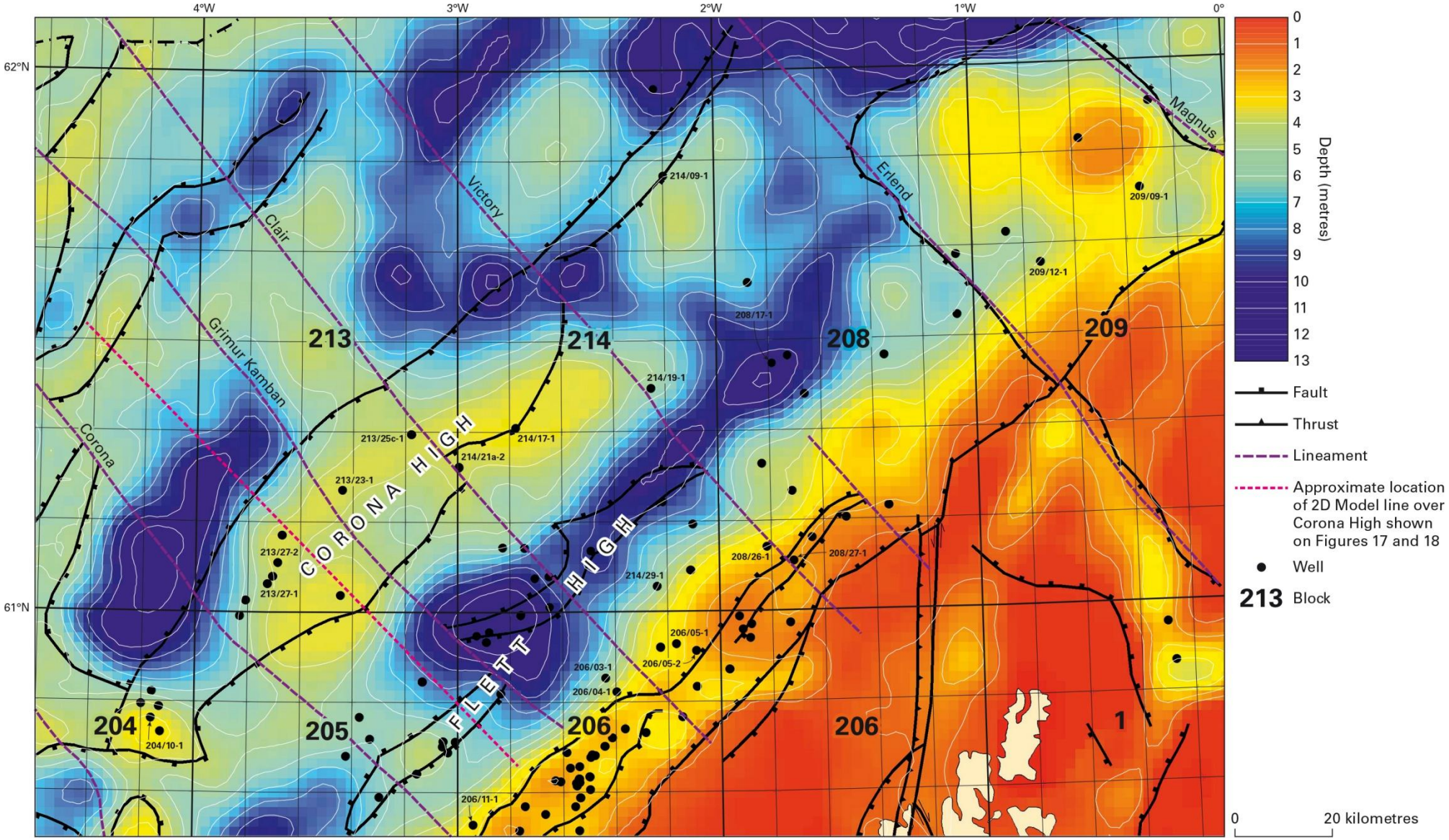

Figure 5. Depth to top crystalline basement based on 3D gravity modelling (Kimbell et al., 2010) superimposed with outlines of structural elements from Ritchie et al. (2011). Note the contrasting extents of the Corona High derived from these two sources.

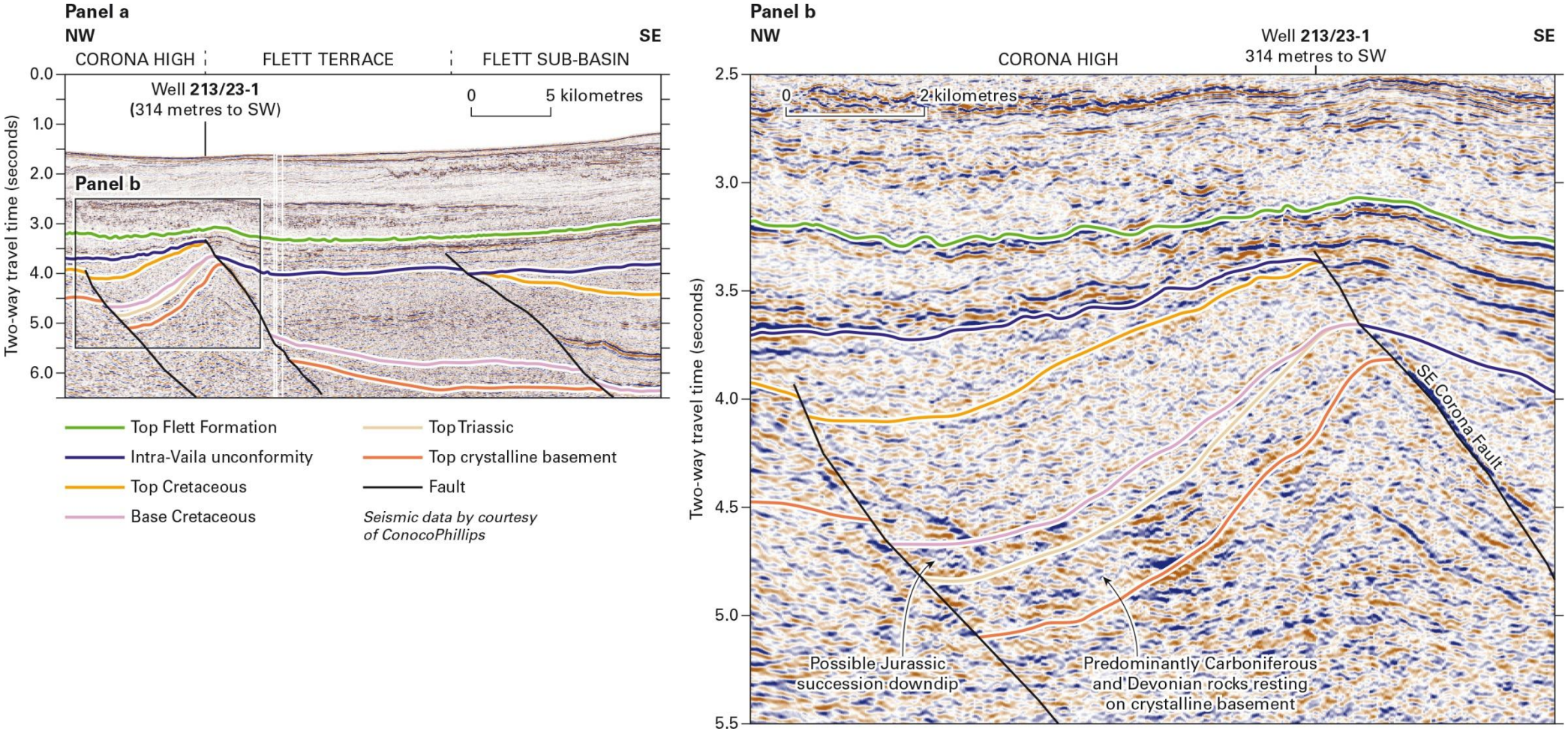

Figure 6. NW-trending seismic profile across Corona High close to well 213/23- 1 and extending across Flett Terrace (Panel a). Note interpreted truncation of the Cretaceous succession beneath the Intra-Vaila Unconformity. See Figure 4 for location of profile.

Figure 7. This figure has been redacted as it was based on 2D seismic data subsequently withdrawn from the project database.

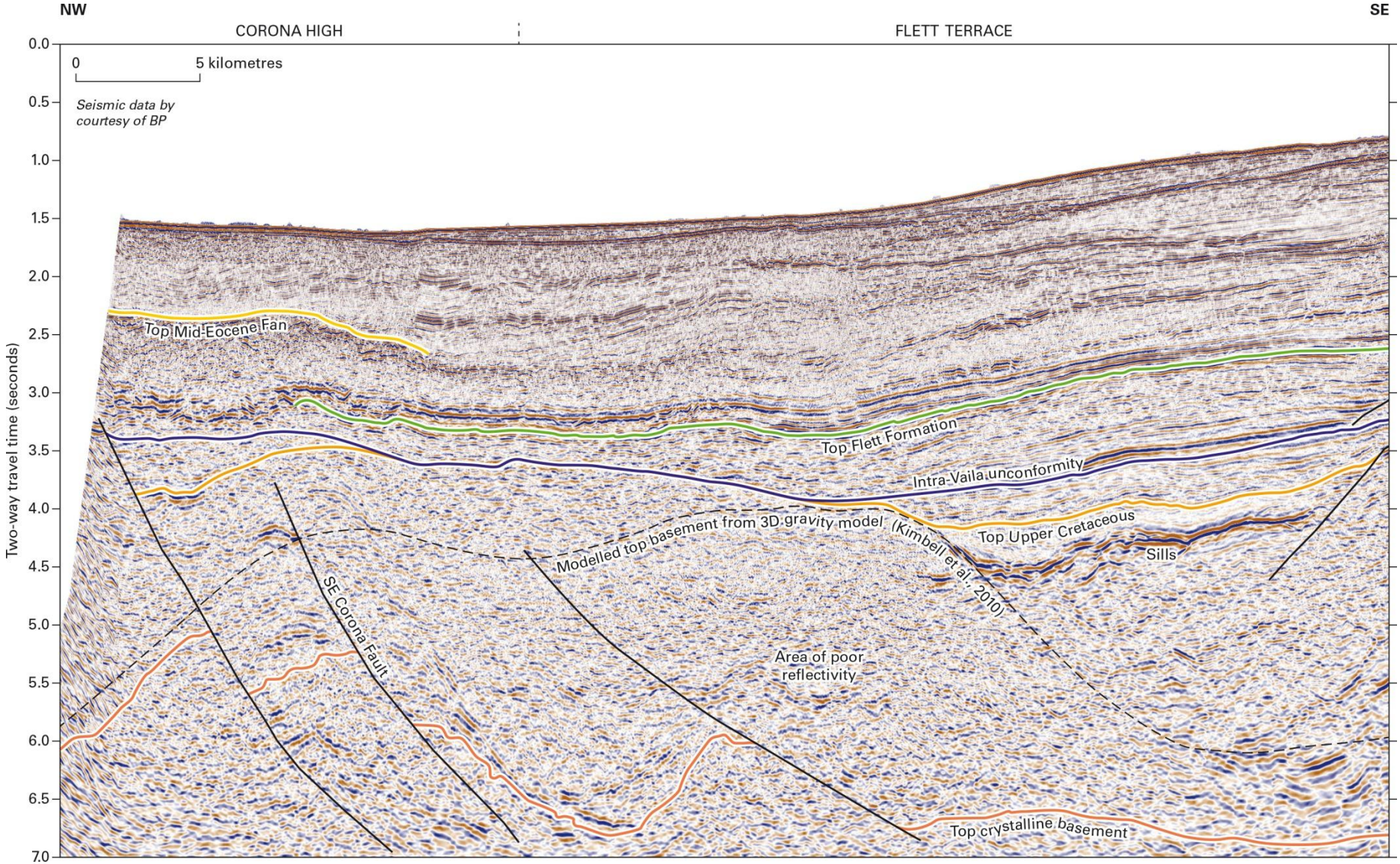

Figure 8. NW-trending seismic profile comparing modelled depth to basement and top crystalline basement pick. Note discrepancy between gravity-derived basement and seismic basement pick over the Flett Terrace. See Figure 4 for location of profile.

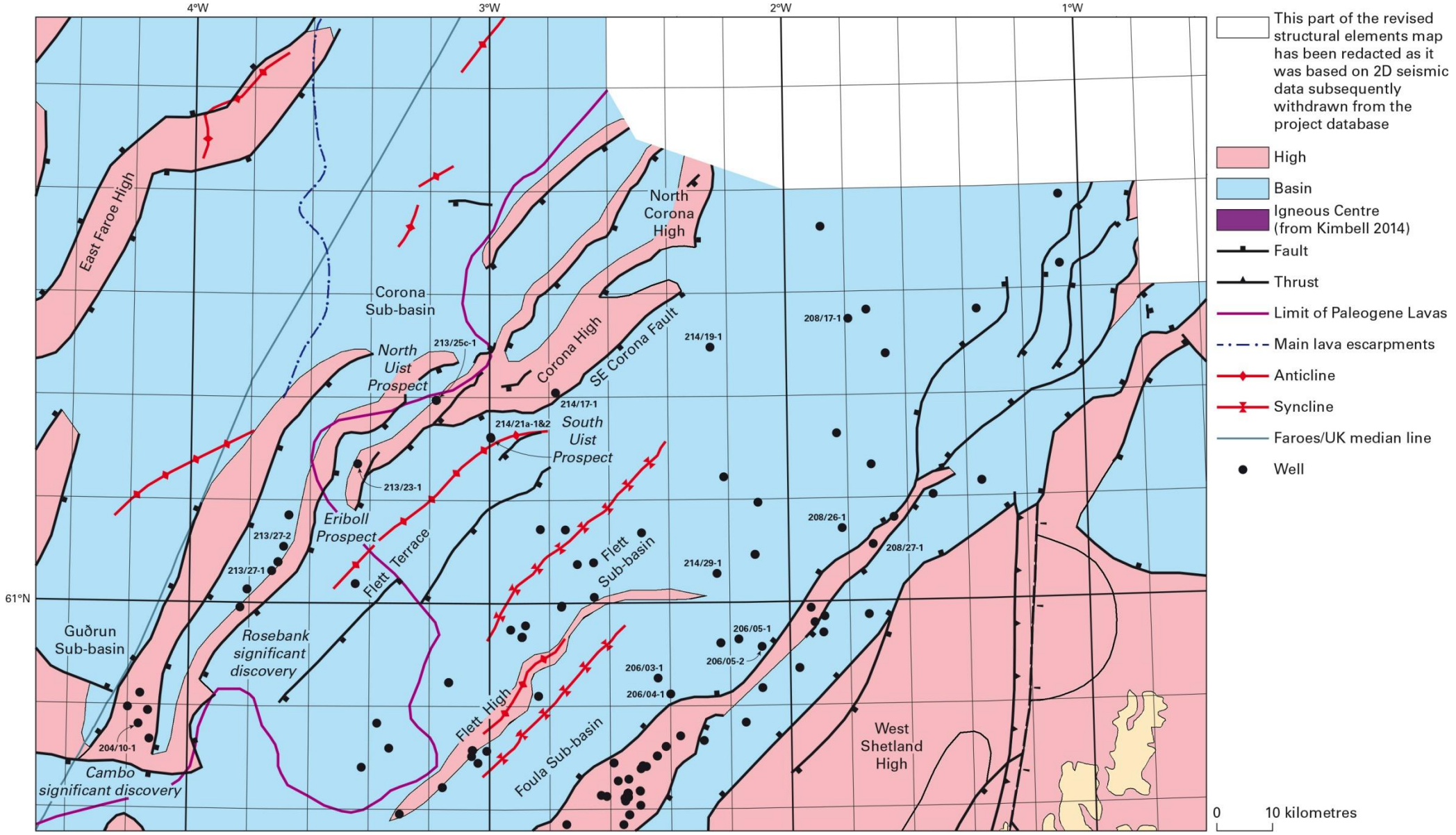

Figure 9. Detail from the revised structural elements map showing the new interpretation over the Corona and Flett highs.

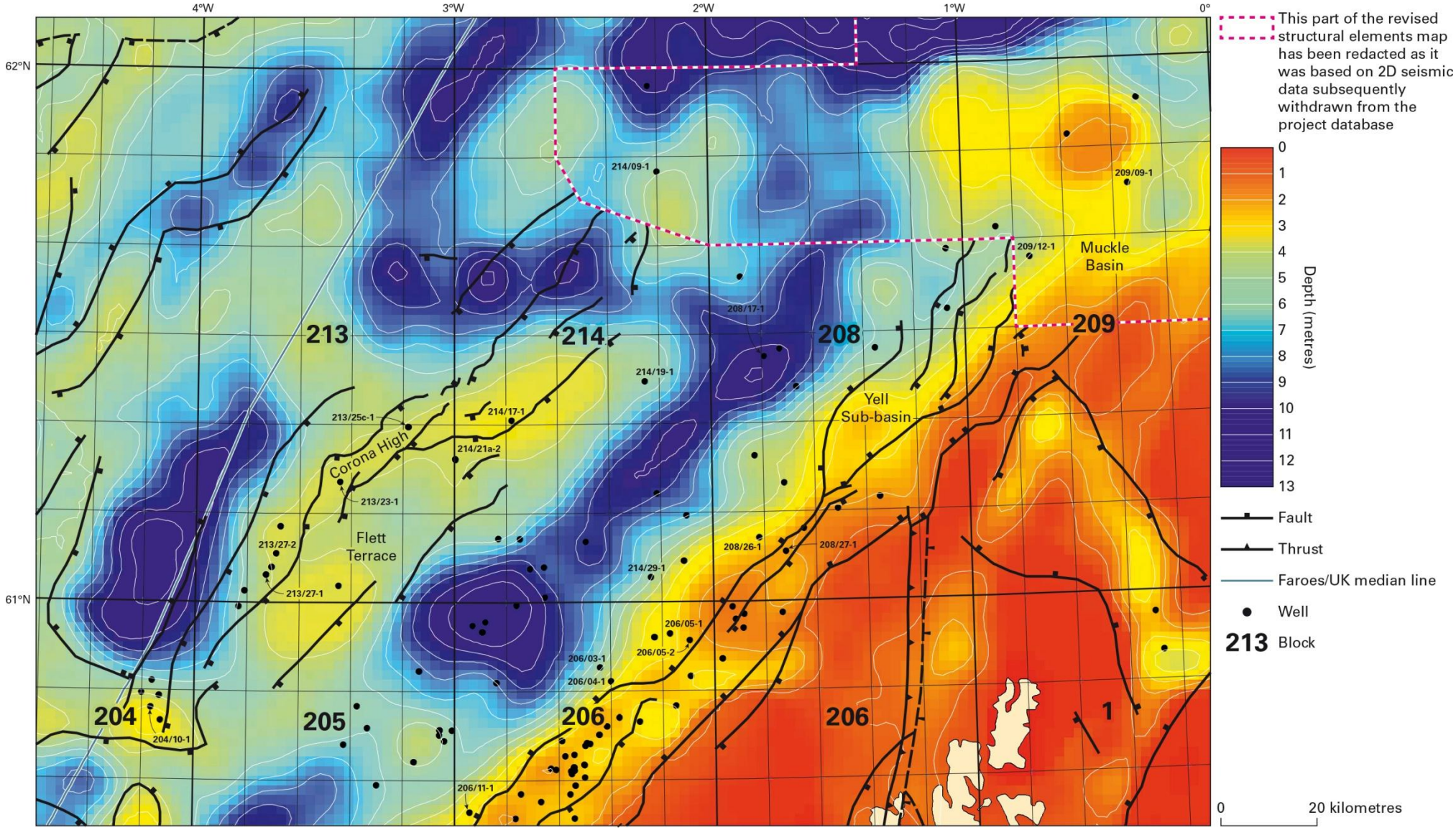

Figure 10. Depth to top crystalline basement based on 3D gravity modelling (Kimbell et al., 2010) superimposed with outlines of the new interpretation over the Corona High.

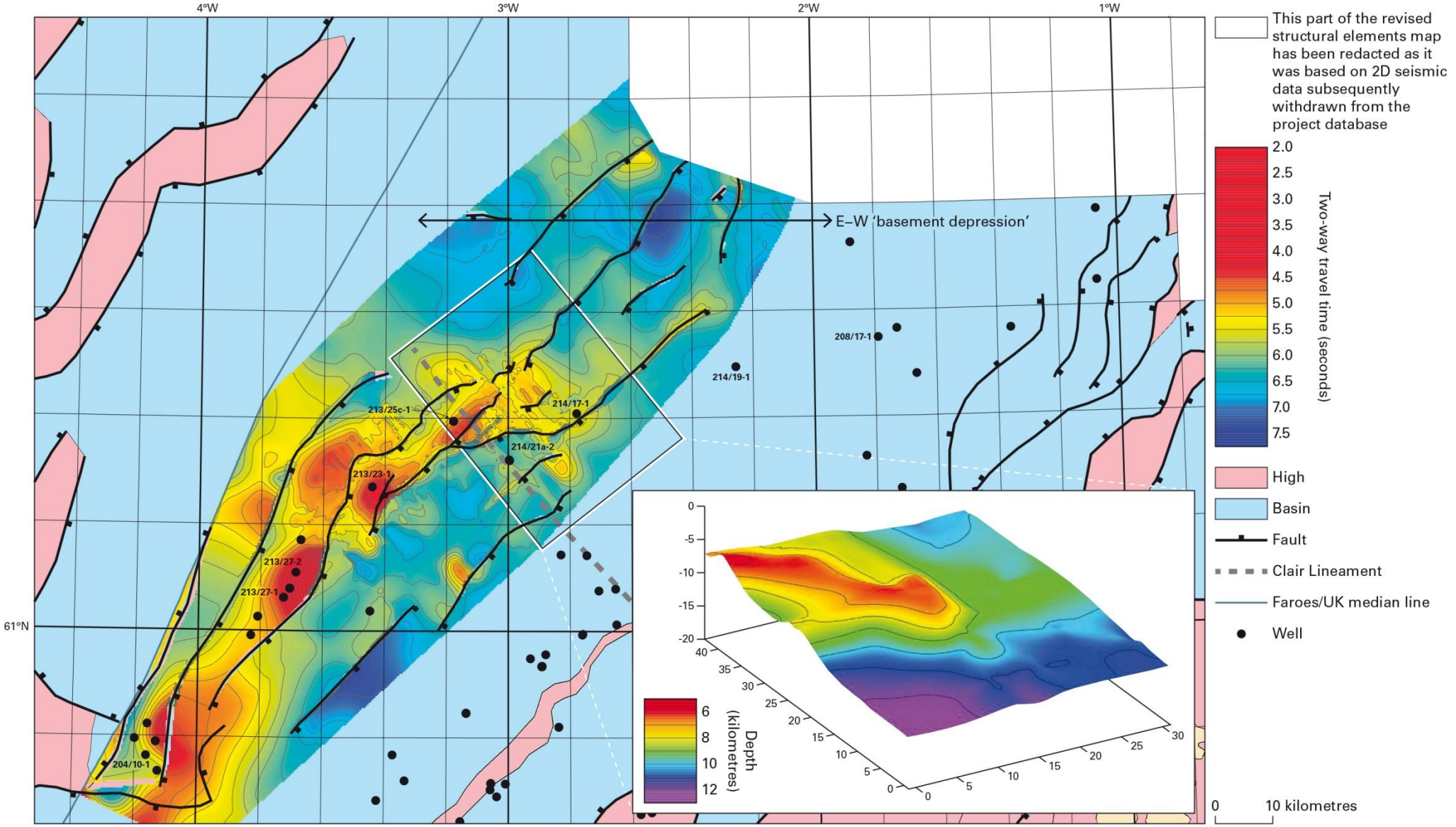

Figure 11. TWTT to interpreted top crystalline basement over the Corona High. Note basement culminations, E-W 'basement depression', horst within the North Corona High. Orientation of and variation in depth to crystalline basement from Makris et al. (2009) shown.

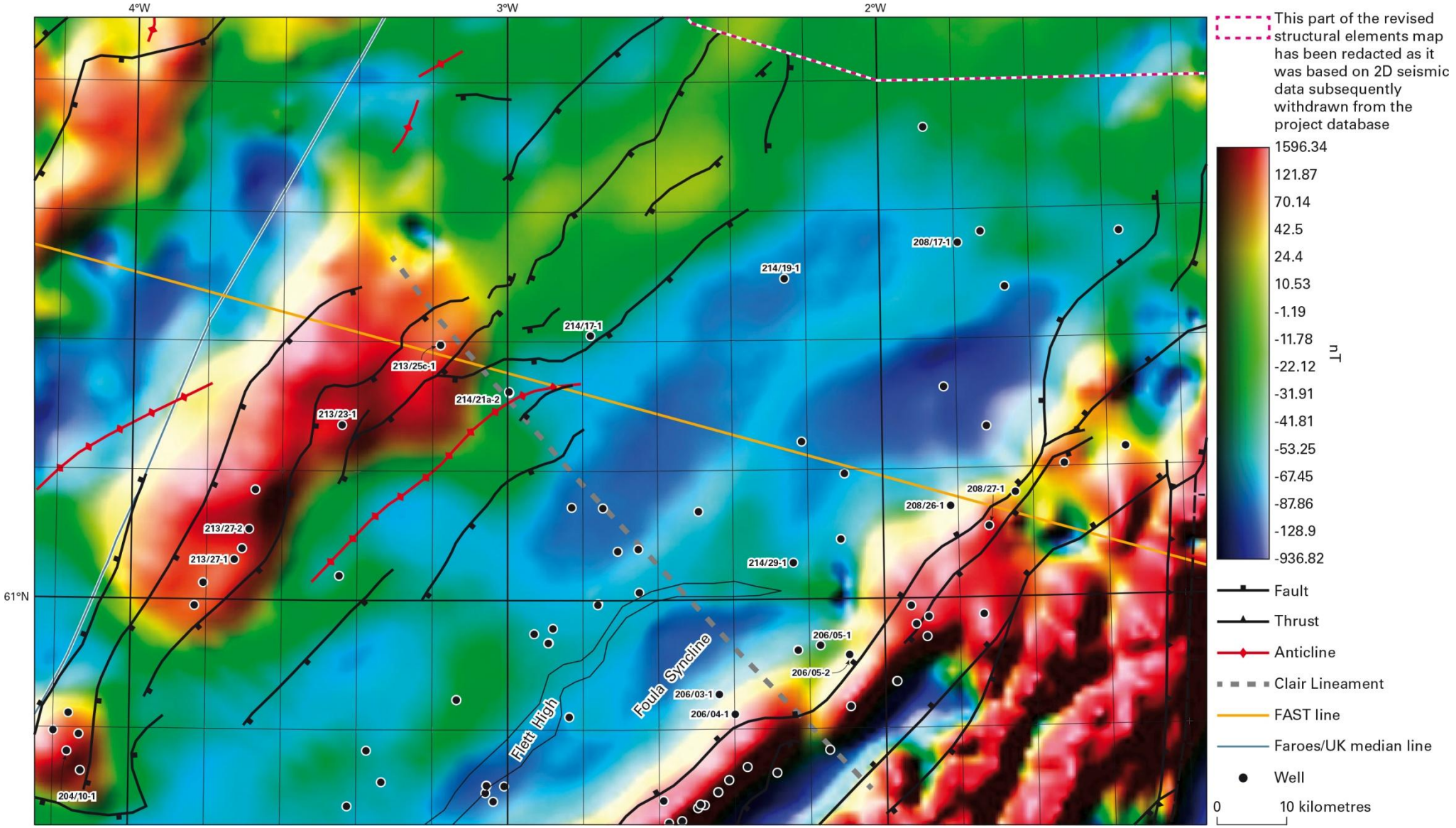

Figure 12. A new image of residual reduced to pole magnetic response over the Corona and Flett highs including location of Clair Lineament. Note relatively sharp decrease in the Corona High magnetic field to NE of postulated lineament.

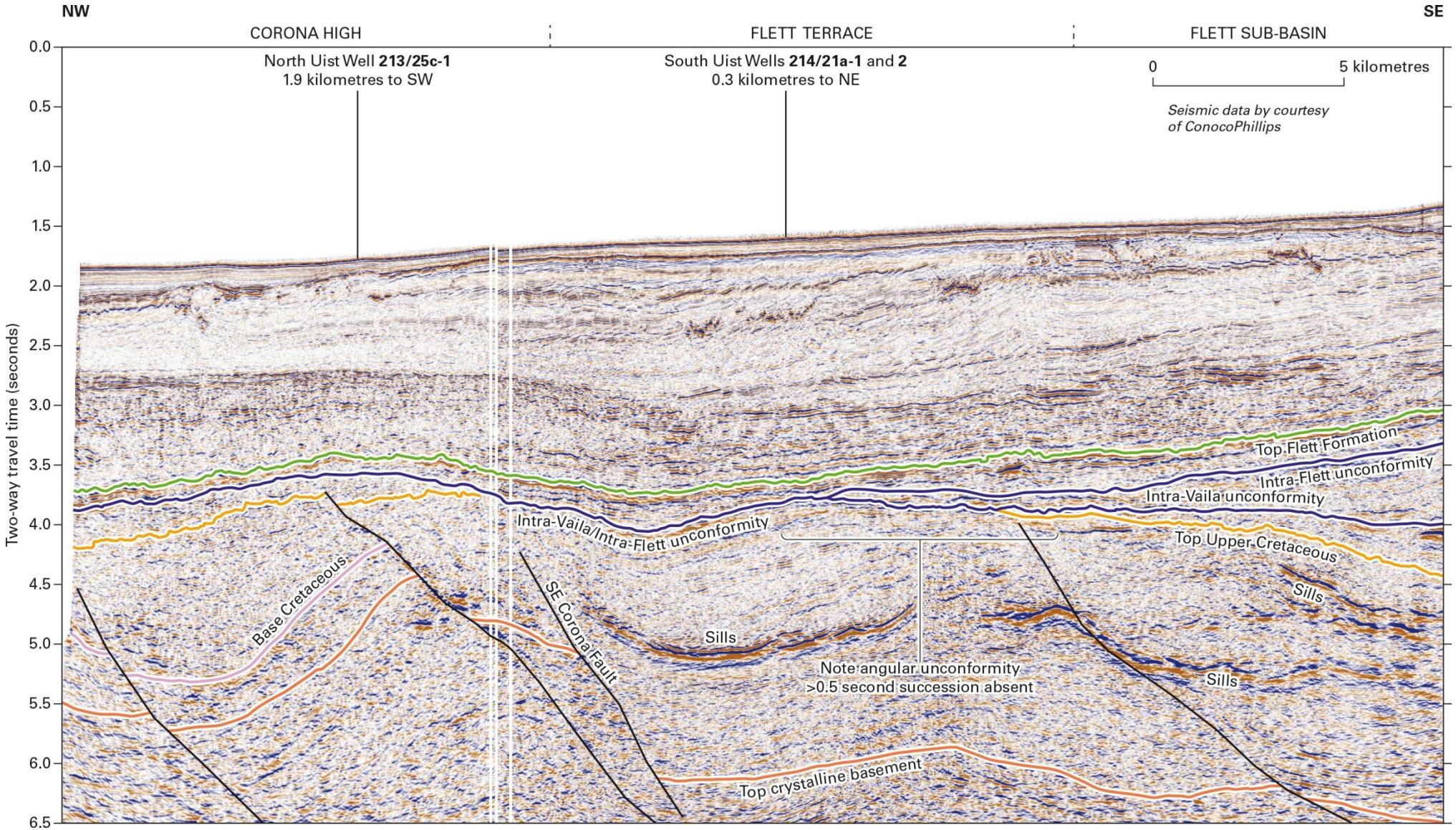

Figure 13. NW-trending seismic profile close to locations of North and South Uist exploration wells showing angular unconformity between the Late Cretaceous and early Paleocene succession. See Figure 4 for location of profile.

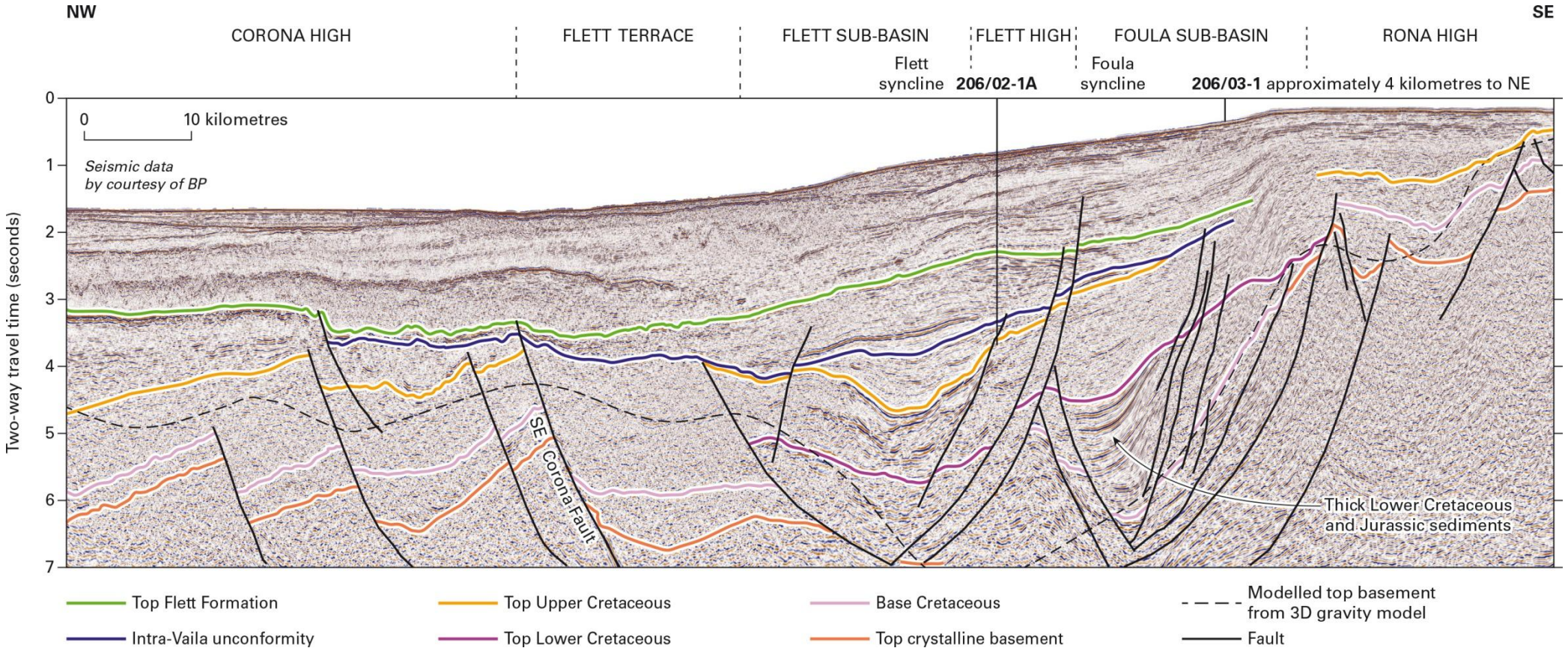

Figure 14. Regional NW-trending interpreted seismic profile showing stratigraphic and structural relationships across the Corona High, Flett Terrace, Flett High, Foula Sub-basin and Rona High. See Figure 4 for location of the profile.

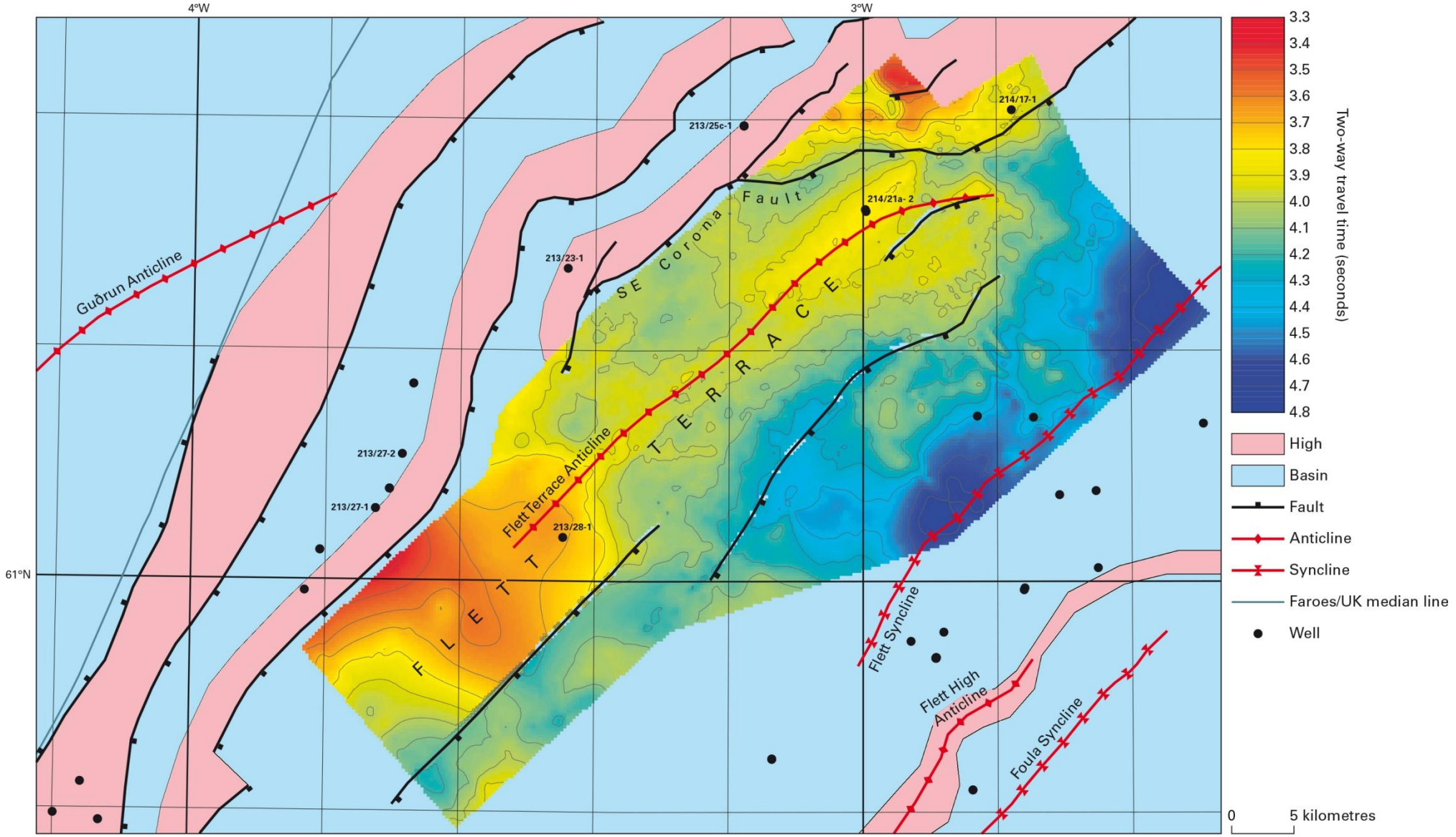

Figure 15. TWTT to interpreted Top Cretaceous Unconformity on the Flett Terrace showing a NE-trending anticlinal structure associated with the 'step-over' in the SE Corona Fault.

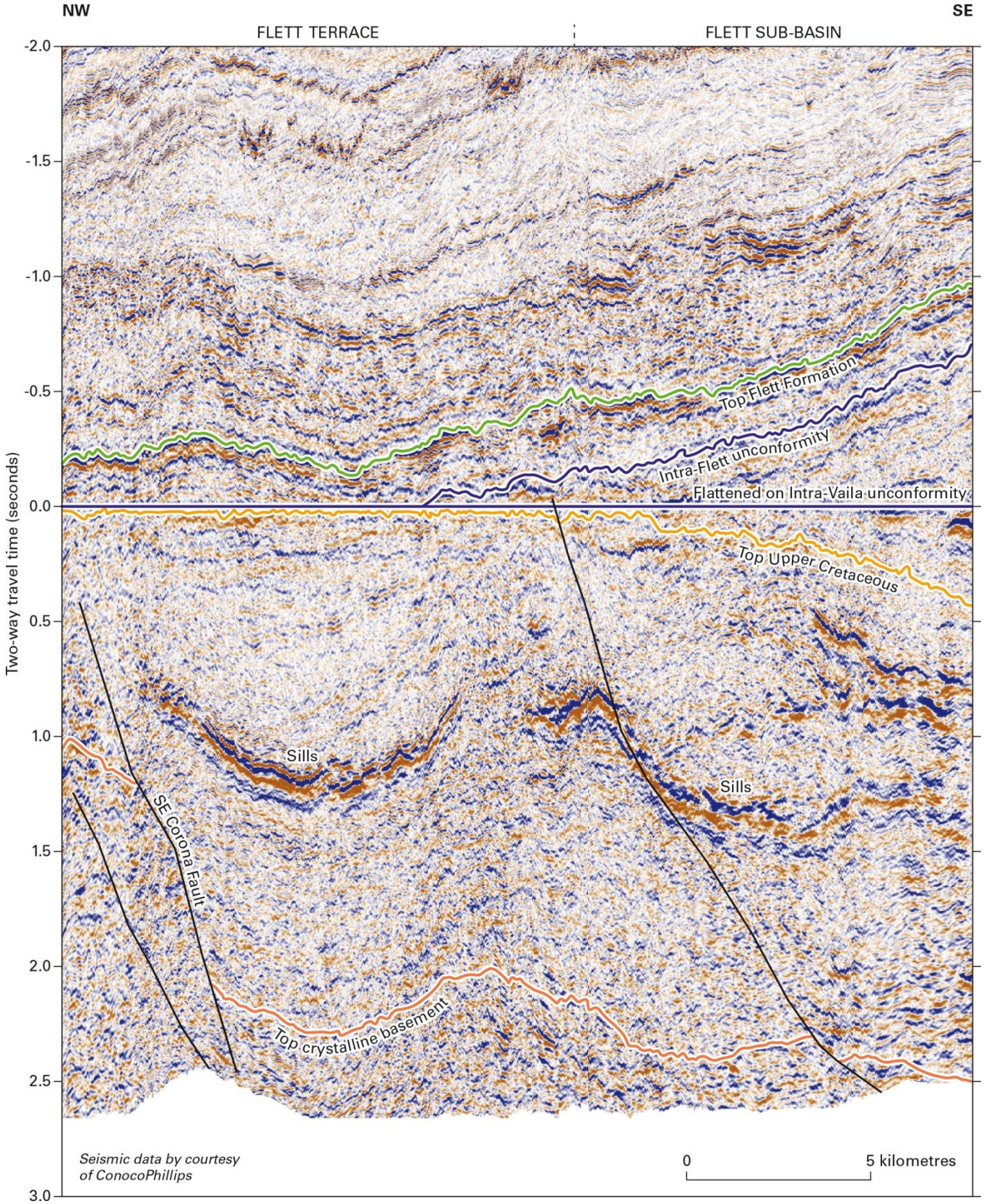

Figure 16. NW-trending seismic profile showing relationship of seismic reflectors on flattened Intra-Vaila Unconformity on the Flett Terrace close to South Uist wells 214/21a- 1 & 2. See Figure 4 for location of profile.

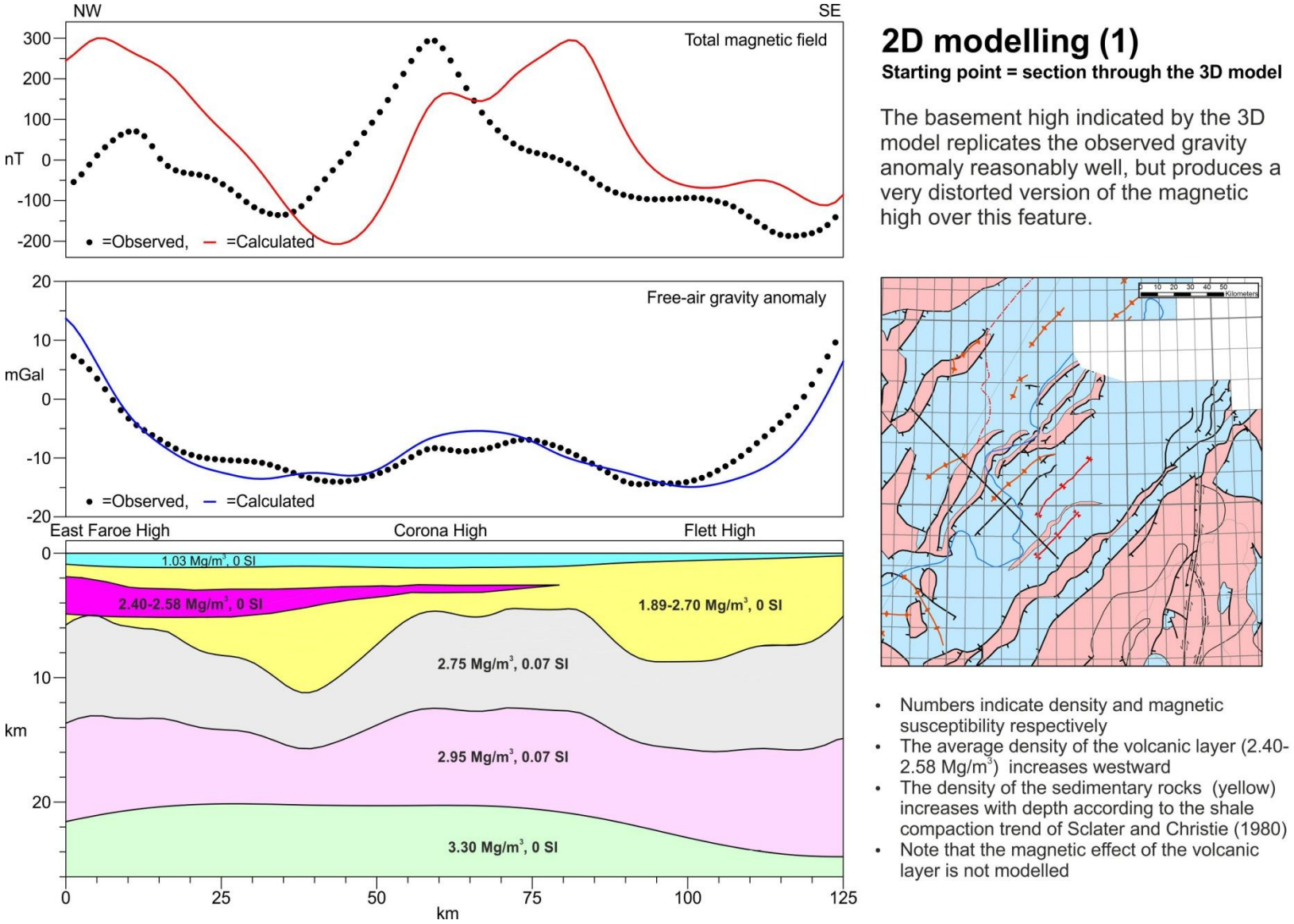

2D modelling (1)

Starting point = section through the 3D model

The basement high indicated by the 3D model replicates the observed gravity anomaly reasonably well, but produces a very distorted version of the magnetic high over this feature.

- Numbers indicate density and magnetic susceptibility respectively
- The average density of the volcanic layer (2.40-2.58 Mg/m^3) increases westward
- The density of the sedimentary rocks (yellow) increases with depth according to the shale compaction trend of Sclater and Christie (1980)
- Note that the magnetic effect of the volcanic layer is not modelled

Figure 17. 2D section through the 3D model of Kimbell et al. (2010) showing calculated gravity and magnetic response compared to that observed over the Corona High. See Figures 4 and 5 for location of the profile.

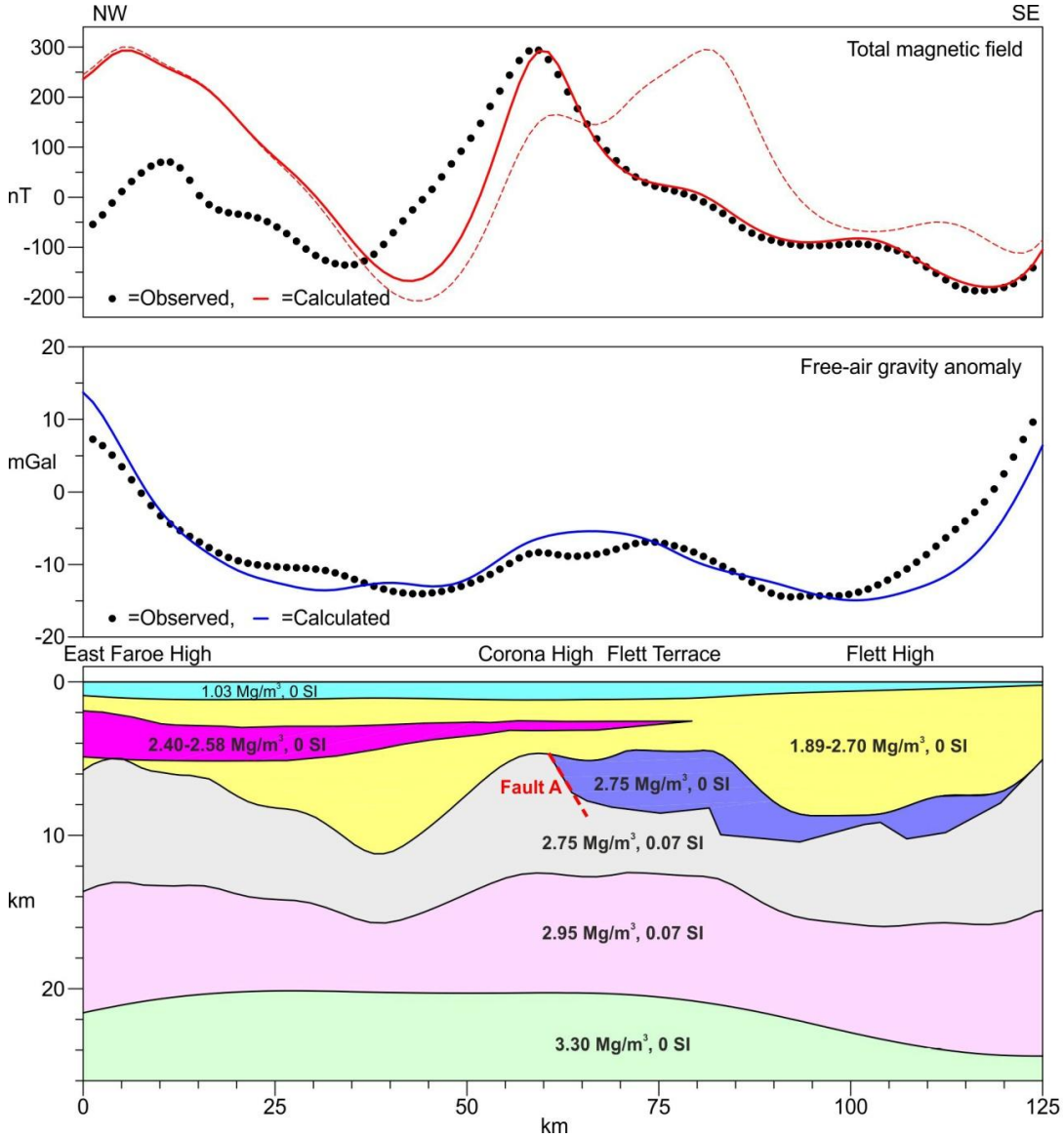

2D modelling (2)

Starting point = section through the 3D model

Introducing a zone of high density, non-magnetic rocks allows better reproduction of the magnetic anomalies on the SE side of the Corona High. The NW edge of this zone correlates well with Fault A inferred from seismic data.

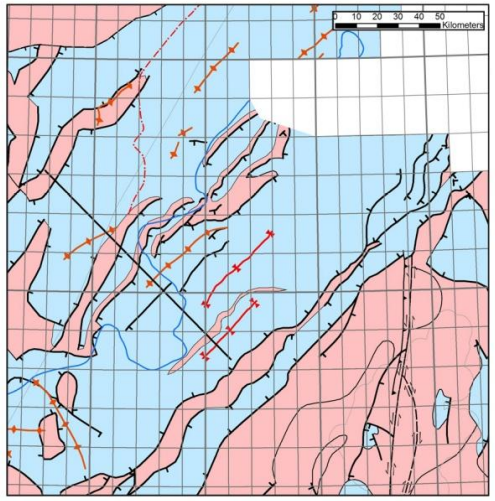

- Numbers indicate density and magnetic susceptibility respectively
- The average density of the volcanic layer (2.40-2.58 Mg/m^3) increases westward
- The density of the sedimentary rocks (yellow) increases with depth according to the shale compaction trend of Sclater and Christie (1980)
- Note that the magnetic effect of the volcanic layer is not modelled

Figure 18. Calculated gravity and magnetic interpretation over a new interpretation of Corona High that includes downfaulted magnetic basement overlain by non-magnetic but relatively dense rocks in hanging wall of Fault A. See Figs. 4 & 5 for location of profile.

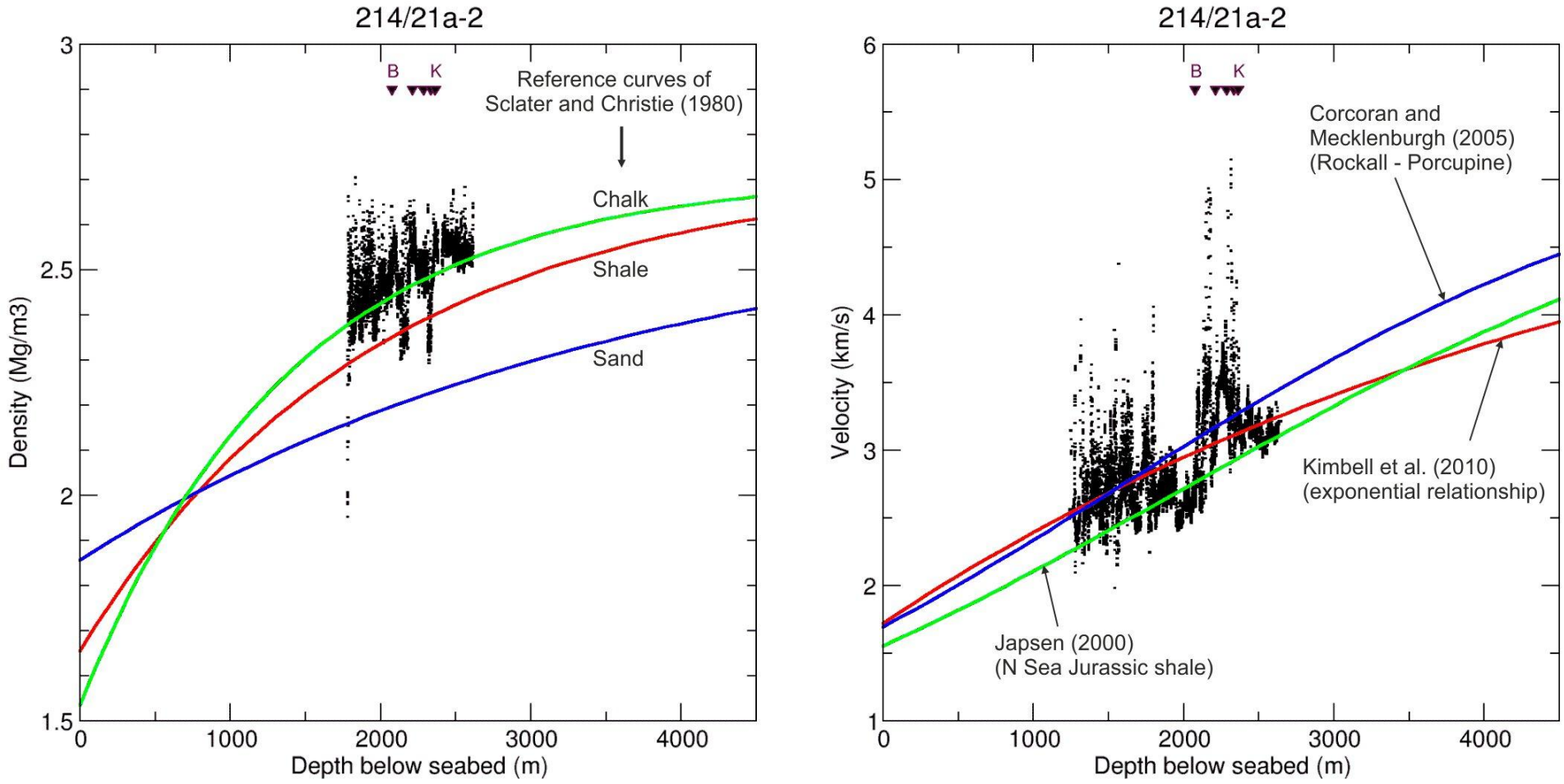

Figure 19. Density and velocity variation with depth below seabed in Upper Cretaceous, Paleocene and Eocene sediments for well 214/21a- 2.

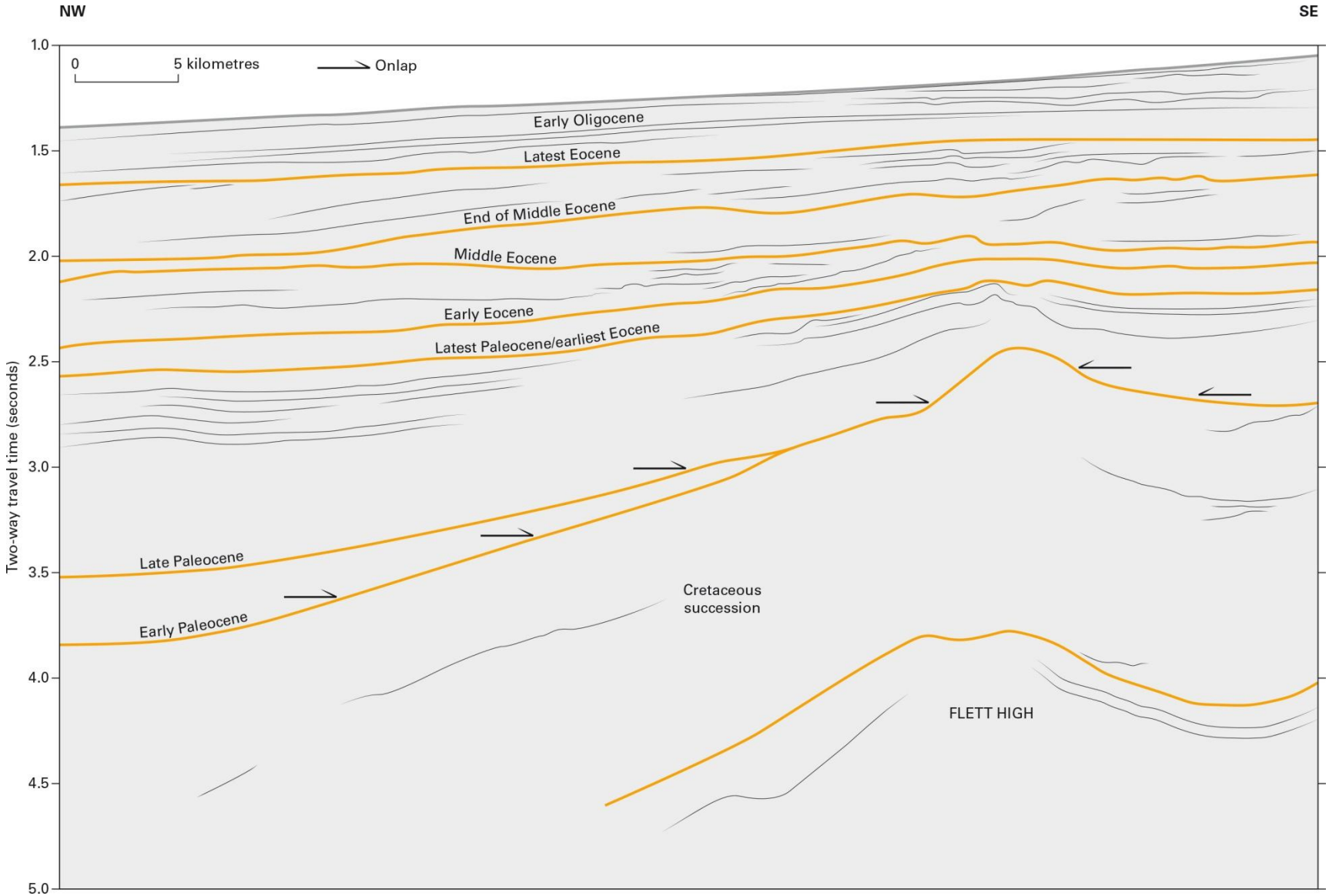

Figure 20. Line drawing of seismic profile interpreted by Robinson et al. (2004) (their Figure 3) showing seismic onlap of Paleocene succession onto the south-western Flett High in Blocks 205/09 and 205/10. See Figure 4 for location of profile.

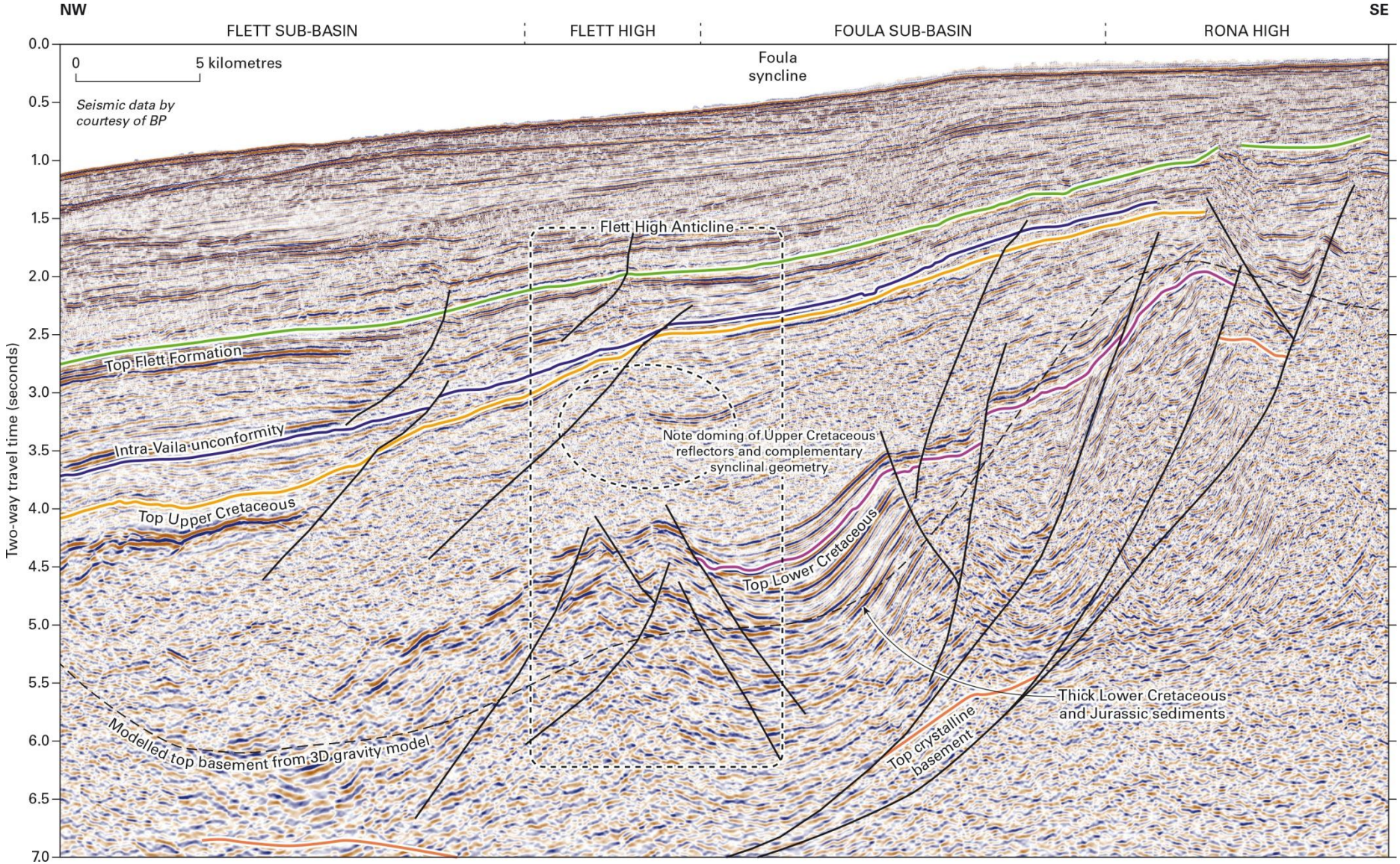

Figure 21. NW-trending interpreted seismic profile illustrating the structure of the Flett High and the adjacent Foula Syncline. See Figure 4 for location of the profile.

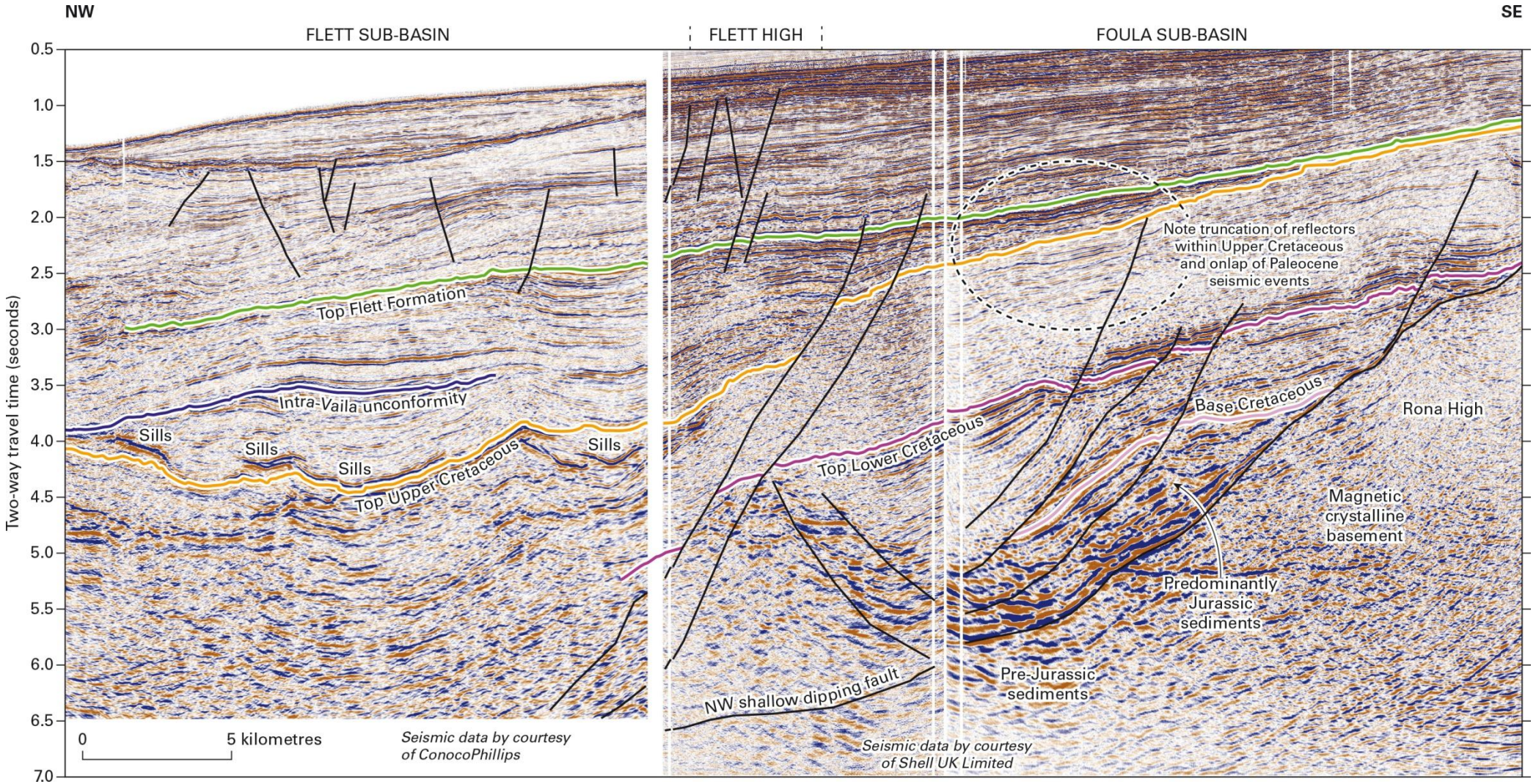

Figure 22. Multipanel display comprising 3 NW-trending interpreted seismic profiles showing the Flett High and adjacent sedimentary successions in the Flett Sub-basin and Foula Syncline and its onlap to the Rona High. See Figure 4 for location of profile.

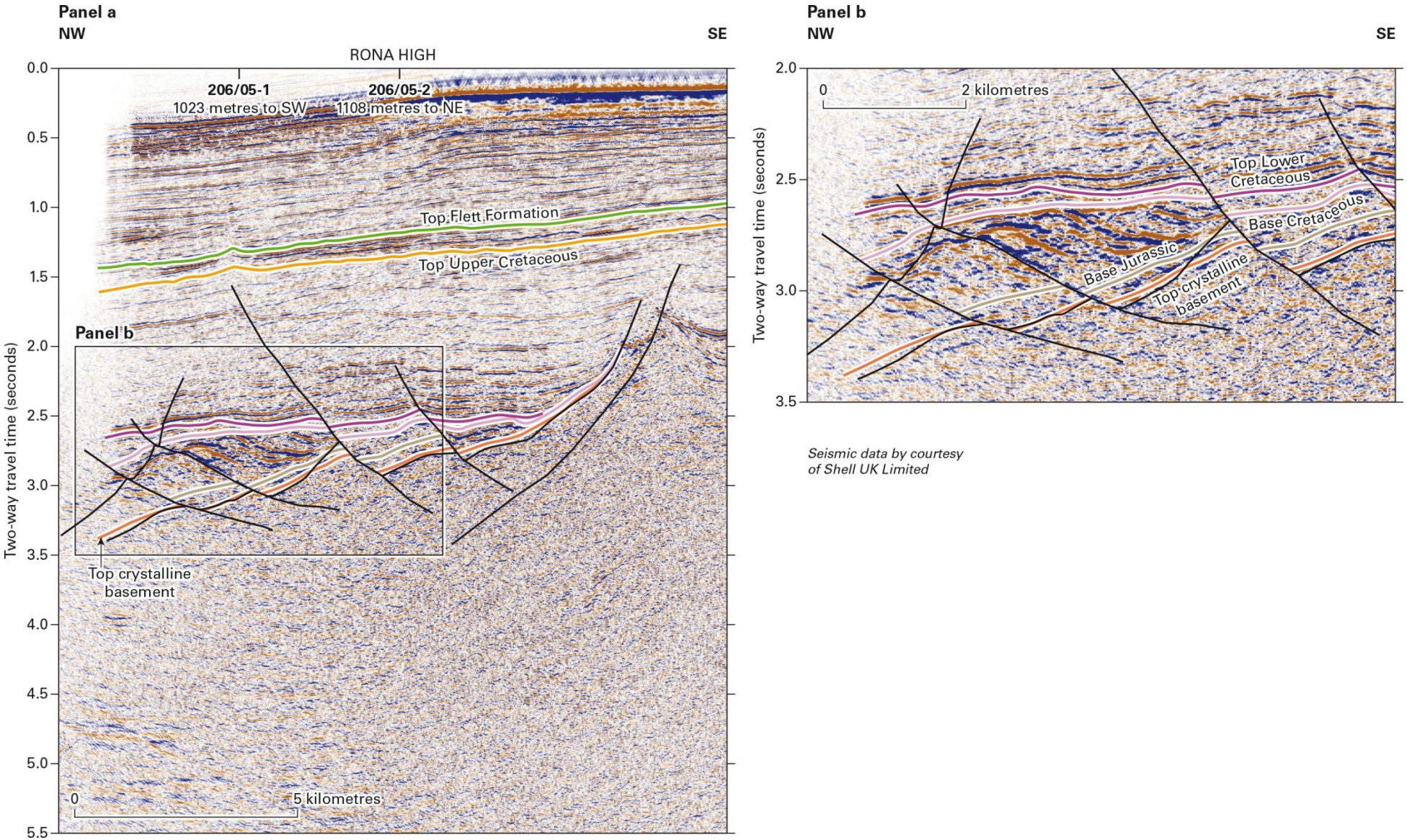

Figure 23. NW-trending interpreted seismic profile over the NW flank of the Rona High, with a more detailed inset (Panel b) showing an angular unconformity between Jurassic and Cretaceous successions. See Figure 4 for location of profile.

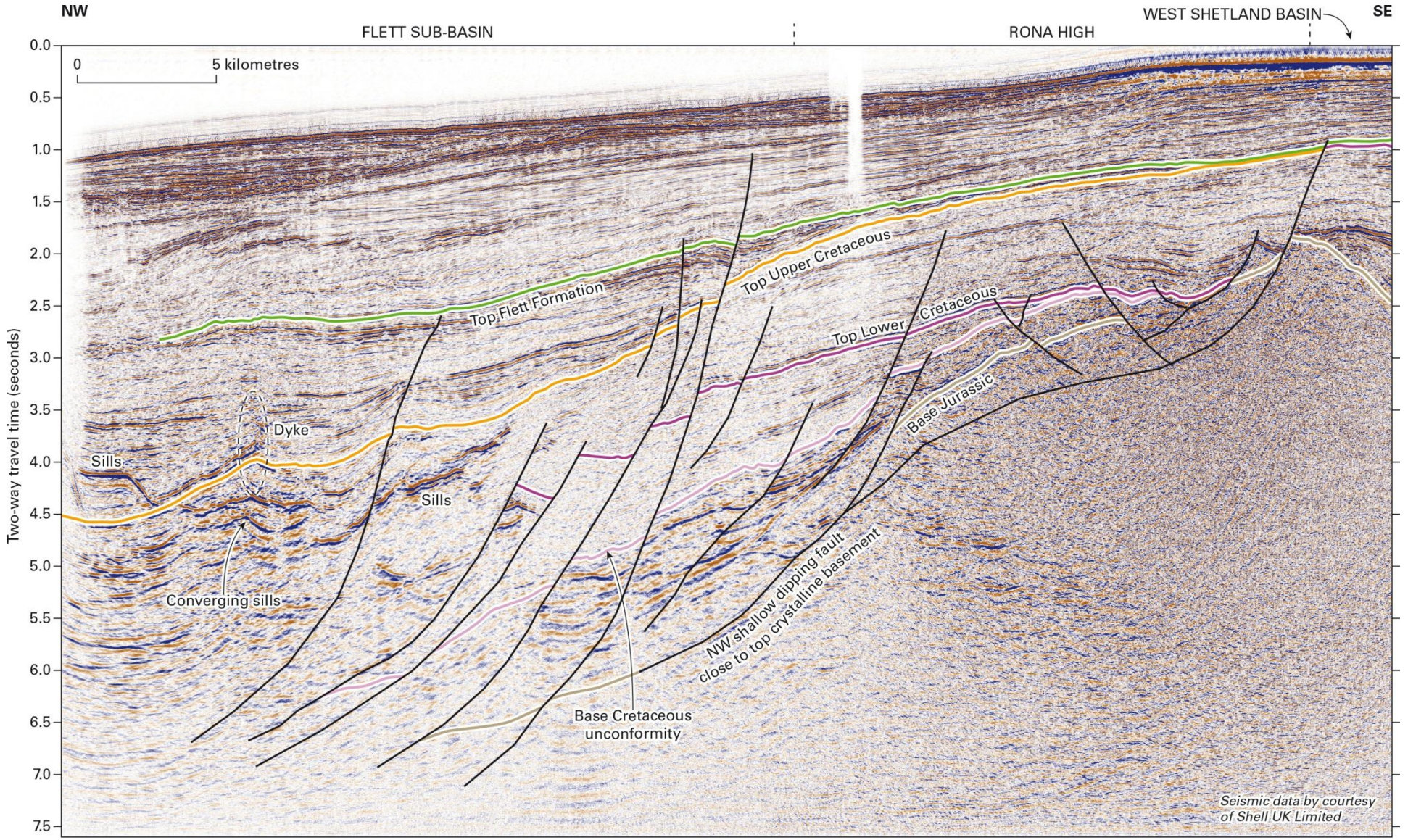

Figure 24. NW-trending seismic profile located NE of the Foula Syncline illustrating the succession on the Rona High and lack of clear seismic imaging further down-dip beneath igneous sills and dykes. See Figure 4 for location of profile.

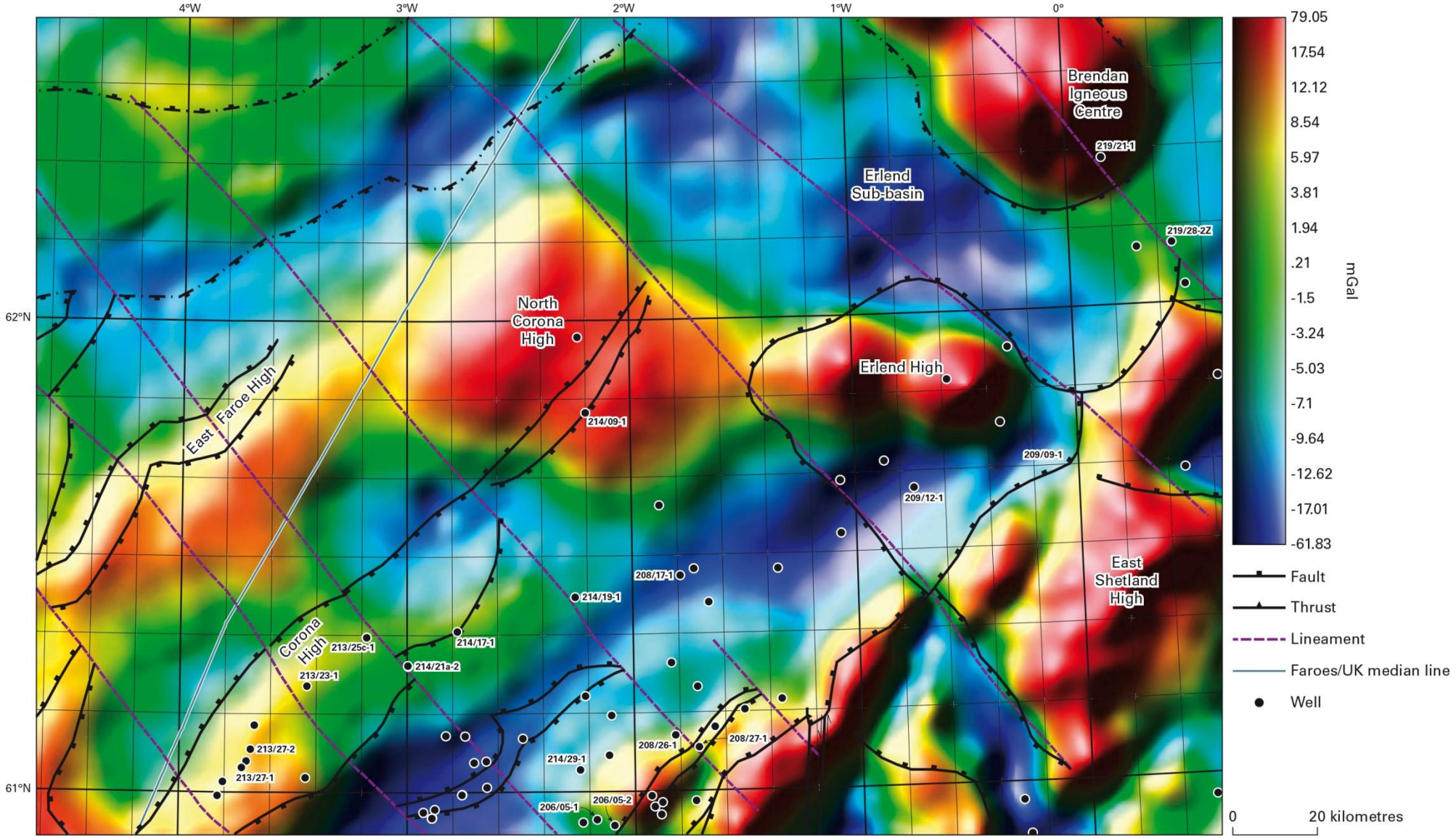

Figure 25. Variation in gravity response (high-pass filtered isostatically corrected Bouguer gravity anomaly; Kimbell et al., 2010) over the Erlend High and adjacent area. Structure outlines from Ritchie et al. (2011) superimposed.

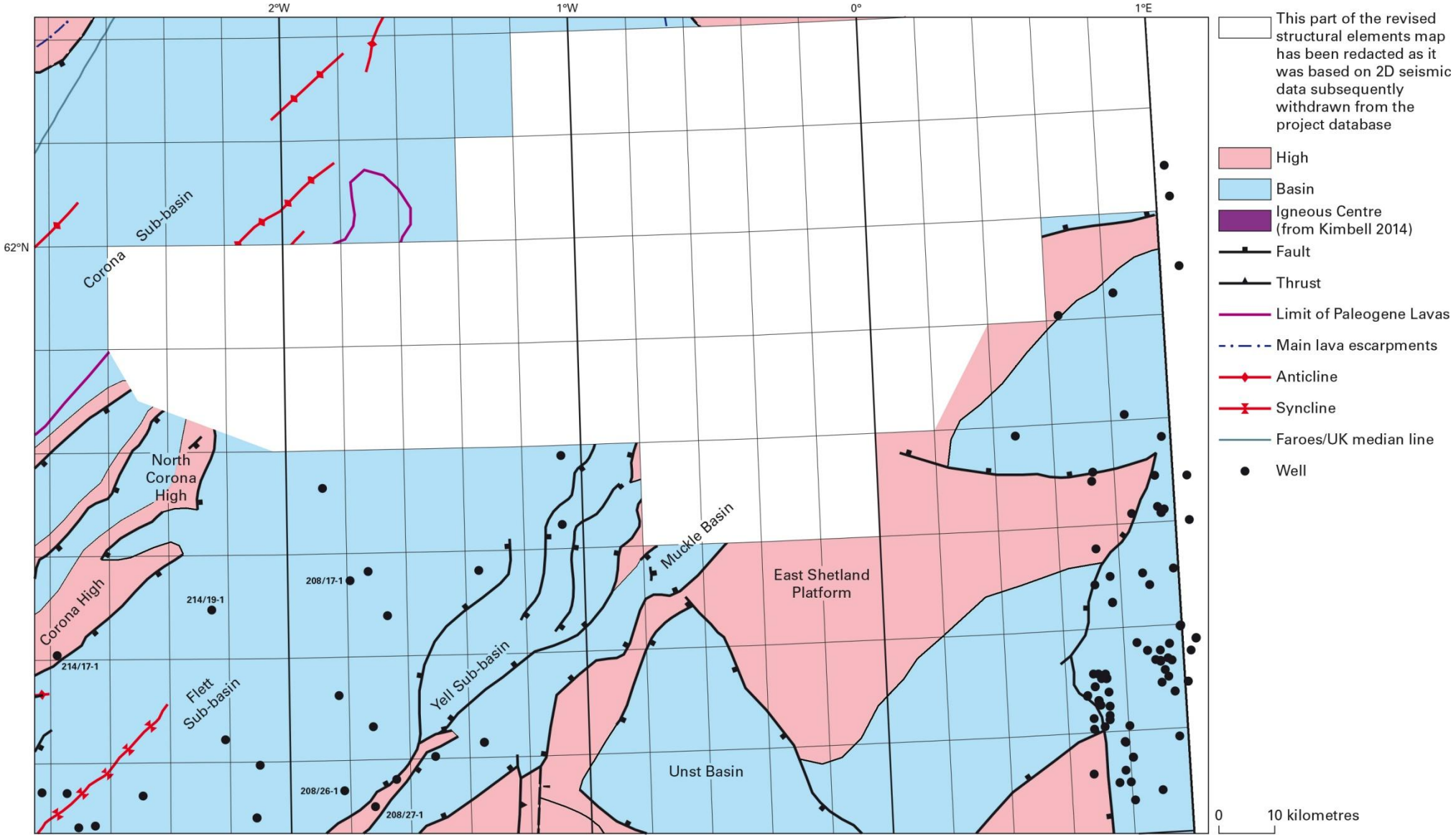

Figure 26. Detail from revised structural elements map partially illustrating the new interpretation across the Erlend High and surrounding area that has otherwise been redacted.

Figure 27. This figure has been redacted as it was based on 2D seismic data subsequently withdrawn from the project database.

Figure 28. This figure has been redacted as it was based on 2D seismic data subsequently withdrawn from the project database.

Figure 29. This figure has been redacted as it was based on 2D seismic data subsequently withdrawn from the project database.

Figure 30. This figure has been redacted as it was based on 2D seismic data subsequently withdrawn from the project database.

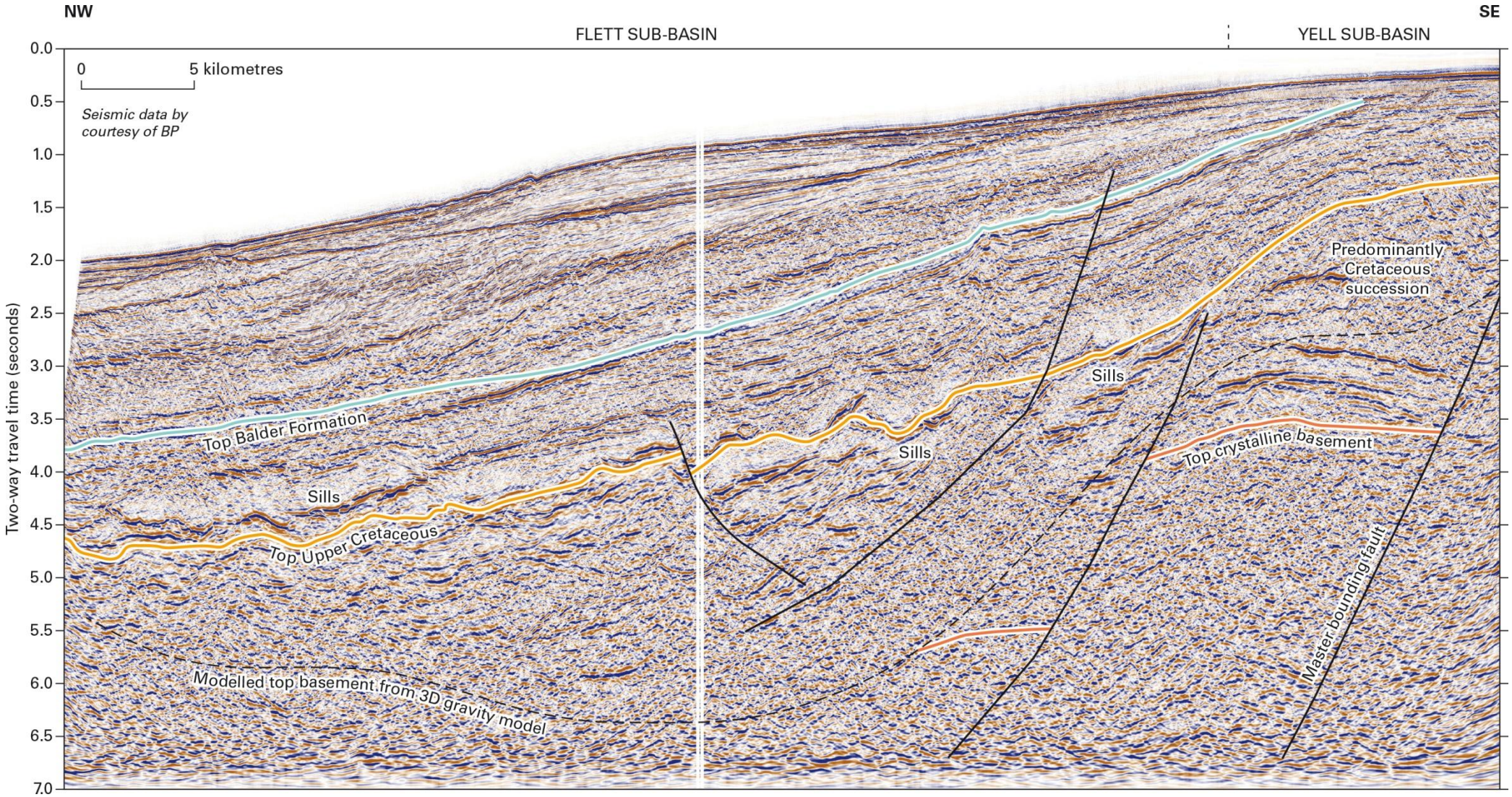

Figure 31. NW-trending seismic profile illustrating the Yell Sub-basin (after Larsen et al., 2010). Note NW-dipping Yell Sub-basin master bounding fault. See Figure 4 for location of profile.

Figure 32. This figure has been redacted as it was based on 2D seismic data subsequently withdrawn from the project database.

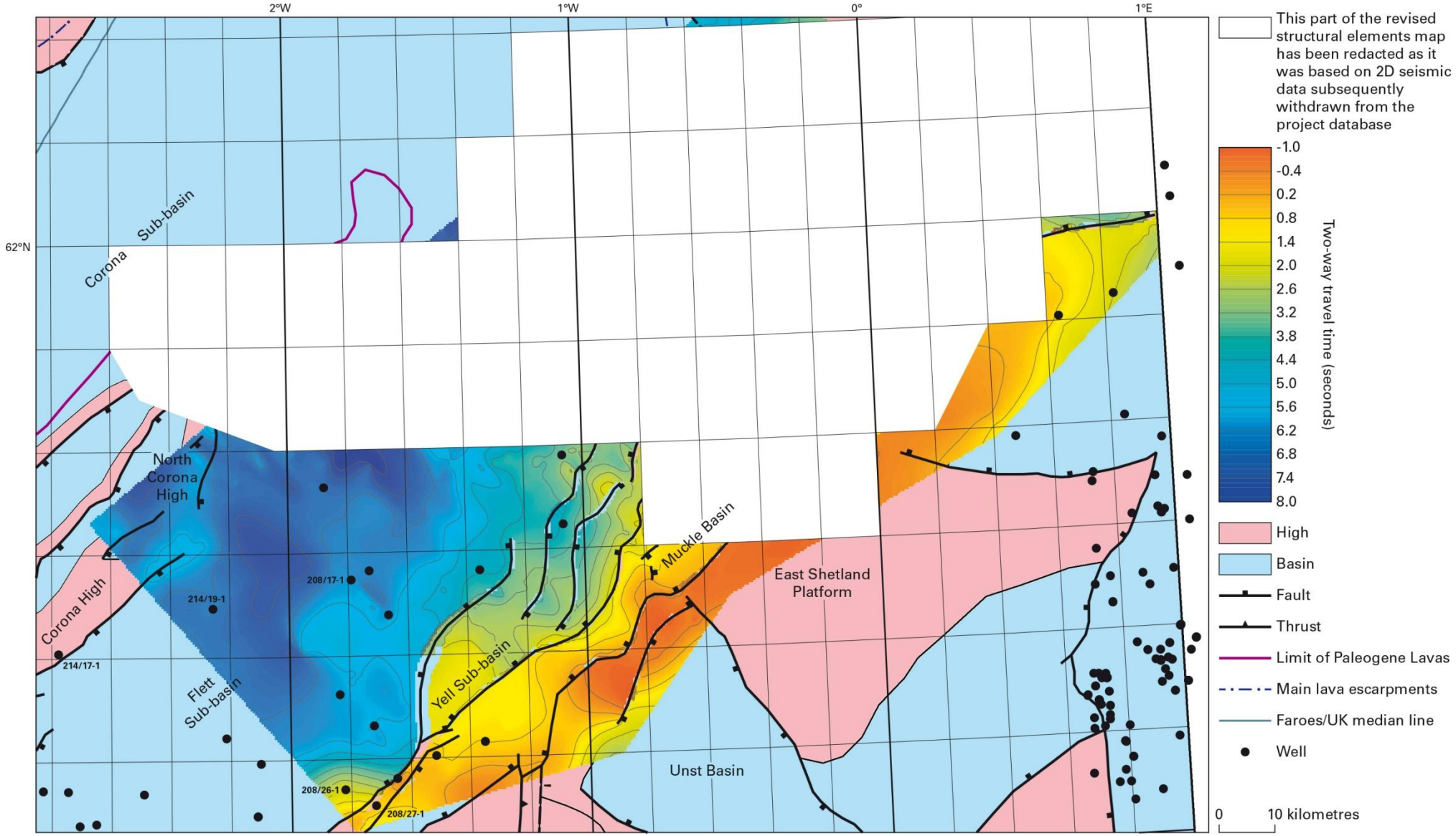

Figure 33. Redacted TWTT to interpreted top crystalline basement over the Erlend High and adjacent areas showing location of the Yell Sub-basin and Muckle Basin (after Larsen et al., 2010).

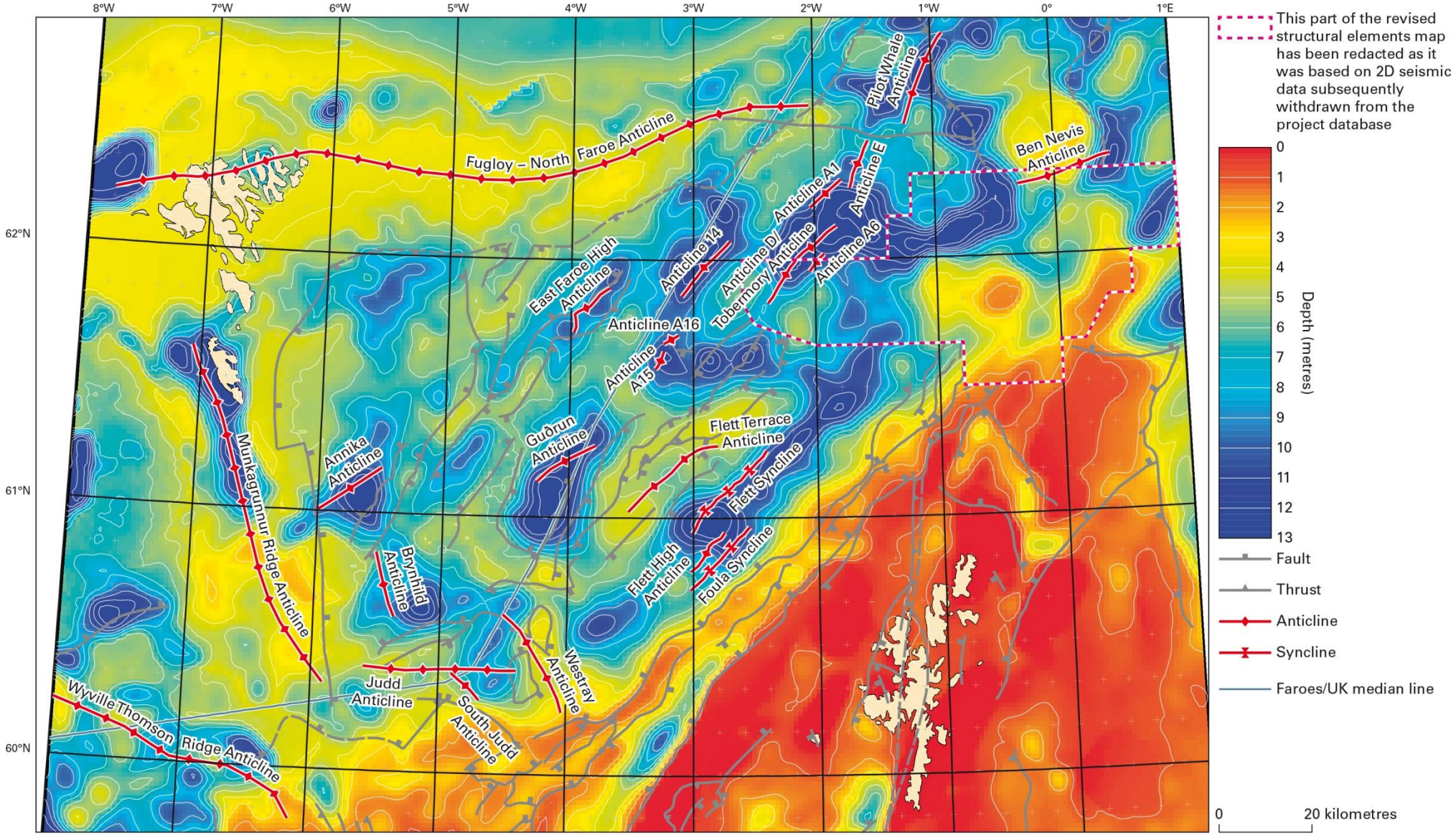

Figure 34. Detail of the modelled depth to basement map of Kimbell et al. (2010) showing the location and names of the rationalised set of fold axes.